

Institut für Anatomie and Zellbiologie
Direktor: Professor Dr. med. Tobias M. Böckers

**Biochemical and functional characterization of RhoSAP:
A RhoGAP of the postsynaptic density**

Dissertation zur Erlangung des Doktorgrades
Dr. biol. hum.
der Medizinischen Fakultät der Universität Ulm

Eingereicht von:
Janine Dahl
aus Ludwigslust

2008

Dekan: Prof. Dr. med. Klaus-Michael Debatin

Erster Gutachter: Prof. Dr. med. Tobias M. Böckers

Zweiter Gutachter: Prof. Dr. rer. nat. Dietmar Fischer

Tag der Promotion:

Abstract

Biochemical and functional characterization of RhoSAP: A Rho GAP of the postsynaptic density

By
Janine Dahl
Ulm University

Glutamatergic synapses in the central nervous system are characterized by an electron dense network of proteins underneath the postsynaptic membrane including cell adhesion molecules, cytoskeletal proteins, scaffolding and adaptor proteins, membrane bound receptors and channels, G-proteins and a wide range of different signalling modulators and effectors. This so called postsynaptic density (PSD) resembles a highly complex signaling machinery. We performed a yeast two-hybrid (YTH) screen with the PDZ domain of the PSD scaffolding molecule ProSAP2/Shank3 as bait and identified a novel interacting protein. This molecule was named after its Rho GAP domain: RhoSAP (Rho GTPase Synapse Associated Protein), which was shown to be active for Cdc42 and Rac1 by a GAP activity assay. Besides its Rho GAP domain, RhoSAP contains an N-terminal BAR domain that might facilitate membrane curvature in endocytic processes. At the C-terminus RhoSAP codes for several proline rich motifs that could possibly act as SH3 binding regions. Therefore, a second YTH screen was carried out with RhoSAP's proline rich C-terminus as bait to discover putative interacting proteins. As an interacting partner syndapin I, a molecule involved in vesicle endocytosis via direct interaction with dynamin I was found. Furthermore, syndapin I contains a C-terminal SH3 domain that is most likely the binding motif for RhoSAP's proline rich region. This novel interaction as well as the interaction with the ProSAP2 PDZ domain was verified by pull-down assays and coimmunoprecipitations.

Coming from the finding that RhoSAP is associated with an endocytosis molecule, an FM4-64 endocytosis assay was performed in cell line to delineate the molecule's significance in endocytic processes in general.

Taken together, RhoSAP is a novel ProSAP2/Shank3 interacting PSD protein, which displays several protein/protein interaction domains. Due to the N-terminal BAR domain, and the interaction with syndapin I, RhoSAP might act within endocytic processes of the postsynaptic membrane.

to my family

Contents

Abbreviations

1	Introduction	1
1.1	The postsynaptic compartment	2
1.2	The Rho GTPases	6
1.3	Rho GTPases-activating proteins (RhoGAPs)	9
1.4	Rho GTPases effector proteins and signaling pathways	12
1.5	Rho GTPases in actin dynamics and membrane trafficking	13
1.6	Nadrin and Rich1	15
	Aim	19
2	Materials and Methods	20
2.1	Declaration of suppliers and basic recipes	20
2.1.1	Materials	20
2.1.2	Recipes	22
2.2	Molecular biological methods	25
2.2.1	DNA/RNA concentration measurement	25
2.2.2	DNA preparation and purification	25
2.2.3	Plasmid DNA isolation from <i>E.coli</i> cell cultures	26
2.2.4	RNA purification, generation of cDNA and PCR	27
2.2.5	Generation of electrocompetent <i>E. coli</i> cells and transformation of plasmids	28
2.2.6	TOPO cloning and restriction analysis	29
2.2.7	DNA sequencing	30

2.2.8 Northern blotting	30
2.2.9 <i>in situ</i> Hybridization	32
2.2.10 Yeast two-hybrid screen	34
2.3 Protein biochemical methods	42
2.3.1 Protein concentration measurement	42
2.3.2 Preparation of GST-tagged fusion protein lysate from <i>E. coli</i> cell culture	43
2.3.3 Preparation of tissue and organ lysates	44
2.3.4 Subcellular fractionation of PSDs by differential centrifugation	45
2.3.5 SDS-PAGE, SDS gel staining and Western blotting	47
2.3.6 IgG purification of polyclonal antisera by (NH ₄)SO ₄	50
2.3.7 Coimmunoprecipitation and pull-down to analyse possible protein-protein interactions	51
2.3.8 GAP activity assay	52
2.4 Cell biological methods	54
2.4.1 Cell passages of cell lines	54
2.4.2 Transient transfection of HeLa and COS-7 cells	55
2.4.3 Generation of primary hippocampal neurons	56
2.4.4 Transfection of primary hippocampal neurons	57
2.4.5 Immunohistochemical staining for confocal fluorescence microscopy	57
2.4.6 DAB staining for confocal light microscopy	58
2.4.7 Immunohistochemical staining for electronmicroscopy (pre-embedding method)	59
2.4.8 Endocytosis assay and statistical analysis	59

3	Results	61
3.1	Gene and protein structural characterization of RhoSAP	61
3.1.1	Identification of RhoSAP as a PDZ domain interacting protein	61
3.1.2	Gene and protein structure of RhoSAP	62
3.1.3	Sequence homologies of RhoSAP	64
3.1.4	Putative splice variants of RhoSAP	64
3.1.5	Generation and characterization of anti-RhoSAP antisera	66
3.1.6	Profiling RhoSAP's expression in brain and other tissue	67
3.1.7	Recombinant expression of RhoSAP in COS7 cells	71
3.1.8	Localization of RhoSAP in hippocampal neurons	73
3.1.9	Subcellular distribution of RhoSAP in neurons	77
3.2	Isolation and analysis of RhoSAP's protein interaction partners	80
3.2.1	Verification of RhoSAP's association with ProSAP2Shank3	80
3.2.2	Identification of novel binding partners by a yeast two-hybrid screen	81
3.2.3	Confirmation of RhoSAP's interaction with syndapin I	82
3.3	Functional analysis of RhoSAP	83
3.3.1	Investigation of GAP activity	83
3.3.2	Investigation of endocytic activity	85
3.3.3	Investigation of intracellular membrane trafficking	89
3.3.4	Investigation of RhoSAP's effect on the cytoskeleton in cell culture	90
4	Discussion	93
4.1	Neuronal localization of RhoSAP and Rho GTPase signaling	93
4.2	RhoSAP: membrane trafficking and actin dynamics	96
4.3	Hypothesis for the function of RhoSAP in neurons	99

4.4 Conclusion	102
5 Summary	104
6 References	106
Acknowledgements	121
Curriculum Vitae	122

Abbreviations

aa	amino acid
ab	antibody
AD	activating domain
AMPAR	1-alpha-amino-3-hydroxy-5-methyl-4-isoxazole propionic acid receptor
Arp2/3	actin related protein 2/3
BD	binding domain
bp	base pair
CAZ	cytomatrix at the active zone
Cdc42	cell division cycle 42
CME	clathrin-mediated endocytosis
COT	the COT1 fraction of human genomic DNA consisting of rapidly annealing repetitive elements
Cortactin	cortical actin binding domain
d	day
DAB	2,3-deaminobenzidine
DIV	days <i>in vitro</i>
DNA	deoxynucleic acid
GAP	GTPase-activating protein
GDI	guanine nucleotide dissociation inhibitor
GEF	guanine nucleotide exchange factor
GFP	green fluorescent protein
mGluR	metabotropic glutamate receptor
GST	glutathione-S-transferase
GTPase	small GDP/GTP-binding protein
IgG	G-class of immunoglobulins

kDA	kilo Dalton
LTD	long-term depression
LTP	long-term potentiation
NMDAR	N-methyl D-aspartate receptor
PCR	polymerase chain reaction
PDZ	PSD95/ Disc-large/ ZO-1 domain
PI	protease inhibitor
PIP ₂	phosphatidylinositol-3-4-phosphate
ProSAP	proline rich synapse-associated protein
PSD	postsynaptic density
PSD95	postsynaptic density protein 95
Rac	Ras-related C3 botulinum toxin substrate
Ras	Roux avian sarcoma
Rho	Ras homologous member
RNA	ribonucleic acid
RhoSAP	RhoGAP synapse associated protein
Shank	SH3 domain and ankyrin repeat containing proteins
SNARE	soluble N-ethylmaleimide-sensitive component attachment protein receptor
SOD	superoxide dismutase
TdT	terminal deoxynucleotidyl transferase
UAS	upstream activating sequence
WASP	Wiskott-Aldrich syndrome protein
WAVE	WASP family verprolin-homologous
Y2H	yeast two-hybrid screen

1 Introduction

Information is integrated, processed and stored in the brain. Therefore, a complex network of trillions of neurons containing a variety of molecules, often unique and crucial to brain and its function, allows neurons to communicate with one another.

Neurons are the largest and most complex cells in the body. They are highly polarized cells, with one axon housing the molecular machinery necessary for action potential propagation and neurotransmitter release and several dendrites containing receptors and signaling components that respond to neurotransmitter emitted.

Neurons mostly communicate through highly specialized cell-cell junctions: the chemical synapses. At these sites, a specific cytoskeletal matrix is assembled at the active zone (CAZ) of an axon terminal organizing the synaptic vesicle release of neurotransmitter (Dresbach *et al.*, 2001). It directly opposes dendritic protrusions called dendritic spines, which are located along the entire length of dendrites in most neurons. The synaptic membranes are separated by the synaptic cleft, a specialized extracellular space typically about 20-30 nm in width (Gundelfinger & tom Dieck, 2000). The dendritic spines harbor the postsynaptic densities (PSD) that contain a multiprotein complex responsible for anchoring neurotransmitter receptors near sites of neurotransmitter release. Thus, synaptic transmission occurs directionally over the synaptic cleft from the pre- to the postsynaptic compartment. In excitatory synapses, glutamate is the predominant neurotransmitter, in contrast to inhibitory synapses which do not show spiny dendrites and release mainly glycine or GABA as neurotransmitter. Excitatory synapses are mainly associated with dendritic spine structures, whereas inhibitory synapses are localized on the somata or dendritic shafts of neurons (Kreienkamp & Dityatev, 2004).

In most regions of the developing brain, the formation of dendritic spines coincides with synaptogenesis in the first weeks after birth. Spine formation, morphogenesis and remodeling induced through synaptic activity, learning and memory or hormonal fluctuations remain a phenomenon, not only restricted to young neurons. Dendritic spines and synapses remain plastic in the adult brain as well (Ethell & Pasquale, 2005).

Consequently, synaptic plasticity depends upon maturation and maintenance of the synapse which in turn, is based on multifaceted protein-protein and protein-lipid interactions within dynamic macromolecular complexes at both, the presynaptic and the postsynaptic side (Gundelfinger *et al.*, 2003; Ziv & Garner, 2004; Kim & Sheng 2004).

1.1 The postsynaptic compartment

Dendritic spines are micron-sized membrane protrusions of neuronal dendrites that are the major sites of contacts for glutamatergic presynaptic inputs in the mammalian nervous system (Hering & Sheng, 2001). Furthermore, spines dynamically change their morphology through neuronal activity and postsynaptic glutamate receptor activation (Lang *et al.*, 2004; Matsuzaki *et al.*, 2004). Newly forming and growing spines in response to repeated glutamatergic stimuli inducing long-term potentiation (LTP) in hippocampal neurons is the contemporary model on a cellular level for learning and memory (Malenka & Nicoll, 1999; Engert & Bonhoeffer, 1999; Matsuzaki *et al.*, 2004). LTP is triggered by an influx of Ca^{2+} -ions at the postsynaptic membrane which in turn depolarizes it and activates signaling cascades in the postsynaptic compartment. It comprises a complex protein network consisting of cytoskeletal and scaffold proteins, receptors, ion channels, adhesion and signaling molecules. This proteome of the PSD is visible as a 40-50 nm thick electron-dense structure located at the synaptic contacts between neurons and is called the postsynaptic density (PSD) (Ziff 1997; Kennedy 2000).

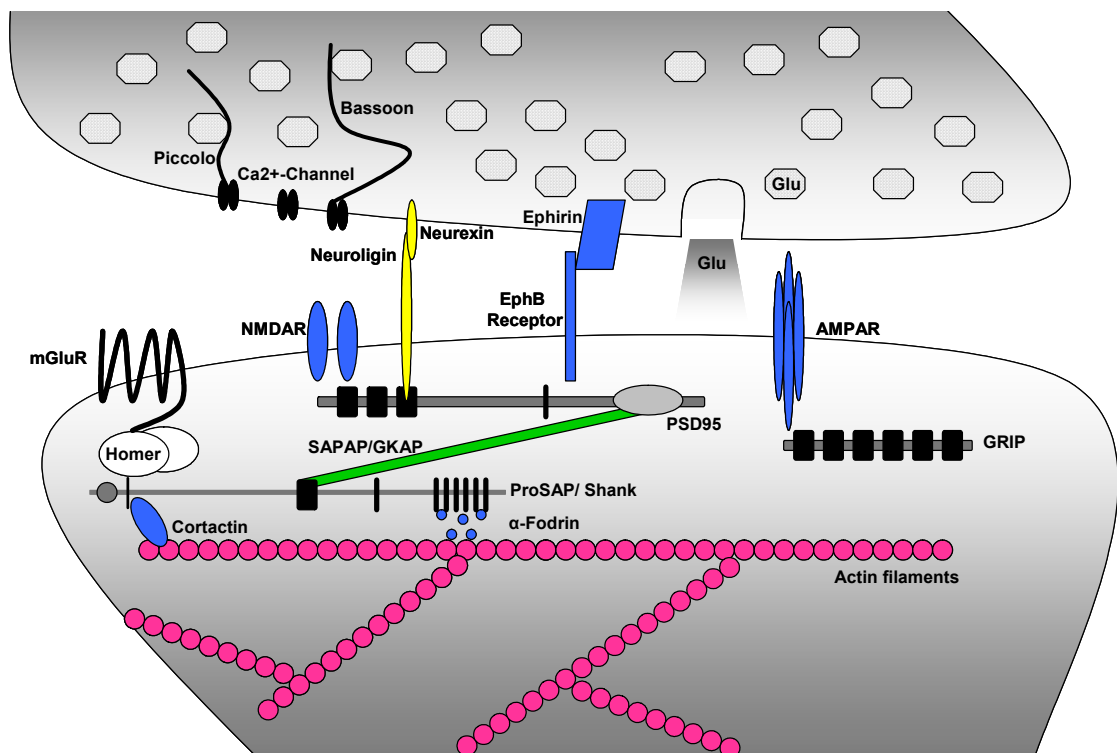


Fig. 1-1 Schematic diagram of the molecular assembly of an excitatory chemical synapse in mammals.

Chemical synapses are highly specialized, complex cell-cell contact sites. The presynaptic site with an axon terminal harbors an apparatus for neurotransmitter release. It is named cytomatrix assembled at the active zone (CAZ). The PSD is a multiprotein complex responsible for anchoring neurotransmitter receptors (AMPA, NMDA, mGlu) near the CAZ to respond to its glutamate release. PSD components further comprise cytoplasmic scaffold proteins, signaling enzymes, and cytoskeletal elements that form a disc-like protein-lipid macrocomplex structure. Indicated are: AMPA (α -amino-3-hydroxy-5-methyl-4-isoxazole propionic acid) receptors, N-methyl-D-aspartate (NMDA) receptors (blue); the serpentin receptor mGluR (black line

spanning the membrane 7-fold); Neuroligin, a postsynaptic adhesion molecule (yellow); the scaffold molecules GRIP, ProSAP/Shank and PSD95 containing one or more PDZ domain(s), typical for PSD scaffold molecule and outlined as black squares; cortical cytoskeletal elements: α -fodrin (blue circle) as a spectrin component and F-actin (pink) are represented; cortactin is shown as blue ellipse as actin associative element; SAPAP/GKAP: SAP90/PSD95-associated protein/guanylate kinase-associated protein.

The presynaptic axonal terminal is depicted with its typical synaptic vesicles, also determined boutons, carrying glutamate to be released after stimulation by an action potential. Presynaptic marker molecules are Piccolo, Bassoon (curved black lines), Neurexin, an adhesion molecule (yellow) and Ca^{2+} -channels (represented as dimer in black). PSD components comprise cytoplasmic scaffold proteins, signaling enzymes, receptors and cytoskeletal elements that form a disc-like protein-lipid complex.

Various types of glutamate receptors are co-clustered in the PSD, including metabotropic GluRs, a seven transmembrane helices receptor type, which mediates signals via trimeric G-proteins and neurotransmitter-gated cation channels: the ionotropic GluRs (iGluRs). Thereby, glutamate as the major excitatory neurotransmitter in the mammalian brain acts primarily on the iGluRs which are separated into two types. AMPA receptors (AMPA) immediately mediate the postsynaptic depolarization and depolarization. Contrastly, NMDA receptors are activated downward as a result of the previous AMPAR activation to initiate synaptic plasticity (Bredt & Nicoll, 2003). This is additionally underlied by the clustering and trafficking of ion channels and receptors in the postsynaptic membrane (Ziff 1997; Esteban 2003).

What is so unique about the PSD structure is the presence of scaffold proteins which multiply cluster and anchor signaling molecules to ion channels, receptors and cytoskeletal elements (Ziff 1997). One such protein class serving as central organizer of the PSD are the membrane-associated guanylate kinase homologs (MAGUKs). MAGUKs are multidomain proteins, usually comprising functional motifs as src homology (SH3), guanylate kinase (GUK) and PSD95/DLG/ZO1 (PDZ) domains. These motifs mediate certain protein-protein interaction patterns with other molecules of the PSD (Montgomery *et al.*, 2004). For instance, synapse associated protein 90 (SAP90)/postsynaptic density protein 95 (PSD95) carries three PDZ domains and is a member of the MAGUKs (Garner *et al.*, 2000). It binds to the NR2 subunit of NMDARs and to another class of scaffold proteins: the proline rich synapse associated protein/SH3 domain and ankyrin repeat containing protein (ProSAP/Shank) family (Boeckers *et al.*, 2002). AMPARs are clustered and anchored to the multicomponent signaling network in the PSD by (glutamate receptor-interacting protein) GRIP, another multi-PDZ domain containing protein. At the same time, they bind to a protein interacting with C-kinase (PICK-1), which is responsible to transduce AMPARs information to downstream signaling cascades (Dong *et al.*, 1997).

Because it is abundant in the brain and can be enriched by a few centrifugation steps, the PSD is a highly suitable structure for mass spectrometrical proteome analysis. The

identified classes of proteins of the PSD comprise: 12% of cytoskeletal actin components (e.g. actin, ankyrins, cortactin, α/β -spectrins), 11% kinases/phosphatases (e.g. PKC γ , Casein kinase 2, PP1, PP2A), 8% GTPases and regulators (e.g. Ras, trimeric G-proteins, GEFs and GAPs), 7% cell adhesion (e.g. Neuroligin, N-Cadherin), 6% scaffold proteins (e.g. ProSAP/Shank, PSD95, Homer, GKAP) and receptors (AMPA, NMDAR, mGluR1), 5% membrane trafficking molecules (e.g. AP1, Clathrin, Syntaxin), 4% motor proteins (e.g. Dynein) and the remaining 47 % are shared among proteins of translation, metabolism, mitochondria, chaperones and others (Li *et al.*, 2004; Peng *et al.*, 2004).

By this method, large numbers of proteins could be identified to be arranged in core subsets in the PSD. The main complexes are the NMDA/SAP90-PSD95 complex (NRC), the mGluR complex (GC) and the AMPAR complex (ARC). Together with the master scaffold proteins of the MAGUK and ProSAP/Shank family, these complexes build a hierarchical structure to ensure an effectively organized signal reception, modulation and transduction in the PSD of excitatory synapses (Boeckers 2006).

ProSAP/Shank family of scaffold proteins

The ProSAP/Shank family of proteins is one of the major scaffold molecules in the PSD that interacts simultaneously with many membrane and cytoplasmic proteins of the postsynapse (Sheng & Kim, 2000). It comprises three members who share a sequence homology of 63-87% due to their highly homologous functional domains: the Ankyrin repeats (ANK), SH3 and PDZ domain, a proline rich region with a Cortactin binding motif (ppI) and a sterile alpha motif (SAM). The ANKs which are localized in the N-terminus interact with α -fodrin and shapin. α -Fodrin connects ProSAP/Shank to the cytoskeleton via its spectrin repeats, a binding motif for F-actin (Boeckers *et al.*, 2001; Lim *et al.*, 2001). At the same time this motif interconnects postsynaptic membrane receptors with the actin cytoskeleton and establishes a link to Ca²⁺-dependent signaling cascades (Boeckers *et al.*, 2002). The ANKs are followed by an SH3 domain, the PDZ domain, a proline rich region which comprises a special segment: the ppI domain. Cortactin interacts with the actin cytoskeleton and is recruited to the PSD through the proline rich region (Du *et al.*, 1998). The QTRL binding motif within the PDZ domain mediates an interaction with the GKAP motif of the guanylate kinase domains that are characteristic for MAKUGs, e.g. PSD95. Thereby, postsynaptic NMDA receptors are linked to the ProSAP/Shank family of proteins (Naisbitt *et al.*, 1999). PDZ domains are repeats of approximately 90 amino acid residues containing the motif Gly-Leu-Gly-Phe (Saras & Heldin, 1996). PDZ domains are

involved in four different classes of interactions; binding to C-terminal or internal motifs, PDZ-PDZ dimerization, and recognition of lipids (Nourry *et al.*, 2003). The domain acts as scaffold close to the plasma membrane to aggregate receptors and signaling molecules of the PSD in large multimeric complexes. In comparison to the ProSAP/Shank family of proteins which contain only one PDZ domain, other postsynaptic scaffold molecules as PSD95, PSD93, GRIP and PICK harbor two or more PDZ domains.

At the end of the C-terminus a sterile alpha motif (SAM) facilitates dimerization of several ProSAP/Shank molecules to localize numerous molecules in the PSD. It is a postsynaptic membrane targeting motif. It has been proposed that assembly of ProSAP/Shank in sheets via its SAM domain in the PSD is a Zn^{2+} -dependent process. Neuronal activity might set free Zn^{2+} -ions which could play an important structural role to support PSD stabilization (Sala *et al.*, 2001; Boeckers *et al.*, 2005; Baron *et al.*, 2006).

Every ProSAP/Shank protein owns several alternative splicing sites (Boeckers *et al.* 1999a; Lim *et al.*, 1999). The expression pattern of each member is distinct and varies from cell-type and tissue. The only brain specific-protein is Shank1 whereas ProSAP1/Shank2 was detected in neuron and glia cells, besides being present in liver and kidney tissue. The same is valid for ProSAP2/Shank3 which could be detected in other tissue as well, *e.g.* heart, muscle and testis (Boeckers *et al.*, 1999b; Lim *et al.*, 1999).

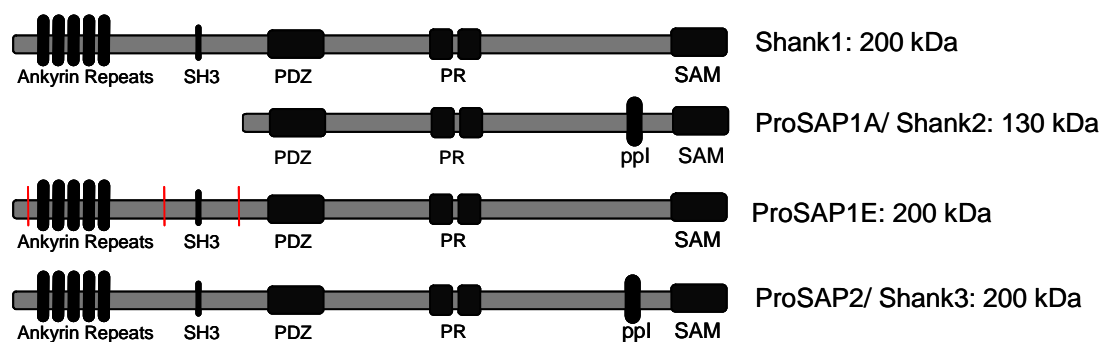


Fig. 1-2 The ProSAP/Shank protein family and the domain structures. ProSAP/Shanks contain several protein-protein interaction domains: ANKs, SH3 and PDZ domain, proline rich regions, ppl and SAM domain. Of three family members Shank1 does not contain ANKs and an SH3 domain. ProSAP1E contains splice variants. Red lines indicate the splice variants domain structures.

Neuropathology associated with abnormalities in dendritic spines and PSD components

Dendritic spines are irregularly shaped and have abnormal postsynaptic densities in a number of neurodevelopmental disorders characterized by mental retardation. Since Rho GTPases have emerged as key regulators of dendritic arborization and spine morphogenesis, it is not surprising that several genes, significant for mental retardation

encode components of Rho family signaling cascades, which underlie the importance of these GTPases in regulating dendritic spine morphology and function. Dendritic spines are irregularly shaped in various forms of nonspecific X-linked mental retardation (XMR), *e.g.* Fragile X syndrome, William's syndrome, Down's syndrome, Angelman syndrome and autism (Ethell & Pasquale, 2005; Newey *et al.*, 2004). For instance, in 1-5% of autistic patients, a mutation in the ProSAP/Shank3 gene is sufficient to cause the neurological disease. Additionally, mutations in neuroligins (NLGN3,4) and neurexin1 have been found to account for autism cases (Jamain *et al.*, 2008; Bourgeron 2007; Durand *et al.*, 2007).

Abnormal dendritic spines are also associated with a number of other neurological disorders, such as schizophrenia, bipolar disorder with psychosis, and epilepsy (Glantz & Lewis, 2002; Rosoklija *et al.*, 2002). Emerging studies implicate a dysregulation of NMDAR trafficking in neuropsychiatric disorder such as cocaine addiction, chronic alcohol abuse, schizophrenia and Alzheimer's disease. In these diseases, permanent neuronal activity drives subunit-specific receptor internalization and degradation through the ubiquitin-proteasome system. Under normal conditions, however, longer neuronal activity is blocked and promotes the alternative RNA splicing of the NR1 subunit, which in turn accelerates forward trafficking of NMDARs through the endosomal-lysosomal pathway (Lau & Zukin, 2007). It follows that NMDARs are tied up in the receptor cycling again and are represented at the dendritic surface again.

1.2 The Rho GTPases

The Ras superfamily of small monomeric 20-40 kDa GTP-binding proteins counts more than 50 members. It can be divided into five major groups based on sequence and functional differences, Ras, Rho, Rab, Sar1/Arf and Ran (Takei *et al.*, 2001; Wennerberg *et al.*, 2005). The three Ras genes, H-Ras, K-Ras and N-Ras were first discovered as oncogenes in rat sarcoma viruses and in neuroblastoma (Downward 1990). The Ras proteins are activated upon ligand engagement of membrane receptors and mainly regulate gene expression influencing cell growth, morphology, differentiation and apoptosis (Shields *et al.*, 2000; Takei *et al.*, 2001). The first signaling pathway found to involve Ras was the Raf/MEK/Erk cascade leading to transcriptional activation (Vojtek & Der, 1998). Other effectors include p120GAP and PI-3 kinase.

Most Ras proteins cycle between an inactive, guanosine diphosphate (GDP)-bound form and an active, guanosine 5'-triphosphate (GTP)-bound form. Five hydrophilic loops, which form the guanine nucleotide-binding site, are the most highly conserved elements in this

binding pocket. Its amino acid residues critical for Mg^{2+} -binding, GTP-binding and hydrolysis are conserved in all members of the Ras superfamily (Takai *et al.*, 2001).

Rho proteins are key regulators in reorganization of the actin cytoskeleton, thereby influencing cellular functions such as cell shape, cell growth, motility and adhesion (Takai *et al.*, 2001). The Rho GTPase subfamily in human includes 22 members, divided into eight subgroups as shown in table 1 (Fransson *et al.*, 2003; Wherlock & Mellor, 2002).

Tab 1-1 The Rho GTPase subfamily

Rho GTPase subgroup	Members
Cdc42	Cdc42, TC10, TCL, Chp and Wrch-1
Rac	Rac1, Rac2, Rac3 and RhoG
Rho	RhoA, RhoB and RhoC
Rnd	Rnd1, Rnd2 and Rnd3
RhoD	RhoD and Rif
RhoH/ TTF	RhoH/TTF
Miro (mitochondrial Rho)	miro1 and miro2
RhoBTB	RhoBTB1 and RhoBTB2

The most extensively characterized of all Rho GTPases are Cdc42 (cell division cycle 42), Rac1 (Ras-related C3 botulinum toxin substrate 1) and RhoA (Ras homologous member A). Initially, Cdc42 was shown to be an important regulator of cell polarity in budding yeast, Rac1 was implicated in regulating superoxide formation of stress fibers (Abo *et al.*, 1991; Adams *et al.*, 1990; Ridley & Hall, 1992). Ras proteins are anchored to various cellular membranes that are critical for their proper function and are regulated by prenyl transferases. In general, Rho GTPases membrane targeting is achieved by a post-translational lipid-modification in the carboxyl terminal CAAX-box and the methylation of a cysteine residue (Seabra 1998).

Members of the Rho GTPase family are the key regulatory proteins that link plasma membrane receptors to the assembly of distinct filamentous actin structures (Hall 1998). As key molecules, Rho GTPases act to regulate signaling convergence of multiple receptors that control processes such as cellular movement, morphology and proliferation. This is achieved by a coordinated interaction with a wide variety of effector proteins. Thereby, signaling cascades that do not only control actin organization but also cell cycle progression in general, gene expression as well as vesicular trafficking is fine tuned to facilitate dynamic change of cell structure (Karnoub *et al.*, 2004). Thus, interconnection of all these important cellular processes by Rho GTPases is of great importance for any kind

of axonal and dendritic development in neurons (Ahnert-Hilger *et al.*, 2004). At this point, it is still unclear how the Rho family affects neurogenesis in detail, yet it has been shown that Rho is a molecular switch to coordinate axonal and dendritic outgrowth and *vice versa* (Bradke & Dotti, 1999).

Over all, the GTP/GDP cycle of small GTPases is tightly regulated by three distinct functional domains which comprise three families of proteins: guanine nucleotide exchange factors (GEFs), GTPase-activating proteins (GAPs), and the guanine nucleotide dissociation inhibitors (GDIs). GEFs activate Rho proteins by catalyzing the exchange of GDP for GTP, therefore increasing the levels of the GTP-bound forms in cells (Schmidt & Hall, 2002).

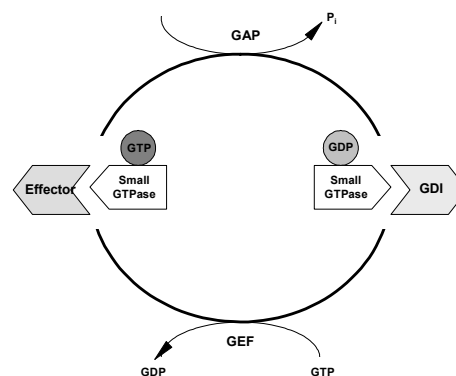


Fig. 1-3 Activation and deactivation of small GTPases by guanine nucleotide exchange and GTP hydrolysis. An activating event triggers the enhanced detachment of bound GDP from the small GTPase. The vacant site is rapidly occupied by GTP and this causes activation of the GTPase. Thus, specific effector enzymes and proteins are in turn activated to switch on downstream signaling cascades. The activation is boosted by guanine exchange factors (GEFs), enabling an accelerated nucleotide exchange. In consistence to the transient activation of G-proteins, the system returns to the resting state following hydrolysis of the bound GTP. In this case, GAP proteins are the effectors to accelerate the rate of GTP hydrolysis, therefore negatively regulating the activity of small GTPases. After returning to there original state of GDP bound form, small GTPases are prevented from going into the next exchange cycle by GDP dissociation inhibitors (GDIs), which bind to the G-protein until it has interacted with the appropriate molecules to be activated again.

More than 70 GEFs for Rho GTPases constitute a class of proteins well known as the diffuse B cell lymphoma (Dbl) family of proteins (Cote & Vuori, 2002). Conversely, RhoGAPs negatively regulate GTPase function by increasing the intrinsic GTP hydrolysis rate, therefore promoting formation of the GDP-bound state (Lamarche & Hall, 1994). Additionally, Rho GTPases are negatively regulated by RhoGDIs which inhibit nucleotide dissociation by interference with GDP/GTP exchange and GTP hydrolysis. Moreover, they promote the release from Rho GTPases from cellular membranes, leading to an inactivation of the GTPase cycle (Keep *et al.*, 1997; Hoffman *et al.*, 2000).

1.3 Rho GTPase-activating proteins (RhoGAPs)

The first RhoGAP identified was p50RhoGAP, and since then more than 30 RhoGAPs have been reported in eukaryotes, ranging from yeast to human. Genome analysis revealed the presence of around 80 human genes containing RhoGAP domains (Moon & Sheng, 2003).

GAPs for the GTPases within the Rho subfamily share high sequence similarity in their GAP domain, whereas the degree of similarity to RasGAPs is low (Scheffzek *et al.*, 1998). Structurally, a common fold for p120RhoGAP and p50RhoGAP could be determined, revealing a core structure motif (RhoGAP domain) made up of seven α -helices and a catalytic arginine residue (arginine finger) that are positioned in approximately the same position (Rittinger *et al.*, 1998; Scheffzek *et al.*, 1996; Barrett *et al.*, 1997). RhoGAP stabilizes the position of glutamine 61 of Rho, which in turn coordinates the attacking water. In addition, the arginine finger is positioned into the phosphate-binding site and stabilizes the transition state by neutralizing negative charge at GTP's γ -phosphate. In some human tumors, glutamine 61 mutation abolishes GAP-induced GTP hydrolysis (Rittinger *et al.*, 1997; Bos *et al.*, 2007).

The substrate specificity of the RhoGAPs toward members of the Rho subfamily varies with each GAP protein, listed in table 1-2 (van Aelst & Schorey, 1997; Bernards 2003).

Very often GAPs exhibit activity for several Rho GTPases in cell-free assays. However their specificity seems to be restricted. Usually, activity measurements involve the well-known Rac, Cdc42, and Rho as substrates, whereas studies on the remaining Rho GTPases are needed to complete the picture. For example, the substrate spectrum of p50RhoGAP *in vitro* encompasses Cdc42, Rac1 and Rho; in contrast, *in vivo*, it appears to display specificity for Rho only. The same is valid for p190GAP which inhibits Rho-mediated stress fiber formation after microinjection but does not induce Rac-mediated membrane ruffling. So far, implication of a direct link between Ras and Rho-mediated signaling pathways remains to be elucidated (Ridley *et al.*, 1993; Settleman *et al.*, 1992). RhoGAPs, in addition to accelerating the hydrolysis of GTP, may mediate other downstream functions of the Rho proteins in mammalian system. Chang *et al.* (1995) demonstrated that p190GAP plays a role in Rho regulation during cytoskeletal rearrangement events in cells. N-chimaerins, representing brain specific RhoGAPs, have been shown to prevent Rac- and Cdc42-induced cytoskeletal rearrangements in fibroblasts (Leung *et al.*, 1993; Kozma *et al.*, 1996).

Tab 1-2 Selected mammalian RhoGAPs for the Rho subfamily of GTPases

RhoGAP	GAP specificity (in vitro)	Tissue distribution	Characteristics	References
p50RhoGAP/ Cdc42GAP (human)	Cdc42, RhoA Rac1	Ubiquitous	Binds PIP ₃ ; 3D- structure determined.	Barfod <i>et al.</i> , 1993; Nassar <i>et al.</i> , 1998
p190-A (human and rat)	RhoA, Rac1 Cdc42	Ubiquitous	Src-substrate and putative mediator of Src-dependent adhesion signals for neural development and neuritogenesis. Overexpression promotes neurite outgrowth in neuroblastoma. Tumor suppressor.	Bouton <i>et al.</i> , 1991; Brouns <i>et al.</i> , 2001
p250GAP	Cdc42 RhoA	Enriched in brain	Interacts with NR2B subunit of NMDA receptors in vivo. Colocalizes with PSD-95. Suppresses Rho family proteins and alters neurite outgrowth.	Takanobu <i>et al.</i> , 2003
p85 α and p85 β (human)	no activity	Ubiquitous	adaptor subunit of PI 3-kinase. Putative target for Cdc42 and Rac1. 3D-structure determined.	Otsu <i>et al.</i> , 1991; Skolnik <i>et al.</i> , 1991; Bokoch <i>et al.</i> , 1996 ; Musacchio <i>et al.</i> , 1996
GRAF2 (mouse)	Cdc42 RhoA	Ubiquitous/highly expressed in brain and liver	Interacts with protein kinase PKN- β and is phosphorylated by this kinase (human). Putative effector for Rho through enhancing neurite retraction in NGF- differentiated PC12 cells (chicken). 3D- structure resolved. Has a BAR domain.	Hildebrand <i>et al.</i> , 1996; Borkhardt <i>et al.</i> , 2000
N-chimaerin	Rac1	brain		Diekmann <i>et al.</i> , 1991

3BP-1 (mouse)	Rac1 Rac2 Cdc42, RhoG	Ubiquitous/abundant in brain and spleen	Binds the SH3 domain in Abl. Has a BAR domain.	Cicchetti <i>et al.</i> , 1992
Rich1 (human)/ Nadrin (rat)	Rac1 Cdc42/ Rac1 Cdc42 RhoA	Ubiquitous/enriched in brain	Rich1 binds CIP4 and several other SH3 domain containing proteins. Nadrin is involved in exocytosis and inhibits neurite outgrowth in PC12 cells. Both effects are proposed to rely on its GAP activity. Both molecules have BAR domains implicated in membrane- trafficking.	Harada <i>et al.</i> , 2000; Richnau & Aspenström, 2001; Furuta <i>et al.</i> , 2002
Rich2	Rac1 Cdc42	Ubiquitous/enriched in brain	Has a BAR domain.	Richnau & Aspenström, 2001
Oligophrenin-1	Rac1 Cdc42 RhoA	Brain	Overexpressed in glial tumors. Involved in neuritogenesis.	

The regulation of GAP activity has been shown to include lipid-binding, protein-protein interaction and phosphorylation (Bernards & Settleman, 2004).

In the case of p190 RhoGAP, it was demonstrated that several phospholipids, including phosphatidylserine, PtdIn(4,5)P₂ and phosphatidic acid, are effective inhibitors of GAP activity *in vitro*. At the same time, phosphatidylserine and PtdIn(4,5)P₂ have been found to stimulate the GAP activity of p190 RhoGAP towards the Rac1 GTPase (Ligeti *et al.*, 2004). Thus, phospholipids can serve as a molecular ‘switch’ to change the GTPases’ substrate preference for a GAP. Thereby, a distinct mechanism for the regulation of GAPs is provided in the cell. In addition to lipid-binding regulation, proteolysis has been observed to be another regulatory tool of the cell to balance GAP concentration. For example, p120 RasGAP is degraded by caspase cleavage and an N-terminal proteolytic fragment is set free to inhibit apoptosis (Yang & Widmann, 2001). Some GAPs also undergo proteolytic degradation via the ubiquitin-proteasome system, as it was described for neurofibromin, a representative of the RasGAP family (Cichowski *et al.*, 2003).

The dysregulation of Rho GTPases activities has been shown to result in diverse neurodegenerative disorders. For instance, the deleted oligophrenin-1 loses its function and

causes an XMR neuropathological disorder with cognitive impairment (Billuart *et al.*, 1998).

1.4 Rho GTPase effector proteins and signaling pathways

Active Rho GTPases interact with a spectrum of functionally divergent groups of proteins. Over 50 effectors have been identified so far for Rho, Rac and Cdc42 that include serine/threonine kinases, tyrosine kinases, lipid kinases, lipases, oxidases, and scaffold proteins. Rho GTPases serve as key regulatory proteins that link plasma membrane receptors to the assembly of distinct filamentous actin structures, gene expression, cell cycle, cell morphogenesis and migration (Hall 1998; Jaffe & Hall, 2005).

In Swiss 3T3 cells, Rac is activated by a wide variety of tyrosine kinase receptors, for example insulin, PDGF and EGF are all strong inducers of Rac-dependent membrane ruffling. Thereby, the key component of activated Rac effector is the lipid kinase phosphatidylinositol 3-kinase (PI-3 K) (Ridley *et al.*, 1992). In the same cell line, Rho was shown to be activated through G-protein coupled receptors (GPCRs) leading to the formation of stress fibers and focal adhesions (Ridely & Hall, 1992). Activation of Cdc42 gave rise to filopodia (Kozma *et al.*, 1995; Nobes 1992).

In brief, Rho, Rac and Cdc42 have distinct effects in several processes that require the reorganization of actin, for example during the cell's development and its associated morphological changes. Rac promotes actin polymerization at the leading edge of the lamellipodia, providing the driving force for forward movement, whereas Cdc42 defines the polarity of the cell and reorientates the Golgi in the direction of movement (Allen *et al.*, 1998, Bishop & Hall, 2000). Actin reorganization influenced by Rac, Cdc42 and Rho has been implicated in neuronal morphogenesis involving neuronal migration and polarization, axon guidance, dendritic spine formation, synaptic organization and plasticity (Luo 2002). Beyond their role in cytoskeletal rearrangements, Rho GTPases control the activity of transcription factors such as SRF, c-Jun, and NF κ B (Minden *et al.*, 1995; Perona *et al.*, 1997). Moreover, Rho GTPases serve functions in promoting or antagonizing apoptosis and cell cycle progression (Welsh 2004; Zhu *et al.*, 2008).

Initially, filopodium formation via Cdc42 was thought to require the ubiquitous N-WASP, allowing an interaction with the Arp2/3 complex for actin polymerization (Rohatgi *et al.*, 1999). However, further findings indicated that N-WASP is dispensable for *de novo* formation of filopodia (Snapper *et al.*, 2001).

Arp2/3-induced actin polymerization can be also triggered by Rac1. The small GTPase interacts with the ProSAP/Shank-associated IRSp53, which binds WAVE and induces actin polymerization. Thus, IRSp53 provides a link between Rac and Cdc42 and an explanation to how Cdc42 can induce Rac-mediated ruffling (Govind *et al.*, 2001).

The main effector pathways activated by Rac, Cdc41 and Rho are depicted in the following scheme.

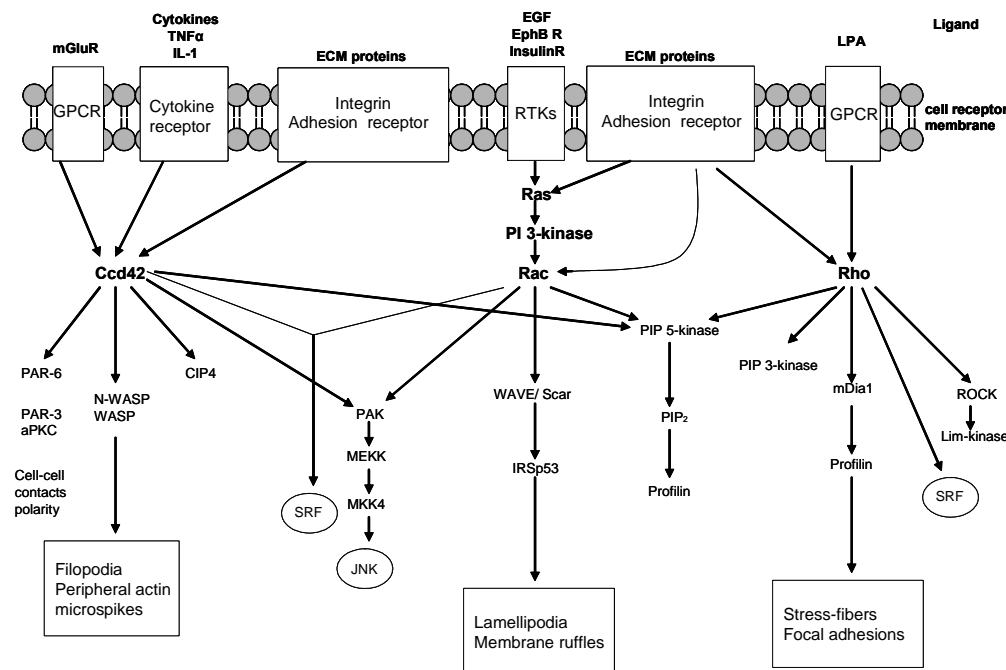


Fig. 1-4 General overview of Rho GTPases signaling pathways and crosstalk interconnections.

Notably, this figure excerpts some of the most important Rho GTPases cascades in non-neuronal and neuronal cells. Rho GTPases can be activated in series, such that one small GTPase stimulates GTP loading of another. Cdc42 is a strong activator of Rac in many cell types, while Rac is able to activate or inhibit Rho to varying degrees. The biochemical events mediating cross-talk between members of the Rho family has to be elucidated. aPKC: atypical protein kinase CCIP4: Cdc42-interacting protein 4; GPCR: G-protein coupled receptor; IRSp53: insulin receptor substrate protein 53; JNK: Jun-kinase; LPA: lysophosphatidic acid; mDia: Diaphanous1; MEKK: MAPK kinase kinase; MKK: MEKK kinase; PAK: p21-activated kinase; PAR6/3: polarity protein 6/3; PI-3/5 kinase: phosphatidylinositol 3/5-kinase; SRF: serum response factor; ROCK: Rho-associated coiled-coil containing protein kinase; WAVE/Scar: WASP-like verprolin-homologous/suppressor of cAMP receptor. Modified and extended from Bar-Sagi & Hall, 2000 and Ethell & Pasquale, 2005.

1.5 Rho GTPases in actin dynamics and membrane trafficking

The ability of neuronal and non-neuronal cells to form a variety of shapes and perform directed movement depends on coordinated arrays of dynamic protein fibers: the cytoskeleton. It also serves as tracks for intracellular trafficking and consists of three types of protein elements: actin, microtubules and intermediate filaments. Phagocytosis, cell adhesion and cell division involve actin cytoskeletal rearrangements (Jaffer *et al.*, 2001; Li 2007). Actin filaments are assembled by polymerization of actin monomers (G-actin) into

fiber-like filaments (F-actin) which polarize into a fast-growing plus end and a slow-growing minus end (Schmidt & Hall, 1998). Actin polymerization is mainly driven by the Arp2/3 complex that creates a branched network. It binds to the side of a pre-existing filament and initiates the formation of a new filament, which in turn branches out from the parent filament (Mullins *et al.*, 1997). Arp2/3 consists of seven subunits, including the actin-related proteins Arp2 and Arp3. For efficient nucleation, the complex alone is not sufficient and has to be stimulated by nucleation promoting factors, such as the Wiskott-Aldrich syndrome protein/WASP family verprolin homologous (WASP/WAVE also names Scar) family of Rho GTPase effectors. WASP and the ubiquitously expressed N-WASP have to be activated by Cdc42 first, until they can in turn trigger actin polymerization (Stradal *et al.*, 2004). Thus, pseudoactin dimer formation by Arp2 and Arp3 is facilitated to act as an actin nucleus, which in turn is the initiation site for nucleation (Goley *et al.*, 2004; Rodal *et al.*, 2005). Dimeric proteins, such as diaphanous (Dia1), dishevelled associated activator of morphogenesis (DAAM) and formin-related protein FRL nucleate unbranched filaments and primarily serve in actin filament elongation but also contribute to depolymerization (Faix *et al.*, 2006; Kovar 2006).

Actin remodeling is also required for cellular events of membrane trafficking, including endocytosis, exocytosis and intracellular transport via the secretory pathway (Lanzetti 2007). Local actin assembly participates in the pinching off of vesicles during endocytosis and the movement away from donor membrane through endosomal recycling events, e. g. the AMPA receptor recycling at the postsynaptic membrane. Endo- and exocytosis are indirectly stimulated via Cdc42 activation of neural (N)-WASP (Bader *et al.*, 2004; Gasman *et al.*, 2004). Furthermore, Cdc42 acts in Golgi to ER transport in an N-WASP dependent manner (Luna *et al.*, 2002). Lamaze *et al.* (1996) demonstrated that constitutively active RhoA and Rac1 mutants have been shown to inhibit clathrin-mediated endocytosis. In addition, other Rho GTPases like RhoD and RhoB localize to endosomes through recruitment of Dia1 and Dia2 splice variants, proposing a promoting effect on actin assembly on endosomes (Fernandez-Borja *et al.*, 2005). Actin coated endosomes enhance association of endosomal structures and compartments with the actin cytoskeleton to slow their dynamics. Recently, it was suggested that RhoB may contribute to the regulation of receptor tyrosine kinases because of its effect on vesicle trafficking and their downstream signaling cascades (Huang *et al.*, 2007).

Moreover, Cortactin, a protein associated with F-actin and the ProSAP/Shank family of scaffold proteins in the PSD, is also a direct binding partner of dynamin I. It was found to

colocalize with clathrin-coated pits and is suggested to be an important component of the receptor-mediated endocytosis (Cao *et al.*, 2003). The removal of glutamate receptors during long-term depression uses clathrin-mediated endocytosis that requires AP2 interactions and dynamin I (Lee *et al.*, 2002; Luscher *et al.*, 1999).

1.6 Nadrin and Rich1

Two representatives of GAPs involved in neuronal developmental processes are: the neuron-associated developmentally regulated protein (Nadrin) and the RhoGAP interacting with CIP4 homologues (Rich1).

Nadrin is the rat homologue of Rich1 in human which in turn is related to Rich2 (KIAA0672). RhoSAP is found to be the rat homologue of the human Rich2 gene.

Both molecules constitute a RhoGAP family of proteins. All of them contain a conserved RhoGAP domain that share a significant sequence homology. It is active for Cdc42 and Rac1 but not RhoA, except for Nadrin that has GTP hydrolysis activating effects on RhoA, too (Harada *et al.*, 2000; Richnau & Aspenström, 2001).

Despite the fact that Nadrin and Rich1 have a very high sequence similarity, their function differs in some respect. Nadrin was found to be a brain-specific protein of 104 kDa which reveals a developmentally regulated expression. Nadrin became detectable at the second postnatal week in the cerebral cortex and the hippocampus. Expression in the cerebellum and olfactory bulb became apparent at the third postnatal week (day 21). The protein could not be detected in glial cells, thus clearly indicating it is a neuron-specific molecule closely related to neuronal differentiation (Harada *et al.*, 2000).

Moreover, Harada *et al.* (2000) demonstrated that Nadrin enhances Ca^{2+} -dependent exocytosis at the neurite termini. This correlates with the suggested function to regulate cortical actin filament networks. Furthermore, the finding is underlayed by the fact that Nadrin colocalizes with synaptotagmin and actin filaments which have been proposed to play an important role in regulating exocytosis (Harada *et al.*, 2000; Trifaro *et al.*, 1993).

Additionally, Nadrin binds to the PDZ domain of the cortical scaffold protein EBP50 through its C-terminal STAL sequence (Reczek & Bretscher, 2001). The motif is conserved in one of the two found splice variants of Nadrin as well, implying a role in the reorganization of the cytoskeleton. Both alternative splice variants: N1 and N2 are characterized by the presence of an additional insert, located in the 5'-prime end corresponding to the C-terminus (Furuta *et al.*, 2002). The two splice variants are localized to the nucleus and show an accelerated nuclear translocation after growth factor stimulated

differentiation. Furuta *et al.* (2002) furthermore suggest that Nadrin's splice variants might act as effectors of additional Rho GTPases' signaling cascades. These pathways could be responsible for a cross-talk between the cytoskeleton and the nucleus.

In contrast to Nadrin, Rich1 is ubiquitously expressed and was found to localize to the Golgi complex but not with early endosomal compartments. It was proposed that the N-terminal BAR domain distorts membranes and liposomes into tubes due to the coiled-coil motif found within the BAR domain. In fact, the notion that Rich1 is facilitating tubulation activity is emphasized by the observation that it forms oligomers (Richnau *et al.*, 2004). Thus, the BAR domain points to an involvement of Rich1 in endocytic events and that it is associated with membranes. In addition, it was shown that one of four proline-rich motifs in the C-terminus is responsible for the interaction with endophilin's and amphiphysin's SH3 domain, two proteins playing a role in clathrin mediated endocytosis. This interaction, together with the aid of oligomerization caused by coiled-coil associations among the proteins' common N-terminal BAR domain, can be considered to promote membrane tubulation (Richnau *et al.*, 2004).

Wells *et al.* (2006) demonstrated that Rich1 is further responsible to maintain tight junctions' integrity (TJ) by interacting with Amot. Here Rich1 is targeted to a TJ protein complex comprising PDZ-domain containing MAGUK proteins: Pals1, Patj and Par3. Because it is known that Cdc42 participates in various cellular processes, including microtubule orientation, actin reorganization and protein trafficking, it was questioned whether Cdc42 regulates TJ maintenance, too. Cdc42 was probed indirectly to function at TJs by proteomic screening all RhoGEFs and RhoGAPs. As a result, Rich1 was identified to maintain TJs integrity through Cdc42 selective regulation (Wells *et al.*, 2006).

BAR domain

Cellular membranes are dynamic structures that can acquire a variety of shapes, thus defining the characteristic of the cell's morphology. Membrane curvature can be determined by several factors. These include extrinsic forces, such as the dynamics of cytoskeletal structures and intrinsic factors, such as the lipid composition or presence of integral membrane proteins with membrane deforming properties (Farsad & de Camilli, 2003). An additional class of bilayer bending and deforming elements is represented by cytosolic proteins transiently and/or reversibly associated with membranes. One class of these proteins with these properties are containing the Bin, amphiphysin, Rvs (BAR) domain (Itoh & de Camilli, 2006). Interestingly, Nadrin and RhoSAP can not only be

classified by their RhoGAP domain but also due to their N-terminal BAR domain. A large variety of BAR domain proteins have been implicated in membrane trafficking, actin cytoskeleton regulation and signaling. Many of such proteins comprise more functional domains, typically involved in these processes, such as SH3 domains, phosphoinositide binding domains and/or regulatory domains for small GTPases. Structurally, BAR domains were predicted to have a coiled-coil domain structure and have been shown to act as homo- and heterodimerization domain (Habermann, 2004).

One of the most thoroughly studied BAR proteins are the amphiphysins (I + II), mostly concentrated at the synapses except house-keeping splice variants are present ubiquitously (Lichte *et al.*, 1992; David *et al.*, 1996). But proteins such as amphiphysin, endophilin 1-3, IRSp53, Bin2, Nadrin, SH3BP1 and Oligophrenin-1, all belong to the N-BAR type of proteins, where a region located within the first 35 - 240 amino acids in the N-terminus displays highest conservation among these molecules (Peter *et al.*, 2004). Subsequent structural analysis revealed hydrophobic and hydrophilic properties, hence establishing an amphiphatic helical structure, also referred to as N-helix region. This structural motif is formed by three roughly anti-parallel helices, the BAR domain. By crystallographic studies, it could be shown that amphiphysin is a dimer, so that two α -helices, oriented oppositely and arranged at an angle, generate a banana shape representing the membrane's interface to allow well suited interaction with curved membranes (Peter *et al.*, 2004).

Thus, BAR domain proteins can also function as curvature sensors and mediate the assembly of protein scaffolds on bent membranes. The liposome tubulating activity of the N-BAR domain was very strong in the BAR domain without the N-helix (Farsad *et al.*, 2001). Taken together, these domains can act to target proteins to specific membranes and/or regulate their activity. As shown in table 1-2, BAR domains are present in the members of a wide variety of protein families (Zhang & Zehhof, 2002; Itoh & de Camilli, 2006).

Tab 1-3 BAR domain-containing proteins in vertebrates

Protein family	Members with BAR domains
Amphiphysin/bridging-integrator (BIN) family	Amphiphysin I Amphiphysin II splice variants: Amphiphysin IIa (brain) Amphiphysin II b (muscle) BIN1 BIN2 BIN3
Endophilin family	Endophilin A1 Endophilin A2 Endophilin A3

	Endophilin B1 Endophilin B2
RhoGAP family	Rich1/ Nadrin and splice variants Rich2 (KIAA0672)/ KIAA0672 3BP-1 Oligophrenin (GRAF2)
RhoGEF	Tuba
ArfGAP	Centaurin β 1 ASAP1/ Ddef1

Another domain with distant relation to BAR domains was identified by data base research based on primary sequences. It was renamed F-BAR due to its N-terminal Fes/Cip4 homology (FCH) domain that is closely followed by a coiled-coil domain and a C-terminal SH3 domain. Oppositely, F-BAR's secondary structure predictions suggest three α -helices, encompassing the FCH domain and downstream sequences, implying that the FCH domain is part of a larger BAR-like domain (Itoh *et al.*, 2005, Frost *et al.*, 2008). Hence the name F-BAR (FCH and BAR). Consistent with BAR domain functions, F-BAR induces massive membrane tubulation, primarily of the plasma membrane. However, the tubules produced by F-BAR domain are larger and appear less flexible than tubules formed by BAR domains (Itoh *et al.*, 2005). Members of the FCH family include CIP4, Toca family, srGAPs and MEGAP1 (mental retardation GTPase-activating protein, also named WAVE-associated RacGAP protein WRP) among other representatives. Like BAR domain proteins they all share the characteristic to have the same interacting partners, such as dynamin, synaptojanin and N-WASP via their SH3-domain (Itoh *et al.*, 2005). Still similarities between BAR and F-BAR domains remain to be assessed on a structural level.

Interestingly, the slit-roundabout (srGAPs) has been recently identified as being critically important in Slit-Robo signal transduction which controls neuronal migration. Slit increases srGAPs binding to Roundabout receptor1 (Robo1), a roundabout transmembrane receptor. In turn, the receptor inactivates Cdc42 as a consequence of srGAP's activity. Thereby neuronal migration can be inhibited (Wong *et al.*, 2001). Yang *et al.* (2006) suggested that the phenotype of 3p⁻ mental retardation syndrome is caused due to the loss of srGAP impairing neuronal migration and axonal connectivity. Moreover, it has been shown that mice expressing a Scar1/WAVE1 lacking the srGAP-binding sites have reduced spine density, abnormal synaptic plasticity and memory deficits (Sonderling *et al.*, 2007).

BAR and F-BAR proteins function as multifunctional adaptors by promoting the assembly of a protein complex at the membrane-cytosol interface. Their roles include the regulation

and coordination of actin dynamics at the membrane and membrane deformations underlying endocytosis, respectively. All kinds of endocytosis, including picocytosis and clathrin-mediated endocytosis are critically dependent on actin function (Engquist-Goldstein & Drubin, 2003). Latrunculin B, a drug that blocks actin polymerization, enhances the growth of BAR and F-BAR domain coated membrane tubules from the plasma, and this effect is reversible upon wash out of the drug (Itoh *et al.*, 2005). Some BAR and F-BAR proteins bind transmembrane proteins that are internalized via clathrin-mediated endocytosis. For example, the BAR protein endophilin binds the synaptic vesicle glutamate transporter v-Glut-1 and disintegrins (Vinatier *et al.*, 2006; Howard *et al.*, 1999). Often, recruitment of BAR and F-BAR proteins from the cytosol to membranes is controlled in time and space by small GTPases, as well as GAPs and GEFs in particular. In a feed-back mechanism, phosphoinositide metabolism is regulated by BAR proteins via binding to phosphoinositide enzymes, e.g. synaptojanin, and the nucleotide cycle of small GTPases (Behnia & Munro, 2005).

Another very interesting functional aspect that has to be further elucidated in the future is the question if membrane binding and GTPase binding of BAR domains takes place independently or associatively. It has been demonstrated that the concave face of the dimerized BAR domain of Arfaptin2 GTPase forms a binding site for Rac1, hence Arfaptin 2 modulates membrane ruffling (Ren *et al.*, 2006; Tarricone *et al.*, 2001).

Aim

The aim of this thesis work was to characterize RhoSAP as a binding partner of the PSD95 associated scaffold molecule ProSAP2/Shank3, in order to elucidate the function of this protein in small GTPase-mediated activities in the postsynapse of neurons.

RhoSAP was isolated from rat brain cDNA library as a binding partner of ProSAP2/Shank3 by a yeast two-hybrid screen using ProSAP2/Shank3's PDZ domain as bait. This work focuses on the basic molecular and protein biochemical characterization of this RhoGAP molecule, and its role in neuronal endocytic activities. Several hints were found that RhoSAP is linked to the F-actin cytoskeleton, suggesting an important function for RhoSAP to interconnect cytoskeletal dynamic events with endocytic turnover during dendritic development, elicited by synaptic input.

Due to the high evolutionary conservation of the synaptic proteins, the results obtained should be also applicable on non-rodents and humans.

2 Materials and Methods

2.1. Declaration of suppliers and basic recipes

2.1.1 Materials

Chemicals, reagents, antibiotics and standards:

Acrylamide (Roth, SERVA), Agarose (PeqLab), Ammonium sulphate (Merck), Ampicillin (Roth) APS (ammonium peroxisulphate, Sigma; Bio-Rad), Bradford Reagent (Bio-Rad), Bromophenol blue (SIGMA), BSA (PAA), Calcium chloride (SIGMA), Coomassie Brilliant Blue G-250 (Roth), DAPI (4,6-Diamidino-2-phenylindol, Invitrogen), Disodium hydrogen phosphate (Merck), DMSO (Dimethylsulfoxide, SIGMA), dNTP mix (Roche), DTT (1,4-dithiothreitol, Roth), EDTA (Ethylenediaminetetraacetic acid, AppliChem), Entellan[®] New (Merck), Ethanol (Fluka), Epon 812 (Fluka), First Strand buffer (5×) (Promega), GelCode[™] Blue Stain Reagent (Pierce), Gel-Dry[™] Drying Solution (Invitrogen), Glucose D-(+)- (Roth), Glutathione sepharose 4B (GE Healthcare), Glycerol anhydrous (Roth), Glycine for elektrophoresis (AppliChem), IPTG (Isopropyl-β-D-thiogalactoside, AppliChem), Kanamycine monosulfate (Roth), Magnesium chloride (Merck), 2-Mercaptoethylamine (SIGMA), Milk powder non-fat (Roth), MOLWOL[®] 4-88 (Calbiochem), Optifect[®] (Invitrogen), Page Ruler[™] prestained protein ladder (Fermentas), Peptone tryptone (Merck), Potassium chloride (AppliChem), Potassium dihydrogen phosphate (Merck), PolyFect[®] (Qiagen), Ponceau Red (SERVA), Protease inhibitor complete (Roche Applied Science), SDS (sodium dodecyl sulphate, Roth), Sodium acetate (Merck), Sodium azide (Merck), Sodium chloride (AppliChem), PCR SuperMix High Fidelity (Invitrogen) TEMED (N,N,N',N'-tetramethylethylenediamine, Fluka), Tris (tris-(hydroxymethyl)-aminomethane, usb corp.), Tween 20 (Roth), Yeast extract (Merck), 100 bp DNA Ladder (Invitrogen), 1 kb DNA ladder (Invitrogen)

Antibodies and enzymes:

Anti-Actin (Sigma), Anti-Bassoon (Assay Designs Stressgen), Anti-FLAG monoclonal antibody (Sigma), Anti-GST (BD Bioscience), Anti-MAP2 (Chemicon), Anti-PSD95 (ABR Affinity Reagents), Rabbit anti-guinea pig immunoglobulins (Ig) (DAKO), Rabbit anti-mouse Ig (DAKO), Anti-RhoA-P (biomol), Anti-RhoSAP (Pineda Antibody Service Berlin), Anti-Snapping I (Transduction Laboratories), Anti-Tubule (SIGMA), Swine anti-guinea pig Ig (DAKO), Encore (Invitrogen), SuperScript[™]II reverse transcriptase (Promega), XhoI (Invitrogen)

Fluorescent dye coupled antibodies, fluorescent dyes and detection reagents:

Anti-Fluor[®]488 goat anti-guinea pig Ig (H+L) (Invitrogen), Anti-Fluor[®]568 goat anti-guinea pig Ig (H+L) (Invitrogen), Anti-Fluor[®]647 goat-anti guinea pig Ig (H+L) (Invitrogen), Anti-Fluor[®]488 goat anti-mouse Ig (H+L) (Invitrogen), Anti-Fluor[®]568 goat anti-mouse Ig (H+L) (Invitrogen), Anti-Fluor[®]647 goat anti-mouse Ig (H+L) (Invitrogen), Anti-Fluor[®]488 goat anti-rabbit Ig (H+L) (Invitrogen), Anti-Fluor[®]568 goat anti-rabbit Ig (H+L) (Invitrogen), Anti-Fluor[®]647 goat anti-rabbit Ig (H+L) (Invitrogen), Biotinylated goat anti-rabbit antibody (Vector), DAPI (Invitrogen), FM[®] 4-64 (Invitrogen Molecular

ProbesTM), ECL plus western blotting detection reagent (GE Healthcare), VisualizerTM Spray & GlowTM ECL Western Blotting Detection System (Upstate)

Instruments and other materials:

Binocular (Schott), CellStar[®] Tissue Culture Flasks T25 (greiner bio-one), Cell Scrapers (greiner bio-one), Centrifuge Avanti CH-AVJ-25 (Thermo Fisher SCIENTIFIC), Chamber Slides (greiner bio-one), Charles River Rats (animal facility, Ulm University), Confocal Microscope Axioscope (Zeiss), Curix60 (Agfa), DNA Speed-Vac (Savant), EM10 transmission electron microscope (Zeiss), Falcon Centrifuge Tubes 15 and 50 mL (Becton Dickinson), Falcon Cell Scrapers (Becton Dickinson), Filtertips (Eppendorf), Fujifilm FLA-3000 Series (Fujifilm), Fuji Imaging Plate and BAS cassette (Fujifilm), Glass Beads (SIGMA), Heraeus Multifuge 3-SR (Thermo Fisher SCIENTIFIC), High Performance Chemiluminescence HyperTM-Film (GE Healthcare), Kodak Hyperfilm (Kodak), Liquid Scintillation Analyzer TRI-CARB 2200CA (Perkin Elmer), MIRAX Scanner (Zeiss), Multiscan RC (Labsystems), Petri Dish 100 mm (greiner bio-one), Sterile working bench (Heraeus LaminAir), Thermomixer comfort (Eppendorf), 24-well cell culture plates (greiner bio-one)

Kits:

Tab. 2-1 Overview of utilized kits

Application	Name	Supplier
Western blot signal detection	ECL Plus Western Blotting Detection Reagents	GE Healthcare Life Sciences
DNA purification	JETquick	GENOMED
	Gel Extraction Spin Kit 50	
	PCR purification kit 25	
	JETstar	
	Plasmid Midi Kit 50	QIAGEN
	QIAprep [®] Spin Miniprep Kit (50)	
	QIAquick [®] Gel Extraction Kit(25)	
	Nucleobond [®] PC500 EF	
RNA purification	QIAshredder TM (250)	Qiagen
	RNeasy [®] Mini Kit	Qiagen
Immunoprecipitation	μMACS GFP tagged Protein Isolation Kit	Miltenyi Biotech
Immunohistochemical staining	VECTASTAIN [®] ABC Kit	VECTOR Laboratories
Molecular cloning	TOPO TA Cloning [®] Kit	Invitrogen
Protein interaction	μMACS TM Epitope Tag Protein Isolation Kit	Miltenyi Biotech
Protein activity assay	RhoGAP Assay Biochem Kit	Cytoskeleton
Protein concentration measurement	BCA TM protein assay kit	Pierce

2.1.2 Recipes

Agar Plates: Luria Broth (LB) was melted in a microwave oven and cooled down to approx. 50°C. For Kan-plates and Amp-plates respectively, the particular antibiotics stock solution was added to a final concentration of 25-50 µg/mL and the agar was poured into plate dishes (approx. 20 mL/plate). Plates were stored at 4°C.

Ampicillin stock solution: Ampicillin was dissolved in distilled water (50 mg/mL), filter-sterilized (0.22 µm), aliquoted, and stored at -20°C.

Bromphenol Blue Solution: 4 mg of solid bromphenol blue were dissolved in 1 mL of sterile water.

Bromphenol Blue Gel Loading Buffer (6×): 0.25 g of bromophenol blue and 3 mL of glycerol were dissolved in 10 mL of deionized water. The solution was stored at room temperature (RT).

Coomassie Brilliant Blue Solution: 0.25 g of Coomassie Brilliant Blue R-250 was dissolved in 90 mL of a methanol/ water ration of 1:1 (v/v) and 10 mL glacial acetic acid. The solution was filtered through a Whatman filter to remove any superfluous particles and stored at RT.

Denhardt's Reagent (50×): 1 g of Ficoll 400, 1 g of Polyvinylpyrrolidone and 1 g of BSA were dissolved in 100 mL deionized water to be sterile filtered, aliquoted and stored at -20°C.

Blotting buffer (10×): 151.5 g of tris and 720 g of glycine were dissolved in deionized water and brought to a final volume of 4 L. To prepare 1× solution, 80 mL of blotting buffer (10×), 200 mL of methanol and 720 mL distilled water were mixed.

IPTG stock solution (1 M): 2.38 g of IPTG were dissolved in 10 mL of deionized water, filter-sterilized (0.22 µm), aliquoted, and stored at -20°C.

Kanamycin stock solution: Kanamycin was dissolved in distilled water (50 mg/mL), filter-sterilized, aliquoted, and stored at -20°C.

LB agar: 10 g of tryptone peptone, 5 g of yeast extract, 5 g of sodium chloride, and 16 g of bacto agar were dissolved in deionized water and brought to a final volume of 1 L to be autoclaved.

LB medium: 10 g of tryptone peptone, 5 g of yeast extract, and 5 g of sodium chloride were dissolved in deionized water and brought to a final volume of 1 L. The medium was autoclaved and stored at 4°C.

M9 minimal medium: 200 mL of M9 salts (5×), 2 mL of a 1M potassium chloride solution, 20 mL of a 20% glucose solution (w/v) and 0.1 mL of a 1 M calcium chloride stock solution were dissolved in 950 mL deionized water. After sterilization by autoclaving, the medium was stored at 4°C.

M9 salts (5×): 2.5 g of sodium chloride, 5 g of ammonium chloride, 15 g of potassium dihydrogen phosphate and 64 g of sodium hydrogen phosphate were solved together in a volume of 1 L deionized water. The solution was divided into 200 mL aliquots and autoclaved for 15 minutes at 15 psi (1.05 kg/ cm²) on liquid cycle. Salts were stored at RT.

Phosphate buffered Saline (PBS) (1×): 8 g sodium chloride, 0.2 g potassium chloride, 1.7 g disodium hydrogen phosphate, and 0.163 g potassium dihydrogen phosphate were dissolved in deionized water and brought to a final volume of 1 L. After adjustment of pH to 7.4 with HCl, saline was autoclaved and stored at RT.

PBS-T: PBS containing 0.1% (v/v) Tween[®] 20.

Sucrose (2 M): 410.76 g were diluted in a final volume of 600 mL deionized water.

SDS-loading buffer (2×): 1.2 mg bromphenol blue were dissolved in 12 mL of 10% SDS (w/v), 6 mL of glycerol, 1 mL of 1M Tris-HCl pH 6.8, and 10 mL of deionized water. Buffer was stored at RT.

SDS-PAGE buffer (5×): 15.1 g of tris base, 94 g of glycine, and 10 g of SDS were dissolved in deionized water and brought to a final volume of 1 L. The buffer was stored at RT.

SOC medium: 4 g of tryptone, 1 g of yeast extract, and 0.1 g of sodium chloride were dissolved in 150 mL deionized water. After addition of 2 mL 0.25 M potassium chloride and 2 mL of 1 M magnesium chloride, pH was adjusted to 7.0 and the solution was brought to a final volume of 200 mL. Medium was divided into 50 mL portions.

SSC (20×): 175.3 g of sodium chloride were dissolved with 88.2 g of sodium citrate in 800 mL deionized water. The pH of the solution was adjusted to 7.0 with high concentrated HCl. After adjusting the volume to 1 L, it was autoclaved, portioned into 500 mL aliquots and stored at RT.

TAE buffer (10×): 242 g of ultrapure Tris base were dissolved in 200 mL deionized water. 57.1 mL of absolute acetic acid and 37.2 g of EDTA sodium salt were added; the pH was adjusted to 8.3 until the volume was replenished to 1 L and stored at RT.

Tris buffered Saline (TBS): 8 g of sodium chloride, 0.2 g of potassium chloride, 3 g of Tris base were dissolved in 800 mL deionized water. After adjustment of the pH to 7.4 with HCl, distilled water was added to 1 L end volume.

TBS-T: TBS containing 0.1% (v/v) Tween[®] 20.

TE buffer pH 7.4: 12.2 g of tris base and 2.9 g of EDTA sodium salt were dissolved in 800 mL of distilled water. The solution was adjusted to pH 7.4. Distilled water was added to 1 L end volume.

Versen solution (0.05%): 8 g of sodium chloride, 0.2 g of potassium chloride, 2.57 g of disodium hydrogen phosphate, 0.2 g of potassium hydrogen phosphate and 0.5 g of EDTA sodium salt were dissolved in 1 L of deionized water to be autoclaved for sterilization.

X-gal solution: 2 g of X-gal (5-bromo-4-chloro-3-indolyl- β -D-galactopyranoside) were dissolved in 100 mL N,N-dimethylformamide and stored in the dark at -20°C.

2-YT medium: 16.6 g of tryptone, 10 g of yeast extract and 5 g of sodium chloride were dissolved in 900 mL of deionized water and adjusted to pH 7 with 5 N NaOH. The solution was stirred, filled up to a total volume of 1 L and autoclaved.

All recipes and following working protocols originate from “Molecular Cloning” by Sambrook & Russel, 5th ed. 2001. All solutions and reagents described in the following subparagraphs were prepared according to these instructions. Due to optimizations in laboratory practice, modified and adapted protocols can be found in some subparagraphs.

2.2 Molecular biological methods

2.2.1 DNA/RNA concentration measurement

For quantization of DNA and RNA, UV/Vis measurements were taken at wavelengths of 260 nm and 280 nm. The reading at 260 nm allows calculation of the concentration of nucleic acid in the sample. An OD₂₆₀ of 1 corresponds approximately to 50 µg/mL for double stranded DNA, 40 µg/mL for single-stranded DNA and RNA, and 20 mg/mL for oligonucleotides. The ratio between the reading at 260 nm and 280 nm (OD₂₆₀/OD₂₈₀) provides an evaluation of the purity of the nucleic acid. Pure DNA solutions have OD₂₆₀/OD₂₈₀ values of 1.8 and 2, respectively.

2.2.2 DNA preparation and purification

DNA was separated via agarose gel electrophoresis, using an appropriate percentage of agarose (0.8-1.8%) and voltage (80-100V), respectively. DNA was isolated from agarose gels and purified by applying Qiaquick Gel Extraction Kit. Ethanol precipitation was performed to concentrate DNA.

Agarose gel electrophoresis and DNA extraction: DNA solutions were mixed 1:5 with 6× Bromphenol Blue Gel Loading Buffer and loaded on an agarose gel, containing 20 ng/mL ethidium bromide. If not otherwise declared, DNA fragments and PCR products were analyzed on 1.2% (w/v) agarose gels, opened plasmid DNA on 0.8% (w/v) gels. Electrophoreses were performed at 80-100V.

Ethanol precipitation of DNA: After determination of the volume of the DNA solution, 2.5 volumes of ethanol and 0.1 volumes of 3 M sodium acetate pH 5.2 were added. DNA was precipitated for 30 minutes at -80°C or overnight at -20°C. After centrifugation for 15 minutes at 13000×g and 4°C in a tabletop centrifuge, the supernatant was discarded, and

the DNA containing pellet was dried by centrifugation in a speed-vac for not longer than 5 minutes.

2.2.3 Plasmid DNA isolation from *E.coli* cell cultures

Plasmid DNA was isolated from *E. coli* cultures and purified, using plasmid DNA preparation kits (GENOMED, MACHEREY-NAGEL, Qiagen). Depending on how much DNA was needed and the experimental intention (DNA sequencing, DNA restriction analysis), plasmid mini- or maxipreparations were performed.

Quick plasmid miniprep without ion-exchange columns: For fast plasmid preparation, a bacteria single clone colony from an ampicillin or kanamycin plate was inoculated in 3 mL LB medium containing 25-50 µg/mL of antibiotic. The culture was allowed to grow under constant agitation at 37°C and 200 rpm overnight. Bacteria were pelleted in 1.5 mL micro-centrifuge tubes at 13000×g for 1 minute. The supernatant was discarded to a volume of 100 µL, which served to resuspend the cells. After mixing the bacteria suspension with 200 µL lysis buffer, tubes were gently inverted and incubated at RT for 15 minutes. Thereby, the procaryotic cell wall is completely lized, except for the murein layer which is conserved. Next, 150 µL of ice-cold buffer 2 were added to the reaction tube, to be inverted and incubated on ice for 5 minutes. To segregate plasmids from cell lysate and genomic DNA, tubes were spun down for 6 minutes at 13000×g. Centrifuging the resulting supernatant under the same conditions again for 10 minutes, was followed by adding 500 µL of isopropanol for precipitation. The sample was then incubated at RT for 15 minutes. After pelleting and washing the DNA sediment with 70% (v/v) ethanol, the resulting DNA containing sediment was resolved in TE buffer containing 0.5 µg/µl RNase. DNA concentration was measured as described (2.2.1) and laid in a range of 0.1-0.3 µg/µL. Plasmid DNA was analyzed by restriction cleavage thereafter (2.2.6).

Tab. 2-2 Buffers for fast miniprep of plasmid DNA

Buffer	Composition	Supplier
Lysis buffer	1% (w/v) SDS 0.2M NaOH in TE	Roth Merck
Buffer 2	3M Potassium acetate 11.5% (w/v) Glacial acetic acid in a. bidest pH 4.8	Roth Merck

Plasmid miniprep: A single bacteria colony from an LB-agar plate was inoculated in 3-5 mL LB medium containing 25-50 µg/mL of antibiotic. The culture was allowed to

grow overnight at 37°C and 200 rpm. Bacteria were spun down either in 1.5 mL centrifuge tubes (2 fractions per sample) for 1 minute at 13000×g or in 30 mL beakers for 10 minutes at 3500×g. Supernatant was discarded, and plasmid DNA was isolated and purified using Diaper Spin Miniprep 250 Kit or GENOMED Mini Preparation Kit, especially if plasmids were specifically for sequence analysis. The procedure was carried out according to the protocols provided by the suppliers. Finally, DNA was eluted from the column, using 25-30 µL deionized water or 50 µL of 10 mM Tris buffer pH 8.5 and stored at -20°C. DNA concentrations of 0.1-0.6 µg/µL have been usually obtained (2.2.1).

Plasmid maxipreparations: A bacteria single clone colony from an LB-agar plate was inoculated in 12 mL of LB medium containing 50 µg/mL antibiotic. The culture was agitated with 200 rpm overnight at 37°C. Upon that, 250 mL of LB medium containing 250 µg/mL antibiotic were submitted to a 2 L flask that was then inoculated 1:20 with *E. coli* pre-cultured cells to grow for 16 hours at 37°C and 200 rpm agitation. Plasmid DNA was isolated and purified, using GENOMED Maxi Kit, according to the protocol provided by the supplier. Finally, DNA pellets were dissolved in 150-200 µL of TE buffer pH 7.4 or deionized water and were stored at -20°C. DNA concentrations of 0.5-2 µg/µL have been usually obtained (2.2.1).

2.2.4 RNA purification, generation of cDNA and PCR

Cytoplasmic total ribonucleic acid (RNA) consisting of rRNA, tRNA and to a lesser extent mRNA, was obtained from rat brain tissue. The isolation was performed following the instructions, according to the RNeasy® Mini Handbook provided by the supplier. The brain tissue was roughly homogenized in a first step by applying Qiashredder™ columns and utilizing RLT-buffer. By ethanol and guanidium salt treatment, RNA had been precipitated to be finally purified with ion-exchange columns. Volumes of 30-50 µL deionized water were used to elute RNA. Subsequently, concentrations varying from 0.05-0.1 µg/mL could be measured (2.2.1). RNA was then stored in a -70°C freezer.

This nucleic acid served as a base for reverse transcription (RT) reaction to generate cDNA, which itself served as template for polymerase chain reactions (PCR).

RT-reaction to generate cDNA and PCR: To accomplish first strand synthesis to generate cDNA from RNA molecules, 100 pmol of random hexamer primers were combined with 2.5 µg total RNA from brain tissue. The mixture was incubated at 70°C for

10 minutes on a thermoblock to denature all secondary structures of the RNA and, was thereafter shortly transferred on ice to prevent renaturation. Afterwards, 4 μ L of First Strand buffer (5 \times), 2 μ L of 0.1 M DTT and 4 μ L of a 10 mM mixture of deoxynucleotides were united altogether with the primed RNA to be incubated at 45°C for 2 minutes. Immediately, 1 μ L (10 U) of SuperScriptTMII reverse transcriptase (*E.C. 2.7.7.49*) was added and the reaction was continued for 1 hour at 45°C. Conclusively, DNA concentration was measured (2.2.1) and DNA was stored at -20°C.

To clone different RhoSAP C-terminal splice variants, the generated rat brain cDNA was amplified with a primer pair yielding to three distinct PCR products. The reaction consisted of three different steps. Primarily, the reaction started by augmenting the temperature to 96°C to denature the DNA. During the second step of the reaction, the temperature (T_A) was decreased to 55°C to facilitate the annealing of primers. The extension of primers through *Taq* and *Pfu* DNA polymerase (*E.C.2.7.7*) occurred at 72°C. Amplification of the C-terminal sequences of RhoSAP came to an extension speed of 1 kb per minute. The chosen primers were annealed at 5'- and 3'- direction of the template brain cDNA, respectively. PCR ran 34 cycles until reaction was stopped by cooling the mixtures down to 4°C. PCR products were detected as subbands on agarose gel and purified as described in paragraph 2.2.2.

Tab. 2-3 PCR array and primers

PCR device/Primers	Composition/DNA sequence 5'-3'	Supplier
dNTP mix (10 \times)	dATP dCTP dTTP dGTP	Roche
PCR array	22.5 μ l Super HiFi Mix 0.5 μ l sense Primer 0.5 ml antisense Primer	Invitrogen
RhoSAP S1426-1444 forward	CCAGACATGGACCCTGCTG	Thermo Fisher SCIENTIFIC
RhoSAP AS2085-2076 reverse	GTAGCTCAGTCCATAGGGTG	Thermo Fisher SCIENTIFIC

2.2.5 Generation of electrocompetent *E. coli* cells and transformation of plasmids

E. coli strains were commercially purchased and stored as stocks. All media were autoclaved prior to use.

DH5 α , XL-1 Blue and BL21 were taken from stocks and grown on a plain agar plate dish overnight at 37°C. 20 mL LB medium in a 50 mL flask were inoculated with fresh bacteria from the plate, and cell culture was allowed to grow overnight at 37°C and 200 rpm agitation. 4 \times 5 mL of this culture were transferred to 4 \times 200 mL 2-YT medium in 1 L flasks

and were agitated at 37°C and 200 rpm until OD₆₀₀ reached 0.5 (approx. 3 hours). Cell culture was divided into aliquots and transferred to 25 mL centrifuge tubes, which were pre-cooled on ice. Cells were centrifuged at 2500×g for 10 minutes at 4°C and supernatants were discarded. The following washing procedure was performed on ice. All four pellets were resuspended in 5 mL of deionized pre-cooled water, pooled and allocated to two 50 mL centrifuge tubes. The tubes were then filled up with cold deionized water to a volume of 20 mL. Bacteria were centrifuged at 2500×g for 10 minutes at 4°C and supernatants were discarded. The pellets were pooled again and the washing step was repeated once. Finally, the remaining pellet was resuspended in 5 mL pre-cooled 10% (v/v) glycerol and transferred to a fresh centrifuge tube that was then filled up to 20 mL volume with 10% (v/v) glycerol. Pelleting occurred at 3000×g for 10 minutes, the supernatant was discarded and the pellet was then resuspended in 1 mL of ice-cold 10% (v/v) glycerol. Thereafter, the suspension was aliquoted into 40 µL portions, pipetted into 1.5 mL micro-centrifuge tubes and shock frozen in liquid nitrogen. Aliquots were stored at -70°C.

Tab. 2-4 *E. coli* strains

Bacterial Strain	Strain's Genotype	Supplier
DH5α	supE44, U169 (φ80 lacZ ΔM15), hsdR17, recA1, endA1, gyr A46, thi-1 relA1	NEB
XL-1 Blue	supE44 hsdR17, recA1 endA1 gyr A46 thi relA1 lac ⁻ , F' [porAB ⁺ lacI ^q lacZ ΔM15 Tn10 (tet ^r)]	NEB
BL21	F ⁻ ompT hsdS _B (r ⁻ _B m ⁻ _B) gal dcm	Invitrogen

The transformation efficiency was tested by transforming plasmid DNA. Therefore, 25-50 ng of pUC19 DNA were mixed with 40 µL of freshly thawed electrocompetent cells and stored on ice for 1 minute in a 2 mm electro cuvette. After electroporation with 2.5 kV, the cuvette was immediately rinsed out with 350 µL of prewarmed SOC medium. The cell culture was agitated for 30 minutes at 37°C in an overhead room shaker. To titer transformed bacteria, 100 µL and 10 µL of the culture, respectively, were plated on agar plates containing the particular selective antibiotic and allowed to grow overnight at 37°C.

2.2.6 TOPO cloning and restriction analysis

RhoSAP splice variants were cloned as purified PCR products into TOPO-TA vector system for further analysis by DNA sequencing (2.2.7). Cloning into pCR[®]2.1 was

performed according to the protocol provided by the supplier. 1 μ L of ligation product was transformed into electrocompetent *E. coli* DH5 α cells (2.2.5).

The analysis of TOPO vectors derived from *E. coli* DH5 α ligation transformants was performed by restriction. 1-2 μ g of DNA were diluted in 18 μ L of deionized water with 2 μ L restriction buffer (10 \times) and 1-2 U of *Eco RI* restriction enzyme (*E.C. 3.1.11_{XX}-3.1.31_{XX}*). The mixture was incubated at 37°C for 1 hour. In order to inactivate the enzyme, the restriction reaction was heated up to 65°C for 20 minutes. DNA fragments were purified (2.2.2) and analyzed by sequencing (2.2.6).

2.2.7 DNA sequencing

DNA sequencing was performed by MWG Biotech. 1 μ g DNA diluted in 20 μ L distilled water was delivered to MWG as standard amount for sequencing analysis.

Tab. 2-5 Sequencing primers

Oligonucleotide	Sequence 5'-3'	Supplier
M13 Forward Primer	CTGGCCGTCGTTTTAC	MWG Biotech
M13 Reverse Primer	CAGGAAACAGCTATGAC	
GAL4 BD GAL4 AD	ATACCACTACAATGGAT	MWG Biotech
pACT	ATACCACTACAAGGAT	Thermo Fisher SCIENTIFIC

2.2.8 Northern blotting

BDTM Multiple Tissue Expression (MTN) Array was used to measure the relative abundance of RhoSAP transcripts in different tissues. The rat MTNTM Array is a positively charged nylon membrane with immobilized poly A⁺ RNAs from heart, brain, spleen, lung, liver, skeletal muscle, kidney and testis tissue (approx. 2 μ g per lane).

A 755 bp cDNA probe amplified from the RhoSAP C-terminus was purified on a 1.2% (w/v) agarose gel and extracted with QIAGEN Gel Extraction Kit.

According to the supplier's user manual, the hybridization was performed as described by Feinberg & Vogelstein, 1983.

Preparation of [α^{32} P]dCTP radiolabeled cDNA probes: 20 ng of cDNA were diluted in 45 μ L TE buffer and shortly denatured by heating at 95°C for 5 minutes in a boiling water bath. The DNA was placed on ice for 5 minutes to cool down. A subsequent brief centrifugation was carried out before adding the denatured DNA to the Rediprime II Random Prime Labeling reaction tube. To generate radioactive labeled DNA, 5 μ L corresponding to 50 μ Ci of Redivue [α^{32} P]dCTP were added to random hexanucleotides to

prime DNA synthesis on the RhoSAP DNA probe. 5'P → 3'-OH directed DNA synthesis is triggered because of the presence of Klenow I fragment (*EC* 2.7.7.7).

Thoroughly pipetting the mixture changes the colour of the solution to purple when the pellet has been completely dissolved. The labeling reaction was incubated at 37°C for 10 minutes at room temperature. 5 µL of 0.2 M EDTA were added to stop the reaction. Afterwards the radiolabeled cDNA probe was again denatured by heating to 95°C for 5 minutes and chilled quickly on ice for 5 minutes. Finally, the radiolabeled probes were purified by centrifugation on Bio-Spin® Tris columns at 1000×g for 4 minutes to remove all unincorporated nucleotides.

To check the efficiency of the Rediprime II Random Prime Labelling system β-actin cDNA was used as control.

Tab. 2-6 Radiolabeling devices

Material	Composition	Supplier
Amersham Rediprime II Random Prime Labelling reaction system	dATP, dGTP, dTTP Exonuclease Free Klenow Enzyme, Random Primers	GE Healthcare
Redivue [$\alpha^{32}\text{P}$]dCTP	50 µCi (3000 Ci/mmol)	GE Healthcare
Bio-Spin®30 Tris Columns	P-30 Polyacrylamide Gel Matrix 10 mM Tris-HCl, pH 7.4	BIO RAD

In preparation for the prehybridization of the MTNTM Array, 15 mL of BD Express Hyb Solution were first prewarmed to 60°C and mixed with 1.5 mg of denatured salmon testes DNA. For incubation of the MTNTM Array, 10 mL were placed in a closed hybridization container. Prehybridization took place at 65°C for 30 minutes in a hybridization oven under continuous agitation.

Hybridization of [$\alpha^{32}\text{P}$]dCTP radiolabeled cDNA probes: 14 µL radiolabeled cDNA probe equaling 20 ng were mixed with 30 µL COT human DNA (interspersed repetitive sequences), 14 µL salmon testes DNA, 50 µL 20×SSC to a total volume of 200 µL and heated at 95°C for 5 minutes and then again at 68°C for 30 minutes. This prepared mixture was added to the remaining 5 mL of prehybridized ExpressHybTM Solution.

The prehybridization solution incubated with the MTE Array was poured out and replaced by the freshly prepared hybridization solution containing the radiolabeled cDNA probe. Bands were already obtained after 1 hour of hybridization under continuous agitation at 65°C. For higher specificity, the blot was incubated in hybridization solution for up to 6 hours.

To complete hybridization, 200 mL of wash solution 1, substituted for the previously discarded hybridization solution, were applied to rinse the blot. Washing took place repetitively for 20 minutes at 65°C under continuous agitation conditions. Finally, wash solution 2 was incubated with the MTNTM Array for 40 minutes under constant shaking at 50°C. The solution was removed and the blot was sealed in plastic wrap.

The northern blot was exposed to X-ray films overnight. Alternatively, the blot was scanned densitometrically by a Fuji IP Reader.

Tab. 2-7 Northern blot material and rinse buffers

Material	Composition	Supplier
Rat MTN TM multiple tissue expression array		BD Biosciences Clontech
ExpressHyb TM hybridization solution	25 mL	BD Biosciences Clontech
Human β -actin cDNA control probe	100 ng	BD Biosciences Clontech
COT human DNA	1 mg/mL	Roche
DNA from salmon testes	11 mg/mL	SIGMA
Wash solution 1	2 \times SSC 1% (w/v) SDS Submitted to DEPC treatment.	Roth
Wash solution 2	0.1 \times SSC 0.5% (w/v) SDS Submitted to DEPC treatment.	Roth

2.2.9 *in situ* Hybridization

In situ hybridization was accomplished under highly stringent conditions to obtain information about the expression of RhoSAP transcripts (mRNA) in rat brain tissue. For investigating possible putative RhoSAP splice variants, oligonucleotides were specially designed to detect possible splice variants of RhoSAP.

Tab. 2-8 DNA-Oligo probes in HPLC pure quality for *in situ* hybridization

Oligonucleotide	Sequence 5' - 3'	Supplier
RhoSAP	TGAGCTTCTTGTGTGTGCTGTGGGACACCTGTTT	Operon
Nadrin	CAGGAAAGATGTTTCGAAGTGATTCAGAAACCCTAGA	Operon
3BP-1	CAGGGGCTTTGGCAGCTCCCGGAGATAGGACTTGA	Operon
A	CTTTGGATTTTCCTAAGGCCATCCTTTTTGTAAAAC	Thermo Fisher SCIENTIFIC
B	AGTTCCTTGCTTTTAGACACACCATCCTTTTTGTGA	Thermo Fisher SCIENTIFIC
C	ACAAGATCTGTAGACATGCTTTCCCCGGCGACAT	Thermo Fisher SCIENTIFIC
D	TCACACAGTAGACATGCTTTCCCCGGCGACAT	Thermo Fisher SCIENTIFIC

16/22	TGGGGACTGGCGCCGGTCAGCAGGGTCCATGTC	MWG Biotech
20.2	CTTACCTGTAGACATGCTTTCCCCCGG	MWG Biotech

Tissue sections were prepared from rat brains at different stages of development. The time-line comprised stages from day 1 (1d), 3d, 7d, 14d, 21d to the adult age. The brain tissues were first frozen, cryo-sliced with 8 μm of thickness and then unfixed frozen on Super Frost Plus slides. Sections were stored at -70°C .

Preparation of $[\gamma^{35}\text{S}]\text{dATP}$ radiolabeled oligonucleotides DNA probes: Oligonucleotides DNA (Oligo-DNA) were diluted to a concentration of 40 ng/ μL . Subsequently, 1 μL of 10 \times terminal transferase buffer, 1 μL of an Oligo-DNA probe and 2 μL aqua bidest were mixed together with 4.5 μL $[\gamma^{35}\text{S}]$ dATP and 1.5 μL of terminal deoxynucleotidyl transferase (TdT, *EC 2.7.7.31*) corresponding to 50 units/ μL were added in the end to a volume of 10 μL . TdT catalyzes the incorporation of deoxynucleotides onto the 3'-OH terminus of DNA. Single-stranded DNA and double-stranded DNA with sticky ends will tail most efficiently.

The heterogeneous mixture was incubated at 37°C for 4 hours in a thermo block. To finish the reaction, 2 μL of 0.5 M EDTA were added to stop the reaction. Then the solution was briefly centrifuged at $4000\times g$ for 1 minute: the mixture was filled up to 48 μL with distilled water. Additionally, 2 μL of a 5 M DTT solution were put in and the reaction was mixed gently again. To purify the radiolabeled nucleic acids, Bio-Spin[®]30 Tris columns were applied according to the manufacturer's instructions.

Tab. 2-9 Components for the radiolabeling reaction

Material	Composition	Supplier
$[\gamma^{35}\text{S}]\text{dATP}$ o. $[\gamma^{35}\text{S}]\text{ATP}\gamma\text{S}$	50 μCi (3000 Ci/mmol)	GE Healthcare
Terminal deoxynucleotidyl transferase <i>FPLCpure</i>	20.900 units/mL	GE Healthcare
10 \times One-Phor-All PLUS terminal transferase buffer	dATP, dCTP, dGTP, dTTP 100 mM Tris Acetate 100 mM Magnesium Acetate 500 mM Potassium Acetate	GE Healthcare Roth Merck Merck
Bio-Spin [®] 30 tris columns	P-30 Polyacrylamide Gel Matrix 10 mM Tris-HCl, pH 7.4	BIO RAD

Hybridization of $[\gamma^{35}\text{S}]\text{dATP}$ radiolabeled Oligo-DNA probes: For *in situ* hybridization of different radiolabeled oligonucleotide probes, humid chambers containing slides with cryo-fixed brain slices were prepared.

Standardly, 50 μL radiolabeled Oligo-DNA were mixed with 300 μL hybridization cocktail, 30 μL salmon testes DNA and 15 μL tRNA. Before mixing all these components together, the DNA components alone were submitted to a denaturation step at 80°C in a water bath for 5 minutes. After chilling the DNAs on ice and centrifuging, the DNA components were ready to use in the hybridization reaction. To enable specific hybridization of the probe to mRNA target sides, excessive amounts of unlabeled competitor nucleic acids (tRNA, salmon testes DNA) were annealed rapidly to unspecific sides in the sample. Thereby specific probe sequences remain single-stranded and thus can properly hybridize to their targets.

After preparation of the Oligo-cocktail mix, an amount of 60 μL was put on each slice that was covered carefully with another slice. Sections were then incubated in humid chambers at 42°C overnight. Subsequently, slices were rinsed 6-fold in cuvettes filled with 1×SSC containing 0.1% (v/v) mercaptoethanol at 55°C for 15 minutes.

As soon as the slides had been cooled down to RT, a second wash step followed by rinsing in 3 changes of 1×SSC to complete the removal of unbound oligonucleotides. For fixation, slides underwent a treatment in 50% (v/v), 70% (v/v), 96% (v/v) and absolute ethanol for some seconds and dried on air for some minutes.

As beta emitters, ^{35}S -isotopes have less emission energy and show longer half-life that is around 87 days. Therefore, exposition of Kodak™ Hyperfilms took about 3 weeks. Radiographs were developed by AGFA Curix60.

Tab. 2-10 Materials for *in situ* hybridization

Material	Composition	Supplier
Hybridization cocktail	5% (w/v) Dextran sulphate 5× Denhardt's reagent 6× SSC 200 mM PBS pH 7.4 50% (v/v) Formamide 1% (w/v) N-Lauroyl-Sarcosine 100 $\mu\text{g/mL}$ Salmon Testes DNA 1 $\mu\text{g/mL}$ tRNA	Fluka SIGMA SIGMA SIGMA
DNA from salmon testes	11 mg/mL	SIGMA
tRNA	10.1 mg/mL	SIGMA

2.2.10 Yeast two-hybrid screen

To identify protein-protein interaction *in vivo*, a yeast two-hybrid screen (Fields & Song, 1989) also referred to as “interaction trap” was conducted. In particular, interacting proteins of ProSAP2/Shank3-PDZ and RhoSAP C-terminus were to be discovered in intact cells. This procedure detecting direct protein-protein interactions on the genetic level

surrounds the disadvantages of biochemical detection of protein associations, *ie.* affinity chromatography. In that method, stringent washing steps disturb the outcome for reasonable results, especially for protein interactions with high dissociation rates.

In contrast, the genetic yeast two-hybrid screen is based upon the biologic effect of the eukaryotic transcription factor GAL4. It originates from *S. cerevisiae* and consists of two functional domains. One DNA-binding domain interacts with the upstream activating sequence (UAS) of the DNA and enables the positioning of the transcription factor to a promoter. The second domain triggers transcription by recruiting and activating the basal transcription machinery. Therefore, this domain is also referred to as activator domain. To evidence basal transcription, the system requires *lacZ* as reporter gene that can be identified by the GAL4 activator domain.

Expressing both domains separately in yeast cells does not result in transcription. The situation changes as soon as both modules are fused with two more protein domains X and Y. That means two hybrid proteins might reconstitute GAL4. Fundamentally, this indirect coupling of binding and activator domain is a necessary prerequisite for the complete function of GAL4. Thus, gene expression of *lacZ* depends on the interaction of these two additional protein domains X and Y although they are not involved in transcription itself. The fusion protein comprising of protein X together with the GAL4 binding domain is used as bait to “catch” unknown interaction partners from a rat brain tissue cDNA library containing possible interacting proteins as coding cDNA.

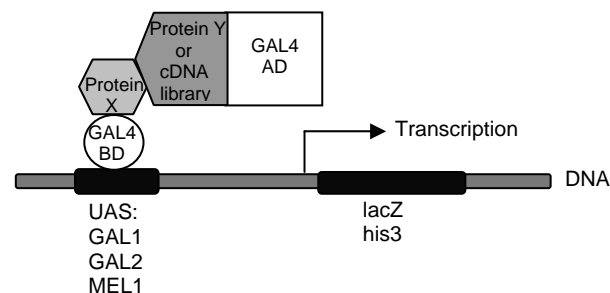


Fig. 2-1 Principle of the yeast two-hybrid system. If the bait and prey proteins bind, then the AD and BD of the GAL-4 transcription factor are indirectly connected, bringing the AD in proximity to the transcription start site (UAS) so that transcription of reporter genes: *lacZ* and *his3* occur.

In this yeast two-hybrid study the cDNA of ProSAP2/Shank3 PDZ domain and RhoSAP C-terminus were integrated into pAS2.1 vector as baits next to the additional coding sequence for the GAL4 binding domain. Before starting the yeast two-hybrid screen, the plasmid itself had to be examined by X-gal filter assay for self-transcriptional activity. To prevent the induction of unspecific transcription of the reporter gene, screens were only performed with small functional domains of the bait protein.

The other part of the system, the rat brain tissue cDNA library is cloned into the pACT2 vector. Thereby possible protein interaction candidates are fused to the GAL4 activator domain. To master the problem of keeping right reading frames after insertion of cDNA-libraries into a prey vector coding for the fused hybrid protein of Y and GAL4s activator domain, an especially representative library had to be generated in order to secure a plural presence of every DNA sequence in a statistical right reading frame.

Tab. 2-11 Yeast two-hybrid plasmids used in the screen

Yeast vector	Description	Supplier
pAS2.1	The pAS2.1 vector expresses proteins fused to the GAL4 DNA-BD. In yeast, proteins are expressed in high levels from constitutive ADH1 and T7 promoter. For selection in <i>E. coli</i> the vector carries a Kan ^r resistance. <i>Trp1</i> is the nutritional marker for selection in yeast.	Clontech
pACT2	pACT2 generates a fusion of the GAL4 AD and a protein encoded by a cDNA in a fusion library cloned into the MCS in the correct orientation and reading frame. The protein is targeted to the yeast nucleus by the nuclear localization sequence from SV40 T-antigen. pACT2 is a shuttle vector which replicates autonomously in both <i>E. coli</i> and <i>S. cerevisiae</i> and contains Amp ^r resistance in <i>E. coli</i> . <i>Leu2</i> as nutritional gene allows auxotroph yeasts to grow on limiting synthetic media.	Clontech

Culturing, generation of competent yeast and transformation of yeast: The yeast two-hybrid screen was performed using two different yeast host strains. Y187 was utilized to maintain transformed pAS2.1 bait vector and could be selected by its auxotrophic marker, the *trp* gene. Expression of the bait plasmid in Y187 resulted in the production of tryptophan, an amino acid that is absent in Y187 due to the deleted *trp* gene. Through complementation, Y187 can be selected on tryptophan supplement deficient SD (SD/-Trp) agar.

The same principle can be adapted for AH109. In this case, the strain lacks a gene for an enzyme, essential for leucine synthesis. Transforming pACT2 into AH109 yeast complements the missing *leu* gene so that this strain can survive on SD/-leu agar.

Tab. 2-12 Yeast strains

Strain	Reporter gene	auxotrophic marker	Reference
Y187	<i>lacZ</i>	<i>trp1</i> <i>leu2</i>	Clontech
AH109	<i>his3</i> <i>ade2</i> <i>lacZ</i>	<i>trp1</i> <i>leu2</i> <i>his3</i>	Clontech

Two different media: YPD and SD were used to cultivate yeast. YPD medium is suitable for yeast strain maintenance and long-term storage. Transformed yeast strains had to be stored in the appropriate SD dropout medium to keep selective pressure on the plasmid. Cultivation of yeast was performed at 30°C in a time scale of four to seven days on YPDA agar plates in an incubator.

Standardly, pure and transformed yeast strains were maintained as glycerol stocks. As a routine 500 µL of cultured yeast cells in YPD medium or appropriate SD dropout medium were resuspended in a 1.5 mL microcentrifuge tube, vortexed vigorously and the same volume of 50% (v/v) glycerol was added to the dispersed cells to a final concentration of 25%.

For preparation of competent yeast cells, 20-50 mL of YPD medium were inoculated with Y187 or AH109 from glycerol stocks stored at -70°C. After incubating the yeast cells overnight at 30°C, 100 mL YPD medium were inoculated with the prepared yeast to an OD₆₀₀ of 0.4 and agitated for approximately 3 hours until the culture reached an OD₆₀₀ of 0.8. Subsequently, yeast was aliquoted and centrifuged for 3 min at 4°C and 2500×g. Initially, the pellet had been resuspended in 5 mL ice-cold deionized water and was filled up to 25 mL. After repeating this wash step twice, the pellet was dissolved in 600 µL deionized water kept the cells competent for nearly 4 days at 4°C.

For plasmid transformation, 60 µL of competent Y187 yeast cells were mixed with 1 µg plasmid DNA, pulsed at 2.5 kV and spilled out with 300 µL of YPD medium. Transformed yeast cells were incubated on a shaker at 30°C and 200 rpm for at least 2 hours. Finally, 100 µL of transformed yeast were plated on the appropriate SD agar.

Tab. 2-13 Media and supplements

Material	Composition	Supplier
Yeast peptone dextrose medium (YPD)	50g/L YPD Autoclave at 121°C for 15 min only.	Q-BIOgene (101 Biosystems)

Synthetic dropout medium (SD)/ and SD agar	43.7 g/L DOB	Q-BIOgene (101 Biosystems)
	+ SD-leu (0.69 g/L)	Q-BIOgene (101 Biosystems)
	+ SD -trp (0.74 g/L)	Q-BIOgene (101 Biosystems)
	+ SD -trp/leu (0.64 g/L)	Q-BIOgene (101 Biosystems)
	+ SD -trp/leu/his (0.62 g/L)	Q-BIOgene (101 Biosystems)
	for screening plates further add	
	+ 0.1 g/L AHS	SIGMA
	+10-15 mg/L Kanamycin	

Autoclave at 121°C for 15 min.

Yeast two-hybrid interaction screen: To conduct the interaction screen, 15 mL SD/-trp medium of prepared Y178 cells transformed with the bait were filled up to 70 mL of SD/-trp medium. The yeast was shaken at 30°C and 200 rpm for at least 24 hours. As soon as the cells had reached a growth of $OD_{600} < 1$, cells were pelleted at $2500\times g$ for 5 minutes and aliquoted into two distinct 50 mL centrifuge tubes. Every pellet was resuspended in 25 mL YPD medium and one aliquot of AH109 pre-transformed with rat brain cDNA was added per tube. The tubes' content was transferred each into 2 L flasks, which already contained 25 mL fresh YPD medium, equaling 50 mL end-volume. The mating approach was shaken with 40 rpm for 24 hours at 30°C on an oscillating incubator.

Thereafter cells were harvested by centrifugation at $1000\times g$ for 10 minutes, resuspended in 20 mL YPD medium and united to a total volume of 40 mL. An amount of 300 μ L of the mated yeast culture was pipetted and distributed on 50 SD/-trp/-leu/-his agar plates of 145 mm size to be incubated at 30°C for 7 days. Generally, first colonies appeared after 4 days of incubation.

To ensure that well-separated colonies were obtained and to provide controls for transformation efficiency, 100 μ L of a 1:1000, 1:100 and 1:10 dilution were also spread on 96 mm SD/-trp/-leu/-his agar plates. To calculate the cotransformation efficiency, the growing colonies (cfu) on dilution plates had to be counted. The cotransformation efficiency could be substantiated by the following equation and should equal more than 10^6 cfu/ μ g:

$$\frac{cfu \times tsv(\mu l)}{vp(\mu l) \times df \times DNA(\mu g)} = cfu / \mu g \text{ DNA}$$

where:

cfu = colony forming unit (counted colonies)
 tsv = total suspension volume
 vp = volume plated
 df = dilution factor

Statistically, on every plate one colony should grow at least. Consequently, 50 colonies could be transferred on master plates. Before restreaking the largest grown colonies again,

a first β -galactosidase assay was performed to verify true interactions and exclude false positive clones from the screening plates. Therefore, the colony-lift filter assay as a means to measure β -galactosidase activity served to screen large numbers of cotransformants. Hence, colonies that survived the *his3* growth selection during the GAL4 two-hybrid library screening could be detected by their blue color occurring after β -galactosidase reaction. Thus, GAL4 was reconstituted functionally to allow LacZ transcription.

As a control, the assay was also used to test the interaction between two known proteins. In this case ProSAP2/Shank3-PDZ and RhoSAP C-terminus as baits were validated to interact with prey proteins from the cDNA library by repeating the determined interactions in a mini-scale mating by simultaneous transformation with pAS2.1 as bait and pACT2 as prey. To confirm the interactions found by yeast two-hybrid screens, a colony-lift filter assay and/or liquid β -galactosidase assay was conducted respectively.

Colony-lift filter assay (β -Galactosidase assay): For each plate of transformants to be assayed, a Whatman filter of 96-145 mm diameter was pre-soaked in 1.5-4 mL of Z buffer/X-gal solution in a clean plate. Then a clean dry filter was placed on the surface of the plate of colonies. The filter was carefully set with a forceps onto the colonies to facilitate their adhesion to the Whatman filter. When the filter has been evenly wetted, it was carefully lifted off the agar plate and transferred to a thermal box filled with liquid nitrogen. The filters were completely submerged for 10 seconds. After the filter had been frozen completely, it was removed from nitrogen and thawed at room temperature again. Freezing and thawing the colonies helped to permeabilize the cells.

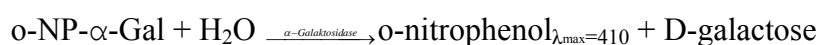
Subsequently, the filters were carefully placed, with colonies side up, on the pre-soaked filter and incubated at 30°C for at least 30 minutes but no longer than 8 hours. Appearance of blue colonies producing β -galactosidase was checked periodically.

Liquid β -galactosidase assay with ONPG as substrate: 5 mL of an overnight culture from a single yeast colony was incubated in SD/-trp/-leu medium at 30°C and 200 rpm. Thereafter, 2 mL of the prepared culture were united with 8 mL YPD medium. Under the same incubation conditions as the overnight culture, yeast was cultivated for 3-5 hours until growth yielded an OD₆₀₀ 0.5-0.8.

Then cell culture was vortexed thoroughly to disperse cell clumps and triple portioned as 1.5 mL aliquots into three micro centrifuge tubes that were centrifuged at 13000×g for 30 seconds. After removing the supernatants, 1.5 mL of Z buffer were added to each pellet

and resuspended until the pellet completely disappeared. Cells were centrifuged again and supernatants were discarded. Each pellet was then resuspended in 300 μL of Z buffer. Thus, the pellet has been concentrated 5-fold before 0.1 mL of the cell suspension were transferred to a fresh microcentrifuge tube and placed in liquid nitrogen for 1 min to freeze cells. The frozen tubes were placed in a 37°C water bath for 1 min to thaw cells. After freezing and thawing had been repeated twice to ensure the cells did break open, blank tubes set up with 100 μL Z buffer were prepared for the assay control reaction.

Subsequently, 0.7 mL of Z buffer supplemented with 0.27% (v/v) of β -mercaptoethanol were added to the reaction tubes and the blank control. Immediately, 160 μL of ONPG solution were added to the reaction and blank control. Tubes were placed in a 30°C incubator and timer could be started to record the kinetics of the following reaction:



After the yellow color developed as result of the β -galactosidase activity, 0.4 mL of 1 M Na_2CO_3 was added to the reaction and blank tube for termination. Elapsed time was recorded in minutes. Time needed to develop the typical yellow color varies from 3 minutes to 24 hours for weaker interactions.

Reaction tubes were centrifuged for 10 minutes at 13000 \times g to pellet cell debris. As any debris impurities interfere with the accuracy of the test, the supernatants were carefully transferred to the clean cuvette. The OD_{420} was measured for the samples relative to the blank control and should lie between 0.2 and 1.0 to be within the linear range of the assay. β -galactosidase units can be calculated by the following definition:

$$\beta\text{-galactosidase units} = 1000 \times \text{OD}_{420} / (t \times V \times \text{OD}_{600})$$

where: t = elapsed time (in min) of incubation

V = 0.1 mL \times concentration factor

$\text{OD}_{600} = A_{260}$ of 1 mL of culture

One unit of β -galactosidase is defined as the amount that hydrolyzes 1 μmol of ONPG to o-nitrophenol and D-galactose per minute per cell.

Tab. 2-14 Reagents and materials required for colony-lift filter assay and liquid β -galactosidase assay

Reagent/Material	Composition	Supplier
Z buffer	16.1 g/L $\text{Na}_2\text{HPO}_4 \times 7\text{H}_2\text{O}$	Merck
	5.5 g/L $\text{NaH}_2\text{PO}_4 \times \text{H}_2\text{O}$	Merck
	0.75 g/L KCl	AppliChem
	0.246 g/L $\text{MgSO}_4 \times 7\text{H}_2\text{O}$	Merck

Z buffer/X-gal solution	100 mL Z buffer 0.27% (v/v) β -mercaptoethanol 1.67% (v/v) X-gal	Fluka
Liquid nitrogen		mti
Whatman filter	125 mm diameter 70 mm diameter	Whatman Schleicher&Schuell
ONPG solution (o-nitrophenyl β -D-galactopyranoside)	4 mg/mL in Z buffer pH 7.0 Solution should be prepared freshly.	Fluka

Isolation of yeast plasmids: To further analyze the prey proteins, their corresponding pACT vectors had to be isolated from yeast colonies. Therefore, a large yeast colony was inoculated from the master plate into 5 mL of YPD medium and incubated at 30°C overnight. The next day, yeast cells were pelleted in fresh 2 mL centrifuge tubes to be resuspended in 200 μ L of yeast lysis solution and chloroform. To completely crack the yeast cell walls, a volume of glass beads corresponding to 50 μ L was added. The resuspension was then vortexed vigorously for 5 minutes. Afterwards cellular debris was harvested by centrifugation at 14000 \times g for 5 minutes. The supernatant was transferred to a proper 1.5 mL microcentrifuge tube and plasmid DNA was precipitated by adding 40 μ L of 3 M sodium acetate pH 5.2 and 1 mL of absolute ethanol. The mixture was incubated at -70°C for 1 hour.

Thereafter, precipitates were centrifuged at 14000 \times g for 10 minutes before pellets could be washed with 500 μ L of 70% (v/v) ethanol. To conclude, pellets were dried in a speed-vac and DNA was redissolved in 30 μ L deionized water.

To obtain a large quantity of plasmids with sufficient purity, as needed for sequencing and restriction enzyme digestion, *E. coli* XL-1 Blue cells were transformed with plasmid DNA isolated from yeast (2.2.5). Bacterial cells were selected by plating transformants on ampicillin containing LB agar for incubation at 37°C overnight.

Tab. 2-15 Yeast lysis solution

Material	Composition	Supplier
Yeast lysis solution	2% (v/v) Triton X-100	Roth
	1% (w/v) SDS	Roth
	100 mM NaCl	AppliChem
	10 mM Tris-HCl (pH 8,0)	usb
	1 mM EDTA	AppliChem

Restriction analysis and sequencing of pACT2 plasmids: Plasmid DNA was isolated (2.2.3) from five *E. coli* colonies and analyzed for each prey vector. DNA was cleaved by *Eco*RI and *Xho*I (2.2.6) to detect all positive prey vectors coding for new interaction

partners. According to the restriction pattern, clones could be selected for sequence analysis to identify the corresponding protein interaction partner for ProSAP2/Shank3-PDZ and RhoSAP C-terminus.

2.3 Protein biochemical methods

2.3.1 Protein concentration measurement

Routinely, protein concentrations were measured spectroscopically at a wavelength of 280 nm. In highly diluted protein solutions, amounts of 5-20 µg of protein could be detected. The absorbance was mainly based on the existence of aromatic amino acids: tryptophan and tyrosine and to a lesser extent on phenylalanine. If the measured protein solutions were not heavily impured by nucleic acids, the absorbance relation $A_{280}/A_{260} < 0.6$ of the protein solution indicates the purity of the solution. In general, spectroscopical methods have the disadvantage of being too insensitive and require highly pure protein concentrations. Colorimetric methods evade these problems partially.

Bradford assay: Protein concentrations were measured using Coomassie Brilliant Blue (CBB) dyes that bind to non-polar, hydrophobic side chains of the protein by complex formation. The most essential interaction is assumed to take place between arginine residues of the protein and the complex dye that might help to stabilize the colouring substance as anionic sulfonate structures.

Bradford reagent (CBB G-250) was prepared by diluting 1:5 in deionized water. 20 µL of the tissue or cell lysate were added to 980 µL of diluted Bradford reagent. The absorbance was measured at 595 nm in an UV/Vis spectrometer as soon as complexation occurred and the reagent's color changed from violet to blue. For every particular measurement, a BSA standard curve spanning a range from 0.25 mg/mL - 1.5 mg/mL was drawn up in lysis buffer. This colorimetric array was applied for measurement of protein lysate samples deriving from GST- and GFP protein purifications.

BCA assay: Protein concentration was measured by BCATM Protein Assay Kit according to instructions, provided by the supplier. The assay was based on bicinchoninic acid (BCA) for the colorimetric detection and quantification of total protein. It combined the reduction of Cu^{+2} to Cu^{+} by proteins in an alkaline medium with selective colorimetric detection of the cuprous cation. The purple- colored reaction product of this assay was formed by the chelation of two molecules of BCA with one cuprous ion. This complex exhibited strong

absorbance at 562 nm. However, the method had no genuine end-point reaction, so that the final color continued to develop but at a very slow rate. Therefore, many samples were assayed at the same time. Relative protein concentrations in a working range from 20-2000 µg per mL were measured. BSA standard curves were laid down for each of the tested sample.

Amido Black 10B assay: To determine protein amounts in tissue or cell lysates, Amido Black 10B as a complexation diazo dye was utilized to fix concentrations in samples already diluted in 2×SDS loading buffer (Chapdelaine *et al.*, 2001).

Basically, 10 µL of each sample, prepared in loading buffer, were put on a nitrocellulose membrane, immersed in staining solution for 10 minutes on an orbital shaker. Then it was treated in destaining solution as long as nitrocellulose foil showed no background. After membranes had drought on air, 1 mL dissolving solution was added to each sample under the extractor hood and probes were incubated at 50°C in a water bath for 30 minutes. The resulting green coloured solution was transferred from the microcentrifuge tube to a 96 well plate. Measuring was performed at 620 nm in an ELISA reader. As reference, different BSA concentrations were measured at 620 nm to be referred to the protein samples' absorbance.

Tab. 2-16 Amido Black 10B staining and destaining solutions

Solutions	Composition	Supplier
Amido Black staining solution	0.5% (w/v) Amido Black 10B 45% (v/v) Methanol 10% (v/v) Glacial Acetic Acid	SIGMA VWR International AppliChem
Destaining solution	47.5% (v/v) Methanol 5% (v/v) Glacial Acetic Acid	VWR International AppliChem
Dissolving solution	80% (v/v) Formic Acid 10% (v/v) Acetic Acid 10% (w/v) Trichloric Acetic Acid	Merck Fluka Merck
Nitrocellulose filter strips	150 mm × 150 mm	Satorius

2.3.2 Preparation of GST-tagged fusion protein from *E. coli* cell culture

To isolate overexpressed GST-RhoSAP-GAP from *E. coli* BL21, the GAP domain of RhoSAP was extracted from protein lysate and furthermore purified by glutathione sepharose affinity chromatography. This procedure was essential to perform the GAP activity assay in order to test the domain's functional specificity (2.3.7).

Preparation of protein lysate: Simultaneously, 4 flasks each containing 300 mL of prewarmed M9 minimal medium containing 500 µg/mL ampicillin were inoculated with 5 mL of pre-cultivated transformed *E. coli* cells. The cultures were allowed to grow for 2-3 hours at 37°C and constant agitation of 200 rpm, until an OD₆₀₀ of 0.4-0.6 was reached. Then, the culture was stimulated with IPTG to an end concentration of 1 mM for 2 hours. Cells were pelleted at 4°C for 15 minutes and 3500×g. After sedimenting the *E. coli* cells, pellets were frozen at -20°C and resuspended in 6 mL ice-cold PBS per pellet. Then lysozyme was added to an end-concentration of 1 mM and the suspensions were kept on ice for 40 minutes to allow the lysis of bacterial cell walls. Thereafter, 5 mL of 0.2% (v/v) Triton X-100 were mixed with each suspension to promote further delipidation of cellular membranes. Furthermore, DNase and RNase solution were added to an end concentration of 5 µg/mL to assure degradation of genomic DNA and cellular RNA. The viscous homogenate was agitated over-head for 10 minutes at 4°C on an orbital shaker. The lysate was centrifuged at 3000×g for 30 minutes and the filtered supernatant (0.45 µm) incubated overnight with pre-washed glutathione sepharose and additional 1 mM DTT, according to the supplier's protocol. Next, an empty plastic column was loaded with the fusion protein coupled to glutathione sepharose and washed twice with 20 mL of 5 mM Tris-HCl pH 8 and thereafter, washing was continued up to 10 times with 2 mL at 4°C. Elution was carried out with 300 µL of 50 mM glutathione and 50 mM Tris-HCl pH 8. Ten fractions were collected and protein concentration measured using glutathione buffer as reference (2.3.1).

2.3.3 Preparation of tissue and organ lysates

All lysed organs and tissues were taken from rats that had been killed by a CO₂ overdose. After organs had been isolated, 10 mL/g of 1×RIPA buffer supplemented with protease inhibitors (Roche Applied Sciences) were added. Organs were homogenized in a Teflon douncer with strokes at 900 rpm and pelleted at 1000×g for 10 minutes. The homogenization to obtain a crude sediment was repeated at least once depending upon the organ. Subsequently, lysates were incubated on an orbital shaker for at least 2 hours or overnight to allow proteins to be extracted. Protein measurements of the lysate samples were performed as described in 2.3.1.

2.3.4 Subcellular fractionation of PSDs by differential centrifugation

For an understanding of the role of PSD proteins at a synapse the proteomic characterization of these structures was required, and this depends on the isolation of a pure fraction (Cotman *et al.*, 1974; Carlin *et al.*, 1980).

PSDs are morphological distinctive entities with special cytochemical properties. To save the majority of biochemical characteristics, the preparation was undertaken using Triton X-100. Thereby, isolated PSDs resembled the most intact *in situ* state (Carlin *et al.*, 1980).

The whole isolation of subcellular brain fractions was performed on ice to stabilize proteins and maintain *in situ* conditions. Three rat brains were removed, shortly rinsed in buffer A and kept on ice. Homogenization was performed thereafter, using 12 up and down strokes with 900 rpm in a Teflon douncer. 10 mL of buffer A per gram of brain weight were applied in each homogenization step. After washing, re-homogenizing and pelleting the homogenates twice the supernatants were combined and pelleted at 12000×g (J-25 rotor) for 15 minutes to obtain crude membrane fraction (P2) which served as the source for the preparation of the PSDs.

This material was resuspended in buffer A again, homogenized by 6 strokes to be finally pelleted at 12000×g for 20 minutes. After resolubilization (Teflon douncer) of the resulting pellets in 1.5 mL per gram of weight in buffer B, the resulting solution was applied to four step gradients of 0.85M-1M-1.2 M sucrose. For the SW28 rotor, each layer comprised a volume of 9.3 mL. By centrifugation at 85000×g (SW28 rotor) for 2 hours, synaptosomes could be harvested at the 1 M-1.2 M sucrose gradient's interface, seen as cloudy bands and were thereafter subjected to osmotic shock. From the same gradient, a myelin membrane fraction was obtained from the top of the 0.8 M sucrose layer and a mitochondrial fraction was isolated as the pellet.

The osmotic shock was induced for further extraction of synaptic junctional complexes. The received synaptosomal material was stirred on ice for 30 minutes after dilution in 5 volumes of 1 mM Tris-HCl pH 8.1 and centrifuged at 33000×g for 30 minutes. To further enrich the received synaptosomal pellets, they were resuspended in 5 mM Tris-HCl pH 8.1 to be fractionated by differential centrifugation again. 2.5 mL of resuspended synaptosomes were resolved on gradients of 0.85M-1M-1.2M sucrose and were then centrifuged at 85000×g for 2 hours. Following the harvest of the synaptosomes layer at the 1 M-1.2 M sucrose interface, synaptic junctions (interphase) were solved in 6 mL/g in buffer B and C to separate soluble postsynaptic and presynaptic proteins from the postsynaptic proteome anchored tightly to the membrane. Delipidation of the interphase

fraction took place by stirring the solution on ice for 15 minutes to finally sediment unpurified PSDs (PSD I fraction) by centrifugation at $33000\times g$ for 30 minutes. To assure a separation of remaining lipids, proteins and integral membrane components not tightly bound to the postsynaptic membrane, a second Triton extraction step was carried out repeating the buffer B and C treatment as described above. The PSD II fraction was pelleted through centrifugation at $33000\times g$ for 30 minutes. To receive normal PSDs, the pellets were united and collected in 1 mL of distilled water, centrifuged at $14000\times g$ and solved in 500 μ L distilled water again. They were stored at -70°C or in liquid nitrogen.

To exclude remaining lipids optimally, a discontinuous sucrose gradient designed for the SW 41 rotor was applied. The gradients consisted of three layers of 1 M-1.5 M-2 M sucrose, each of 3.5 mL volume. The PSD II fraction was then ultracentrifuged at $200000\times g$ overnight to yield highest purification. Next day PSDs were harvested as weak cloudy banding at the 1.5 M-2 M sucrose interface. The harvested layer amounted to a volume of approx. 1 mL. Thereafter, the collected material was diluted in 10 mL distilled water, resuspended, pelleted at $200000\times g$ for 2 hours and rediluted in 200-500 μ L of distilled water (Super PSD fraction). Storage proceeded in a -70°C freezer.

To clarify the abundance and the enrichment of proteins, a sample of each fraction was investigated by Western blot analysis (2.3.4).

Tab. 2-17 Materials of the PSD preparation

Material	Composition/Rotor	Supplier
Buffer A	0.32 M Sucrose 5 mM HEPES pH 7.4 PI	Roth SIGMA Roche
Buffer B	0.32 M Sucrose 5 mM Tris pH 8.1	Roth usb corp.
Buffer C	0.32 M Sucrose 12 mM Tris pH 8.1 1% (v/v) Triton	Roth usb corp.
Tris-HCl solution	1 mM Tris pH 8.1	usb corp.
Tris-HCl solution	5 mM Tris pH 8.1	usb corp.
Sucrose/ Tris-HCl gradients	<u>Solutions had an final volume of 200 mL.</u> <i>0.85 M</i> (85 mL 2M Sucrose, 2 mL 0.5 M Tris-HCl) <i>1 M</i> (100 mL 2M Sucrose, 2 mL 0.5 M Tris-HCl) <i>1.2 M</i> (120 mL 2M Sucrose, 2 mL 0.5 M Tris-HCl)	usb corp.

<u>Solutions had an end volume of 50 mL.</u> 1.5 M (37.5 mL 2M Sucrose, 0.5 mL 0.5 M Tris-HCl) 2 M (49.5 mL 2M Sucrose, 0.5 mL 0.5 M Tris-HCl)		
Beckman Avanti centrifuge	Rotor J-25 v _{Max} = 25000 rpm/75 600×g	Thermo Fisher SCIENTIFIC
Beckman ultracentrifuge L8-55M	Rotor SW 28 (v _{Max} = 28000 rpm/141000g) Rotor SW 41 v _{Max} = 41000 rpm/288000g	Thermo Fisher SCIENTIFIC

2.3.5 SDS-PAGE, SDS gel staining and Western blotting

To detect and verify proteins from cell and tissue lysates, PSD fractions and coimmunoprecipitations were separated by polyacrylamide gel electrophoresis (PAGE) and subsequently analyzed by Western blotting. SDS is a strong anionic detergent, which strongly binds to hydrophobic areas in the protein, hence, it denatures the proteins structure. SDS treatment induces negatively charges all side residues of a protein. As a result, protein-SDS complexes completely migrate to the anode. In an electrical field amino acid composition as well as the isoelectrical point of the proteins are of no significance to mobility. The pace itself, with which the charged protein is running through an electrical field, is determined by its mobility depending upon its size and the electrical field strength. Furthermore the pH and ionic strength of the buffer medium influence the charged mobility of the proteins.

SDS-PAGE: Gel electrophoresis was performed at 100 V for 3 hours (7.5 cm × 10 cm × 1 mm), respectively, in SDS PAGE buffer. Samples were dissolved at a 1:1 proportion with SDS-loading buffer containing DTT to completely reduce proteins by breaking their disulfide bonds completely. Heated at 95°C for 5 minutes to destroy all secondary-tertiary protein structures, 2-20 µL of each denatured sample were loaded on a 8% (v/v), 10% (v/v) or 12% (v/v) acrylamide gel depending on the size of the protein to be analyzed.

Tab. 2-18 Component volumes (mL) per gel volume of 10 mL solutions for SDS-PAGE gels

Polycrylamide end concentration	Composition	Supplier
10% SDS gel	30% (v/v) Acrylamide	3.3 mL SERVA, Roth
	1.5 M Tris pH 8.8	2.5 mL usb corp.
	10% (w/v) SDS	0.1 mL Roth
	10% (w/v) APS	0.1 mL Bio Rad
	0.04% (v/v) TEMED	0.004 mL Merck
	deionized water	4 mL

12% SDS gel	40% (v/v)	Acrylamide	4 mL	SERVA, Roth
	1.5 M	Tris pH 8.8	2.5 mL	usb corp.
	10% (w/v)	SDS	0.1 mL	Roth
	10% (w/v)	APS	0.1 mL	Bio Rad
	0.04% (w/v)	TEMED	0.004 mL	Merck
	deionized water		3.3 mL	
5% SDS stacking gel	30% (v/v)	Acrylamide	3.3 mL	SERVA, Roth
	1 M	Tris pH 8.8	2.5 mL	usb corp.
	10% (w/v)	SDS	0.1 mL	Roth
	10% (w/v)	APS	0.1 mL	Bio Rad
	0.04% (w/v)	TEMED	0.004 mL	Merck
	deionized water		4 mL	

Coomassie Blue R-250 staining of SDS-gels: Gels were stained with Coomassie staining solution for 1 hour at room temperature on an orbital shaker and subsequently the colour was rinsed out for 2×45 minutes in 30% (v/v) methanol and 10% (v/v) glacial acetic acid. Alternatively, GelCode[®] Blue Stain Reagent solution was utilized in order to avoid several changes of destaining solutions. In this procedure, the gel was shortly swirled in distilled water, agitated in GelCode[®] staining solution for 1 hour and washed for another hour in distilled water. Thereupon, gels were fixed in Gel-Dry[™] solution.

Silver staining of SDS-gels: To detect small amounts of protein in the micro-range from 1-10 µg, gels were silver stained (Heukeshoven & Dernick, 1988). First, gels were fixed 2×20 minutes in an 1:2 acetic acid and ethanol mixture on an orbital shaker to be incubated in potassium sulfide oxide twice for 1-4 hours or overnight. Then gels had to be washed by shaking 5×30 minutes in distilled water to be stained then with silver nitrate for another 30 minutes. Continuously, the proceeding with the developing reaction for 5 minutes was undertaken by incubating in sodium formaldehyde. To finalize the silver staining, gels were washed 2×10 minutes and the whole reaction was conclusively stopped by shaking the gel in 2% (v/v) glacial acetic acid, supplemented with 5% (w/v) Tris for 15 minutes on an orbital shaker. Gels were dried with Gel Dry Blotting[™] Drying solution to be shrink-wrapped in foil. Therefore, gels were shortly rinsed in deionized water, agitated in Gel-Dry[™] solution for 1 hour and finally shaken in deionized water for another 1 hour on an orbital tumbler to eliminate all excess solution.

Tab. 2-19 SDS gel staining solutions and equipment

Material	Composition	Supplier
Fixation solution	15% (v/v) Glacial Acetic Acid	AppliChem
	30% (v/v) Ethanol	VWR International
Incubation solution	30% (v/v) Ethanol	SIGMA
	0.4 M Potassium Acetate	Merck
	0.2-0.4% (w/v) Na ₂ S ₂ O ₃ ×5H ₂ O	SIGMA

	pH 6 with acetic acid	
Staining solution	2.5% (w/v) AgNO ₃	Merck
	0.01% (w/v) Formaldehyde	Merck
Developing solution	0.001% (w/v) Na ₂ S ₂ O ₃ ×5H ₂ O	Bio-Rad
	2.5% (w/v) Na ₂ CO ₃	Merck
	0.01% (w/v) Formaldehyde	Merck

Western blot and protein detection: The gel, nitrocellulose membrane and Whatman filter papers were prepared for blotting by soaking shortly in electroblotting buffer. The following packing order in blot-apparatus was used: 2 Whatman filter papers, nitrocellulose membrane, SDS gel and again 2 Whatman filter papers were packed from cathode to anode. Transfers of proteins were carried out at 100 V for 90 minutes (5.5 mA/cm²) in electroblotting buffer in a tank blot apparatus. To examine the quality of protein transfer, the membrane was stained with Ponceau Red to visualize all protein bands. The following incubations occurred on an orbital shaker, when not otherwise stated.

After washing the membrane in deionized water, blocking of non-specific binding sites was performed by immersing the membrane in 5% (w/v) non-fat dried milk in TBS-T or PBS-T for 1 hour at 4°C. The membrane was rinsed briefly with 2 changes of TBS-T. For binding of the primary antibody, dilutions in a range from 1:1000 to 1:10000 in PBS-T were used, and the membrane was incubated overnight at 4°C. After binding, the membrane was rinsed, incubated for 15 minutes and subsequently 2×10 minutes washed with fresh changes of PBS-T. To detect the primary antibody, routinely the secondary horse radish peroxidase (HRP)-conjugated antibody was diluted 1:1000 in PBS-T and the membrane was incubated for 1 hour at room temperature. After precipitation, the membrane was rinsed, incubated for 10 minutes and washed twice for 5 minutes with fresh changes of PBS-T.

Visualization of proteins was performed on HyperfilmTM ECL film with an ECL Plus Western blotting detection kit, according to the experimental protocol provided by the supplier.

HRP catalyzes the oxidation of the Lumigen PS-3 Acridan substrate. The amount of intermediates relates to the basic level of detected protein recognized through the secondary HRP-conjugated antibody.

These acridinium intermediates again react with peroxide under slight alkaline conditions to produce a sustained chemiluminescence that is then detected by autoradiography. The maximum emission wavelength is 503 nm (green light) and can be already detected

visually in the dark when huge amounts of protein had been transferred to the membrane previously. Different exposure times were tested.

Alternatively, VisualizerTM ECL detection spray was utilized to trigger the same chemiluminescence reaction as described previously.

2.3.6 IgG purification of polyclonal antisera by (NH₄)SO₄ precipitation or protein A

Precipitation is one of the eldest methods to purify proteins. It is non-protein specific, except for the precipitation of IgMs and IgGs by antigens, *e.g.* protein A or G. It is standardly used to remove protein impurities from heterogeneous antiserum mixtures.

Ammonium sulfate precipitation: To separate the major non-specific proteins and other disturbing components from RhoSAP antiserum to yield optimal immune reactions, *e.g.* Western blots or coimmunoprecipitations, 2 mL of RhoSAP antiserum was centrifuged at 500×g for 10 minutes to take off cells. The supernatant was recentrifuged at 10000×g for 10 minutes at 4°C to remove the remaining debris. An equal volume of saturated ammonium sulfate was added slowly drop by drop to the solution while the mixture was gently stirred on ice for 1 hour. After sedimenting the solution at 10000×g for 10 minutes at 4°C, the supernatant was discarded and the pellet was then resuspended in 1.5 mL starting buffer. This material was dialyzed against two changes of starting buffer, each of 2 L volume. The dialysate content was then centrifuged at 10000×g for 10 minutes to pellet any remaining debris.

Western blots (2.3.4) probed with brain homogenate were used to detect RhoSAP by using differentially diluted antiserum concentrations in a range from 1:1000 to 1:6000.

Purification on protein A-agarose: Protein A is a bacterial cell wall constituent that specifically binds to the F_c parts of certain classes of Immunoglobulins (Igs) from various species. It has a very high affinity to rabbit IgM, IgA, IgD and most subclasses of IgGs. In contrast, protein G that is also a bacterial cell wall component shows lower affinity for rat IgGs but is high affine to mouse IgGs.

A column, filled with 2 mL volume of protein A-agarose was pre-equilibrated with 2×2 mL starting buffer. RhoSAP rabbit antiserum was clarified by centrifugation (4°C) at 10000×g for 10 minutes. 200 µL of 1 M Tris-HCl pH 8 were added to the supernatant to adjust the pH of the crude antibody solution to pH 7.5. After the sample had been slowly passed through the protein A-agarose column, it was washed 6×2.5 ml with starting buffer.

The same procedure was repeated using washing buffer 2 until no protein could be measured UV-spectroscopically ($A_{280\text{nm}}$) in the effluent. To elute Igs, 500 μL of elution buffer were applied to the column and 12 fractions of eluate were collected in tubes containing 100 μL of neutralization buffer. Fractions were mixed gently and kept on ice. By measuring the fractions at 280 nm, the IgG-containing fractions were identified, relating 1 $A_{280\text{nm}}$ unit were equivalent to 0.8 mg of IgG protein per mL. Conclusively, 2 mL of purified protein A-agarose were dialyzed against 2 L of PBS. Different dilutions of RhoSAP antiserum were subsequently examined by Western blot analysis (2.3.4).

Tab. 2-20 IgG purification buffer and column matrix

Material	Composition	Supplier
Starting buffer	100 mM Tris-HCl pH 8 PI	usb corp. Roche
Washing buffer	10 mM Tris-HCl pH 8 PI	usb corp Roche
Elution buffer	100 mM Glycine pH 3 PI	usb corp Roche
Neutralization buffer	1 M Tris-HCl pH 8 PI	usb corp. Roche
Protein A-agarose	Recombinant protein A was covalently coupled to 6% (w/v) cross-linked agarose at a concentration of 3 mg/mL.	Roche

2.3.7 Coimmunoprecipitation and pull-down assays to analyse possible protein interactions

To verify interactions between RhoSAP and proteins found through the yeast two-hybrid screen, coimmunoprecipitations and pull-down studies were undertaken. Both assays were performed using the μMACS MicroBead Kit according to the suppliers' protocol. A suspension of super-paramagnetic MicroBeads were conjugated to anti-GFP tagged specific antibodies that were already provided by the supplier. Unloaded MicroBeads were conjugated to anti-RhoSAP as well as to the interaction partners antibodies. The magnetically-labeled proteins are retained on a μ Column placed in the magnetic field of a μMACS Separator.

For coimmunoprecipitations, brain lysate (2.3.2) was loaded onto the μ Column to allow interaction of specific brain proteins with the protein of interest, cross-linked to the μ Columns matrix by its magnetically tagged antibody. For pull-down investigations of interactions between two proteins, exclusively, Heal cell lysate which contained the overexpressed GFP interaction candidate was applied to the μ Columns, to allow direct

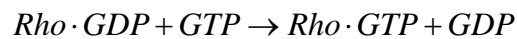
interaction with the particular protein of interest coupled to the matrix via anti-GFP μ MACS.

Eluates were analyzed by SDS-PAGE and Western blot analysis (2.3.4) to investigate the binding behavior with the defined interaction partner. Thus, it was possible to suggest if proteins were part of an interaction complex.

2.3.8 GAP activity assay

The small GTPases are molecular switches, which control cellular processes such as cytoskeletal reorganization, axonal guidance, vesicle trafficking, gene expression and cell motility. The balance of the GTP to GDP bound state underlies the switch mechanism as they turn from an activated GTP form to an inactive state that is the GDP form. The balance of GTP to GDP bound states is controlled by catalytic proteins that either increase the rate of exchange of GDP to GTP (GEFs), decrease the GTPase activity GTPase activating proteins (GAPs), or prevent the exchange of GDP (GDIs).

The rate-limiting step in the exchange reaction is the nucleotide off rate, and the reaction:



is, therefore, pseudo first-order. GAPs stimulate the intrinsic GTPase nucleotide exchange rate of small GTPases to act as downstream regulators for representatives of the Ras superfamily that are Rho, Rac and Cdc42.

The best-studied GAPs that have been proved so far to have GAP activity are p50RhoGAP, p120RasGAP, and p190RasGAP. However, the majority of assumed GAP proteins have been implicated by homology to contain GAP activity. Because of this circumstance, RhoSAP's RhoGAP domain was tested for genuine GAP activity by measurement of intrinsic nucleotide exchange and GTP hydrolysis rate (Self & Hall, 1995).

In this array, RhoSAP's purified RhoGAP domain was applied as GST fusion protein. Cdc42, Rac1 and RhoA were the selected small G-protein candidates to be tested for their ability of inducing downstream RhoGAP activity. p50RhoGAP recombinant His-tagged protein served as positive control.

Preloading the small GTPase: 0.1 μ g of recombinant His-tagged small G-protein was first incubated in a total volume of 20 μ L preloading buffer containing 10 μ Ci [γ - 32 GTP]-GTP in a water bath for 10 minutes at 30°C. To stop the reaction, 5 μ L of a 0.1 M potassium chloride solution were added to a final concentration of 17 mM and the mixture

was placed on ice. In this way, the GTPase was loaded with radiolabeled guanosine triphosphate.

GTPase activity assay: 3 μL of the preloaded protein to give a final concentration of 6 nM was diluted with reaction buffer to a final volume of 30 μL . The reaction buffer contained an excess of freshly added unlabeled GTP corresponding to an end concentration of 10 mM.

For GAP-stimulated GTPase assays, an aliquot of 0.5 μL equaling 0.1 μg of RhoSAP-GAP-GST protein with a final concentration of 0.3 $\mu\text{g}/\mu\text{L}$ was added at this stage to the reaction. In general, equimolar amounts of small G-proteins and the GAP proteins (p50RhoGAP-His and RhoSAP-RhoGAP-GST) were used. Incubation continued at 30°C. A 5 μL sample was removed immediately (time zero) and then after 3, 6, 9 and 12 minutes to be diluted into 1 mL of cold buffer that finished the reaction. All samples were subsequently filtered through prewetted 25 mm nitrocellulose filters. The filters were washed three times with 3 mL of cold reaction buffer and air-dried. Measuring the amount of radioactive nucleotide remaining on the small G-protein was determined by scintillation counting. Therefore, the filter's relative radioactivity resulting from the bound [γ - ^{32}GTP]-GTP was recorded as cpm and the time zero number for each array was set as reference. Cpm numbers corresponding to the other time points could be calculated relatively as GTP remaining in per cent (%) when related to time zero. To evaluate data for each array, GTP hydrolysis was measured for Cdc42, Rac1 and RhoA activity reaction without supplementing p50RhoGAP-His and RhoSAP-RhoGAP-GST, respectively, as negative control. To minimize deviations, every measurement was repeated three times.

Tab. 2-21 Used materials and reagents for the GAP activity assay

Material	Composition	Supplier
small GTPases: Cdc42, Rac1 and RhoA	small GTPases delivered as 100 μg purified His tagged proteins lyophilized. Reconstitution to 250 μM in 20 μL equal 5 mg/mL. Storage at -70°C	Cytoskeleton
p50 Rho-GAP	small GTPases delivered as 50 μg purified His tagged proteins lyophilized. Reconstitution to 170 μM in 10 μL equal 5 mg/mL. Storage at -70°C	Cytoskeleton
GTP stock	100 mM GTP in 100 μL deionized water	Cytoskeleton

[γ - ³² GTP]-GTP	250 μ Ci 6000 Ci/mmol	GE Healthcare
Preloading buffer	20 mM Tris-HCl pH 7.5 25 mM NaCl 5 mM EDTA 0.1 mM DTT	usb corp.
Reaction buffer	20 mM Tris-HCl pH7.5 0.1 mM DTT 0.87 mg/ml BSA 1 mM nonradioactive GTP, freshly added due to instability of GTP in solutions	usb corp. Roth PAA
Stop buffer	50 mM Tris-HCl pH7.5 50 mM NaCl 5 mM MgCl ₂	usb corp. AppliChem Merck
Nitrocellulose filter	NC20 0.2 μ m; 2.5 μ m	Whatman Schleicher & Schuell

2.4 Cell biological methods

2.4.1 Cell passages of cell lines

All cell lines were incubated in 5 mL of the corresponding medium in T25 cell culture bottles at 37°C, 5% CO₂ and 90% air humidity in an incubator. Every 3 days, cells were passaged to fresh T25 bottles depending on cell's formation of confluent layers. Therefore, cells were washed with 5 mL of PBS and treated with 1 mL of Trypsin solution at 37°C for up to 5 minutes in an incubator. After cells had dissociated from the bottle's surface, either autonomously or by shaking the bottle manually, they were spilled with 5 mL of their particular medium and gently resuspended. 250 μ L of the resuspended cells were added to 5 mL fresh medium in a new T25 culture bottle. Cells were then recultured at 37°C, 5% CO₂ and 90% air humidity containing incubator.

Tab. 2-22 Cell culture media and supplements

Material	Composition	Supplier
<i>Mod. Eagle Medium</i> (MEM)	110 mg/mL NaCOCH ₃ non essential amino acids	Invitrogen
DULBECCO'S <i>Mod. Eagle Medium</i> (DMEM)	4.5 mg/mL D-Glucose 110 mg/mL NaCOCH ₃ non essential amino acids	Invitrogen
Trypsin-EDTA	2.5% (v/v) Trypsin 0.125% (v/v) Versen in PBS without Ca ²⁺ and Mg ²⁺ .	Biochrom
Fetal Calf Serum (FCS)	Heat inactivated at 65°C for 30 minutes.	Invitrogen

L-Glutamine (100×)	200 mM	Invitrogen
Penicillin-Streptomycin	10,000 units/mL Penicillin 10,000 units/mL Streptomycin	Invitrogen

Tab. 2-23 Eukaryotic cell lines

Material	Composition	Supplier
COS-7	A simian kidney cell line derived from CV-1 by transformation with an origin-defective mutant of SV-40. Cells were cultured in DMEM.	DSMZ ACC 60
HeLa	Established from the epitheloid cervix carcinoma due to an adenocarcinoma. It is the first aneuploid cultured human cell line. Cells were cultured in MEM.	DSMZ ACC 57

To store cell lines, after first or second passage, cell lines resuspended in MEM or DMEM, respectively, were mixed with 10% (v/v) FBS and 10% (v/v) DMSO solution. The suspension was aliquoted in 100 μ L portions and transferred to cryo tubes that were frozen in liquid nitrogen.

2.4.2 Transient transfection of HeLa and COS-7 cells

Transfection efficiencies depend on a variety of parameters. Factors as cell culture, the effect of serum on the transfection reagent, the type of vector construct, the quality of plasmid DNA and the ratio of transfection reagent to DNA have to be taken into account to yield optimal transfection results.

DNA was diluted in cell growth medium containing no serum and other supplements. Finally, the PolyFect[®] transfection agent was added to be vortexed for 10 seconds. Samples were incubated for 10 minutes at room temperature to allow complex formation. While complexation took place, the growth medium was gently aspirated; cells were washed once in PBS, and added to fresh cell growth medium containing serum and antibiotics. Some cell growth medium was added containing supplements to the transfection complexes reaction, mixed and immediately transferred to the cells in the dish. To ensure homogenous distribution of the complexes, dishes were swirled gently before they were reincubated at 37°C and 5% CO₂. Cell line lysates were prepared as described under 2.3.2.

Tab. 2-24 Detailed parameters for transient transfection

Approach	Assay
100 mm Petri dish (1×10 ⁶ cells)	4 μ g DNA 300 μ L DMEM/MEM without supplements 25 μ L PolyFect and adding 7 mL fresh DMEM/MEM to cells.

2 chamber slides	0.75 µg DNA
(4×10 ⁴ cells)	50 µL DMEM/MEM without supplements
	5 µL PolyFect
	adding 1.5 mL fresh DMEM/ MEM to cells

2.4.3 Generation of primary hippocampal neurons

To cultivate primary hippocampal neurons (Goslin & Banker, 1991), 24 well plates containing one coverslip in each well, were coated with 500 µL of Poly-L-Lysine solution for at least 1 hour in a 37°C incubator and washed twice with PBS before preparation.

A pregnant rat, bearing embryos of an 18-day pre-natal stage was killed by CO₂ to take out the embryos that were immediately decapitated. Subsequently, embryonic brains were dissected and kept in a Petri dish containing HBSS buffer on ice to preserve cell's vitality as long as possible. In a second step, hippocampi were dissected under a binocular and collected in 15 mL test tube filled with HBSS. The following preparation steps were continued in a clean bench.

Then cells were triply washed in 10 mL of HBSS and the buffer was decanted leaving a rest volume of approximately 1.8 mL. To destroy cell associations, 200 µL of a 2.5% Trypsin solution were added to a total volume of 2 mL and the cells were incubated in a 37°C warm water bath for 15 minutes and washed 5×5 mL with HBSS.

The buffer was filled up to a volume of 1.6 mL to add 400 µL of DNase solution to an end concentration of 0.01% and cells were resuspended to be passaged through a cell strainer. The strainer's membrane was spilled with 18 mL of DMEM medium in total, pipetting in 1 mL steps, one after the other. To determine the cell concentration of this suspension, the cell number was counted by using a Neubauer chamber and the suspension was diluted to 2×10⁴ cells/500 µL per well for immunohistochemical staining or 4×10⁴ cells/500 µl for hippocampal transfections. If hippocampal neurons were seeded onto Petri dishes, 6×10⁶ cells/mL were solved in Neurobasal medium. The next day, DMEM medium was substituted by 600 µL of freshly added Neurobasal medium containing all supplements (FCS, glutamate, and penicillin-streptavidine). Primary hippocampal neurons were maintained at 37°C, 5% CO₂ and 90% air humidity for 28 days. Cells died when exceeding this time range.

Tab. 2-25 Cell culture media and supplements

Material	Composition	Supplier
Neurobasal Medium	Without Glutamine	Invitrogen
B-27 Supplement (50×)	Vitamin A and E, Catalase SOD, Glutathione	Invitrogen
Hank's Balanced Salt Solution (HBSS) 1×	Without Ca ²⁺ and Mg ²⁺ With/without Phenol Red	PAA

2.4.4 Transfection of primary hippocampal neurons

Primary hippocampal neurons were transfected under sterile conditions at day 1 (d1) in 24-well plates. First, 3 μL OptifectTM were mixed with 50 μL neurobasal medium without supplements in a separate micro-centrifuge tube and incubated for 5 minutes at room temperature in the clean bench. In another test tube 1 μg DNA was combined with 50 μL neurobasal medium free of additives. Both probes were mixed and incubated for 30 minutes at room temperature. In the mean time, 24 well plates were washed twice with 650 μL of HBSS per well. After that, 500 μL of prewarmed Neurobasal medium containing B27 and glutamine but without antibiotics were pipetted in each well and 100 μL of the transfection mixture were added to the well. Hippocampal neurons were incubated for 4-7 days in a 5% CO_2 incubator and then fixed with paraformaldehyde solution. Immunohistochemical stainings (2.4.5) and microscopical analysis finished transfection investigations in neuronal cells.

2.4.5 Immunohistochemical staining for fluorescence microscopy

Hippocampal neurons were grown on coverslips in a 24-well plate and fixed at day 3 (d3), d5, d7, d14, d21 or d28 with 500 μL of fixation solution for 10 minutes at room temperature. 1.5×10^5 cells per well were seeded in chamber slides overnight and fixed with 500 μL of fixation solution per chamber. Then cells were washed twice with PBS and 500 μL of permeabilization solution was pipetted in each well for 3 minutes on ice. The cells were washed again twice in PBS. Subsequently, nearly all unspecific binding sites were quenched by incubation in 500 μL of blocking solution on each coverslip and incubating at room temperature for 1 hour. Thereafter, the primary antibodies, diluted 1:1000 or 1:4000 in blocking solution, respectively, were applied to allow antibody precipitation overnight in a refrigerator. Following the incubation, cells were washed three times in 500 μL of PBS for 5 minutes while the second HRP-conjugated antibody was prepared by diluting 1:1000 in blocking solution. 500 μL of this mixture were added per well and incubated at 4°C in the dark for 2 hours. Then cells were washed 3×5 minutes with PBS and were immersed in deionized water containing DAPI in a dilution of 1:10000. To embed the cells, 10 μL of MOLWOL[®] solution, prepared according to the instructions provided by the supplier, were dropped on separate slides, so that coverslips directed with the cell-side down, were put into this drop. Probes were analyzed using a fluorescence microscope.

Tab. 2-26 Immunohistochemical staining solutions

Material	Composition	Supplier
Fixation solution	10% (w/v) Paraformaldehyde pH 7.4	Merck
Blocking solution	1% (v/v) Horse Serum 2% (w/v) BSA 0.1% (v/v) Triton X-100 in PBS	PAA PAA Roche
Phosphate buffer	1.14% (w/v) $\text{NaH}_2\text{PO}_4 \times \text{H}_2\text{O}$ 1.86% (w/v) $\text{Na}_2\text{HPO}_4 \times 2\text{H}_2\text{O}$	Merck Merck

2.4.6 DAB staining for light microscopy

Immunohistochemistry was used to analyze RhoSAP distribution pattern in rat brain. Therefore, paraffin sections were used and the developing reaction occurred indirectly by enzymatic cleavage of a reporter substance: 3,3-diaminobenzidine (DAB).

Brain sections of 4-8 μm thickness, immobilized on slides, had to be deparaffinized first in 3 changes of xylene for 15 minutes. Then, brain slides were hydrated in four steps, for 5 minutes each, in isopropanol, absolute ethanol, in 96% (v/v) ethanol and finally, in 70% (v/v) ethanol. The sections were briefly washed with deionized water, and incubated in hydrogen peroxide for 10 minutes to suppress all endogenous peroxidase activity. The brain sections were rinsed in three changes of PBS, transferred into a humidified chamber and further blocked in 1% (w/v) BSA diluted in PBS at room temperature for 1 hour. The primary RhoSAP antibody diluted 1:1000 in 0.5% (w/v) BSA and PBS was pipetted on the sections that were then incubated at 4°C overnight. After washing the slides 3×5 minutes in PBS, the biotin-conjugated anti-rabbit antibody was applied. Then, the slides were incubated for 2 hours at room temperature and rinsed in PBS again. To visualize the formation of precipitated antigen-antibody complexes, the VECTASTAIN® ABC kit was applied, according to the protocol provided by the supplier. Thereby, HRP conjugated to the avidin-biotin complex catalyzed the oxidation of DAB. That resulted in the formation of insoluble brown complexes. The procedure was stopped by washing the slides with 2 changes of deionized water for 10 minutes. Finally, the sections were dehydrated in 5 steps for 5 minutes each by rinsing in 70% (v/v) ethanol, 96% (v/v) ethanol, isopropanol and two changes of xylol. Embedding occurred through Entellan® New fixation. The slides were documented by Zeiss MIRAX scanner.

2.4.7 Immunohistochemical staining for electronmicroscopy (pre-embedding method)

Cells were fixed with 4% (w/v) paraformaldehyde, 0.1% (w/v) glutaraldehyde and 1% (w/v) sucrose 10 min at 4°C and permeabilized with 0.004% (w/v) digitonine for 4 minutes on ice. Pre-incubation was carried out 1 hour at room temperature with 10% (v/v) normal goat serum, 1% (w/v) BSA in PBS followed by incubation with the primary antibodies (rabbit anti-RhoSAP 1:1000) in 3% (v/v) goat serum and 1% (w/v) BSA in PBS overnight at 4°C. After washing, biotinylated goat anti-rabbit antibodies were added in dilution, 1:100 for 2 hours at room temperature. Cells were covered with a 1:100 dilution of the avidin-biotin-horseradish peroxidase complex (Vector, Burlingame) for 30 min. As substrate for the peroxidase, DAB was applied followed by a postfixation with 2.5% (w/v) glutaraldehyde and 1% (w/v) sucrose in 0.1 M phosphate buffer pH 7.3. Cells were contrasted with silver stain. Therefore, they were treated with 0.5% (w/v) osmium tetroxide/ 0.8% (w/v) $\text{K}_3\text{Fe}(\text{CN})_6$ for 20 minutes at room temperature, contrasted with 0.5% (w/v) tannic acid and 2% (w/v) uranylacetate and embedded in epoxy resin. Ultra-thin sections of 70-80 nm were examined using an EM10 transmission electron microscope at 80 kV.

2.4.8 Endocytosis assay and statistical analysis

To investigate activity-dependent vesicle cycling in HeLa cells, FM[®] 4-64, a lipophilic styryl dye was applied to assay the influence of RhoSAP alone and in combination with its associative molecules ProSAP2/Shank3 and syndapin I, on endocytic activity in HeLa cells. The water-soluble dye is believed to insert into the outer leaflet of the surface membrane, so that if the cell is endocytically active, the dye becomes internalized within the recycled vesicles that are brightly stained and excluded to extracellular space. The amount of FM[®] 4-64 taken up per vesicle by endocytosis equals the amount of dye released upon exocytosis. This indicates there is no transfer from internalized vesicles to endosomal compartments within the cell.

First, a working staining solution of five µg/mL of FM[®] 4-64 dye was prepared in ice-cold HBSS buffer and kept on ice. The medium from transfected HeLa cells (3.1.2) was removed quickly and the cells were briefly rinsed with HBSS. Immediately, slides were immersed in 600 µL of the staining solution, on ice, for 10 minutes. After removal of staining solution, cells were immediately fixed (3.1.4) for 10 minutes with 4% paraformaldehyde (w/v) and were then examined under the microscope to analyze vesicle formation.

To determine effects of GFP-construct transfection on endocytic behavior statistically 30 HeLa cells were analyzed in every experiment, by counting their vesicle number and evaluating statistical significances to refer to an augmentation or diminution of endocytosis. Every approach was repeated three times to assure documentation of representative cells. Results were depicted in charts indicating the average value and standard deviation. To compare different groups of transfection approaches, data were examined for their normality. The Mann-Whitney Rank Sum Test showed statistically significant differences among the groups. Indication occurred as asterisk symbols marked as * $p = 0,002$ and * $p < 0,001$ in the chart.

3 Results

3.1 Gene and protein structural characterization of RhoSAP

3.1.1 Identification of RhoSAP as a PDZ domain interacting protein

The yeast two-hybrid system was used to identify novel binding partners for ProSAP2/Shank3 PDZ domain. Therefore, a rat brain cDNA library cloned into pACT-2 vector as prey was screened, employing 142 amino acids (aa) of ProSAP2/Shank3 representing the molecule's PDZ domain. A total of 3 clones were isolated that encoded a protein consisting of 818 aa named RhoSAP for RhoGAP synapse associated protein. The cDNA consists of 2457 bp. By means of alignment search, three segments were found corresponding hypothetically to protein domains: BAR, RhoGAP and proline rich motifs.

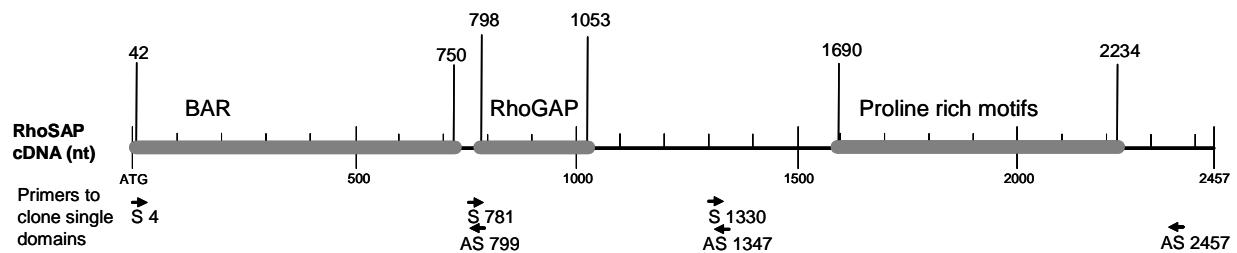


Fig. 3-1 Scheme of RhoSAP's cDNA structure. Via a yeast two-hybrid screen with ProSAP2/Shank3's PDZ domain, a cDNA corresponding to RhoSAP was detected as novel interaction partner. The cDNA sequence was of 2457 bp lengths. Three potentially functional domains (BAR, RhoGAP, proline rich motifs) could be assigned to cDNA sections. Primers (S, AS) were chosen to amplify these sections for cloning.

Additional data base search and literature analysis revealed a relation to the human RhoGAP interacting with CIP4 homologues: Rich2 molecule (EMBL-EBI: BC089950; also named KIAA0672, EMBL-EBI: BC117412) which was related to Rich1 (Richnau & Aspenström, 2001). Additional sequence search revealed that Nadrin (EMBL-EBI: AB042827) is the rat homologue of Rich1 and is related to RhoSAP.

KIAA0672	MKKQFNMRQLAN	OTVGRAEKTEVLSEDLQVEKRELVKQVSHSTHKKLTACLQGGQGA	60
RhoSAP	MKKQFNMRQLAN	OTVGRAEKTEVLSEDLQVEKRELVKQVSHSTHKKLTACLQGGQGA	60
KIAA0672		EADWRSKKLPLTTLAQCLMEGSAILGDDTLLGKMLKLCGETDELAQELIHFELRVERDV	120
RhoSAP		EADWRSKKLPLTTLAQCLMEGSAILGDDTLLGKMLKLCGETDELAQELIHFELRVERDV	120
KIAA0672		IEPLFLLAEVEIPNIQKQKRLAKLVLDMDSSRTWQQTSSSGSSSLQPAGAKADALR	180
RhoSAP		IEPLFLLAEVEIPNIQKQKRLAKLVLDMDSSRTWQQTSSSGSSSLQPAGAKADALR	180
KIAA0672		SEMEEAANRVEICRDQLSADMYSFVAKEIDYANYPQTLLIEVQAEYHRKSLTLLQAVLPQI	240
RhoSAP		SEMEEAANRVEICRDQLSADMYSFVAKEIDYANYPQTLLIEVQAEYHRKSLTLLQAVLPQI	240
KIAA0672		KAQQEAWVKKPSFGKPLEEHLTISGREIAFPICVITMLLECGMQEGLFRVAPSASKLK	300
RhoSAP		KAQQEAWVKKPSFGKPLEEHLTISGREIAFPICVITMLLECGMQEGLFRVAPSASKLK	300
KIAA0672		KLKAALDCCVVDVQEYSADPHAIAAGALKSYLRELPEPLMTFELYDEWIQASNIQEQDKRL	360
RhoSAP		KLKAALDCCVVDVQEYSADPHAIAAGALKSYLRELPEPLMTFELYDEWIQASNVQEQDKKI	360
KIAA0672		QALNNACEKLPKANHNIRYLKFLSKLSEYQDVNMTSPSNMAIVLGNLLMPQSEGNIIT	420
RhoSAP		QALNNACEKLPKANHNIRYLKFLSKLSEYQDVNMTSPSNMAIVLGNLLMPQSEGNIIT	420
KIAA0672		EMMTTVSLQIVGIIIEPIIQHADWFF	480
RhoSAP		EMMTTVSLQIVGIIIEPIIQHADWFF	480
KIAA0672		DRRQPEQARRPLSVATDNMMLEFYKKGDLRKIQSMGVRVMDTSWVARRGSSAGRKAACA	540
RhoSAP		DRRQPEQARRPLSVATDNMMLEFYKKGDLRKIQSMGVRVMDTNWVARRGSSAGRKVSCA	540
KIAA0672		PSMQPPAPPSELAAPLPSPLPEQVDSAPAPALSPGASLQPTPERPVSQSKELSPG	600
RhoSAP		PSMQPPAPPSELAAPLPSPLPEQVDSAP--APALSPGSLGLQGPERTSTTKSKELSPG	598
KIAA0672		SAQKGSPPQSIQTTICPGTQGPQP	654
RhoSAP		SAQKGSPPQSIQTTICPGTQGPQP	658
KIAA0672		FEVQPGTVSDQPTGQPSPVSLSPPTSPYGLSYPPGYSMASQSLSPASAPPLASPSV	714
RhoSAP		FEVQPGTVSDQPTGQPSPVSLSPPTSPYGLSYPPGYSMASQSLSPASAPPLASPSV	718
KIAA0672		FTSLAKSRPTTKFRORFTLPP	774
RhoSAP		FTSLAKSRPTTKFRORFTLPP	778
KIAA0672		VPSIHILGSLTLRLSPLEHARRHSVTDKRDSEEESESTAL	814
RhoSAP		VPSIHILGSLTLRLSPLEHARRHSVTDKRDSEEESESTAL	818

Fig. 3-2 Alignment of RhoSAP and Rich2 (KIAA0672). RhoGAP synapse associated protein (RhoSAP) was identified by a yeast two-hybrid screen to search for proteins implicated in ProSAP2/Shank3 signaling via the PDZ domain which functioned as bait. After screening a rat brain cDNA library, a clone was isolated that corresponded to KIAA0672 which is named Rich2 alternatively. Alignment was performed by EBI-EMBL Clustal W program. Coloured indication: F-BAR Domain (Blue), RhoGAP (Yellow) and SH3 binding motif (green).

3.1.2 Gene and protein structure of RhoSAP

The chromosomal structure of RhoSAP in the *R. norvegicus* genome (10q23) is characterized by 22 exons and 21 introns of different size. The exons form an open reading frame (ORF) comprising 2457 base pair which encode for an 818 aa protein.

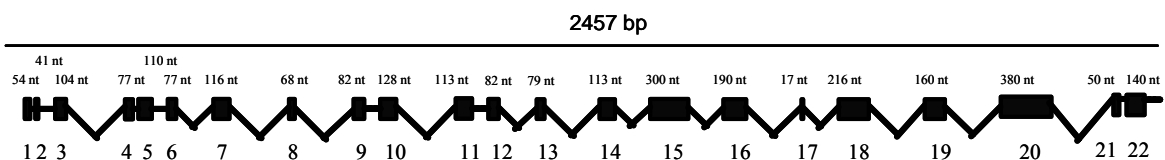


Fig. 3-3 Exon-intron structure of RhoSAP as found on *R. norvegicus* genome. By means of a yeast two-hybrid screen of a rat brain cDNA library with ProSAP2/Shank3 PDZ domain as bait, a cDNA of 2457 bp was found which corresponded to the human Rich2 (KIAA0672). Analysis of the rat contig DNA (chromosome 10q24) to clear RhoSAP exon-intron structure, revealed 22 exons for this gene on the chromosome and 21 introns. The prey cDNA however did not contain exon 21. In exon 22 the cDNA runs into a stop signal TGA.

By using tools as EBI Data Bank and Swissprot, structural investigations on protein level revealed that RhoSAP contains an N-terminal BAR domain (aa: 14-246). In accordance

with studies on the BAR domain-containing proteins amphiphysin I and endophilin A1, the BAR domain in RhoSAP might also bind lipids, and could deform lipid bilayers *in vitro*, thus, suggesting a role in membrane-trafficking (Itoh & de Camilli, 2006).

It is postulated that the protein's RhoGAP domain (aa: 252-442) could act as potential modulation module for monomeric GTP-binding proteins (small GTPase) of the Rho family, including Cdc42, Rac-1 and RhoA. GTPase activating domains act as negative regulators of small GTPases, accelerating the rate of GTP hydrolysis, thus, switching off the GTPase's activity. During the stoichiometrically interaction between RhoGAPs and the small GTPases, the conserved arginine finger GLFRVAP acts as cationic residue to stabilize the transition state of the reacting GTP (Bos *et al.*, 2007).

Moreover, sequence alignments of RhoSAP showed that four proline-rich motifs can be found in the C-terminal part of the protein. They confer binding to a number of SH3 domain-containing proteins and are often referred to as SH3-binding motif.

Finally, a further significant motif was detected: STAL. It is present in the C-terminus and determines the interaction with the PDZ domain.

A

```

MKKQFNRMRLANQTVGRAEKTEVLSEDLQVEKRLVLVKQVSHSTHKKLTACLQGGQGAEDKRSKKLPLTTLAQCLMEGSAILGDDTL 90
LGKMLKLCGETEDELAQELIHFELPVERDVIEPLFLAEVEIPNIQKQKHLAKLVLDMDSSRTFWQQTSSKSSGLSSSLQPAKADALR 180
EEMEEAANRVEICRDQLSADMYSFVAKEDIDYANYFQTLIEVQAEYHRKSLTLLQAVLPQIKAQGEAWVEKPSFGKPLEEHLTISGREIAF 270
PIEACVTMLLECGMQEEGLFRVAPSASKLKKLKAALDCCVVDVQEYSADPHAIAGALKSYLRELPEPLMTFELYDEWIQASNVQEQDKKL 360
QALWNACEKLPKANHNINIRYLKFLSKLSEYQDVNKMTPSNMAIVLGNLLWPQAEGNITEMMTTVSLQIVGIIIEPIIQHADWFFPGEIE 450
FNITGNYSPPVHVHNHANYSSMPSDMDPADRRQPEQARRPLSVATDNMMLEFYKDKGLRKIQSMGVRVMDTNWVARRGSSAGRKVSCAP 540
PSMQPPAPPAELAAPLPSPLPEQLDSPAAPALSPSGLGQLQGPERTSTTKSKELSPGSAQKSGSPGSSQGTACAGTQPGAQPGAQPGASP 630
SPSQPPADQSPHTLRKVSKLAPIPPKVFPQPGAMADQSAQQLSPVLSPTPPSTPSPYGLSYFPQGYSLASGQLSPAAAPPLASPSVFT 720
STLSKSRPTPKPRQRPTLPPQPPSVLSASSPQSTEHMPLDGMSPGESMSTDLVHFDVPSIHIELGSTLRSLPLEHARRHSVTDKRDSE 810
EESSESTAL 818

```

B

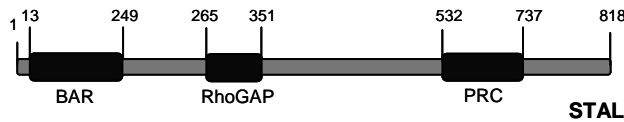


Fig. 3-4 Protein structure of RhoSAP. The newly discovered rat brain protein: RhoSAP, comprising a total of 818 aa, was furthermore investigated by its amino acid structure. All corresponding structural motifs were calculated through Swissprot Prosite program. (A) RhoSAP aa sequence. The BAR domain, highlighted in italic capitals consists of 236 aa. In contrast, the RhoGAP domain (86 aa) was set in frame and its arginine finger, responsible for small GTPase interaction was underlined in red. Through amino acid alignments, three proline rich motifs were detected in the C-terminus that ends with the PDZ interaction sequence: STAL. (B) Protein motifs of RhoSAP are depicted schematically according to their size and location within the protein directed from N- to C-terminus.

3.1.3 Sequence homologies of RhoSAP

By DNA alignment studies, RhoSAP was found to be the rat homologue of Rich2 in humans. To ultimately categorize the newly explored molecule RhoSAP in regard to its sequential relation to the Rich proteins, all three DNA sequences (Rich1, Rich2 and RhoSAP) were searched on the human, rat and mouse genome. RhoSAP and Rich2 fell exactly on the same loci in each investigated species' genome, implicating a homology. Further sequence search revealed that Nadrin (EMBL-EBI: AB042827) was the rat homologue of Rich1. Another protein related to Nadrin and RhoSAP was SH3-binding protein1 (3BP1) which contained an F-BAR domain, a RhoGAP domain and an SH3-binding motif in accordance with RhoSAP and Nadrin. These findings implicate to group the molecules into a protein family. The amino acid sequence identity among RhoSAP, Nadrin and 3BP1 ranges from 30% to 50% comparing the whole sequences.

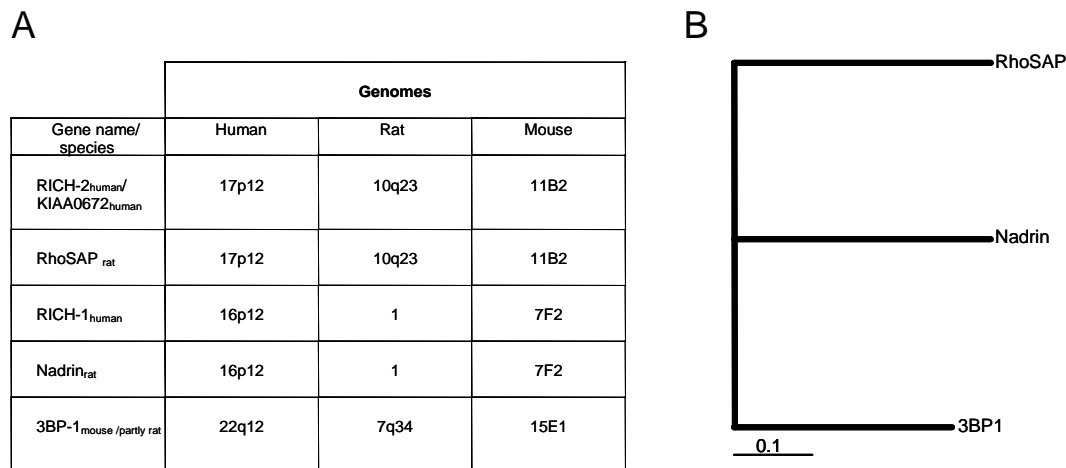


Fig. 3-5 Proteins related to RhoSAP. (A) Loci determination by EMBL alignment tools for Rich1, Rich2, RhoSAP, Nadrin and 3BP1 in the human, rat and mouse genome. The human protein Rich2 and RhoSAP isolated from rat brain are localized on the same locus (10q23) in *R. norvegicus*. Alignment studies revealed that Rich1 is the human homologue of Nadrin. Both are found on chromosome 1 in *R. norvegicus*. (B) Phylogenetic analysis of RhoSAP, Nadrin and 3BP1 by use of Treeview program. The bar has a relative value. Branch lengths are proportional to the inferred evolutionary change.

3.1.4 Putative splice variants of RhoSAP

Rat brain RNA was transcribed reversely and amplified by RT-PCR. Interestingly, performing RT-PCR with S1330 and AS 2457 primers did not result in one PCR product only. Instead of one main band of 450 bp, two additional bands between 506 bp and 1018 bp were detected on agarose gel. To address whether these bands were putative splice variants, their DNAs were subcloned into the TOPO-TA[®] vector and sequenced. The obtained results correlated well with the fragments' sizes found on the agarose gel and furthermore showed that RhoSAP was detectable in at least three alternative transcripts. To

elucidate a relation between these alternative splice variants of RhoSAP mRNA and their expression pattern in specific brain regions, *in situ* hybridizations were performed. The findings imply that RhoSAP splice variants II (2237 bp) and III (2000 bp) prevalingly play a role in the cerebellar area of the brain. They show only marginal transcript abundance in the cortex. In contrast, the RhoSAP splice variant of 2462 bp containing a further exon 21, named RhoSAP SI here, illustrates a high level of transcripts in the cortex, mainly during the developmental stages from day 9 (d9) until 3 weeks. In the adult stages of brain development (3 months and 1 year), RhoSAP SI transcript signals were weak and it appeared that they vanish gradually when compared with the development stages from d9 to d21.

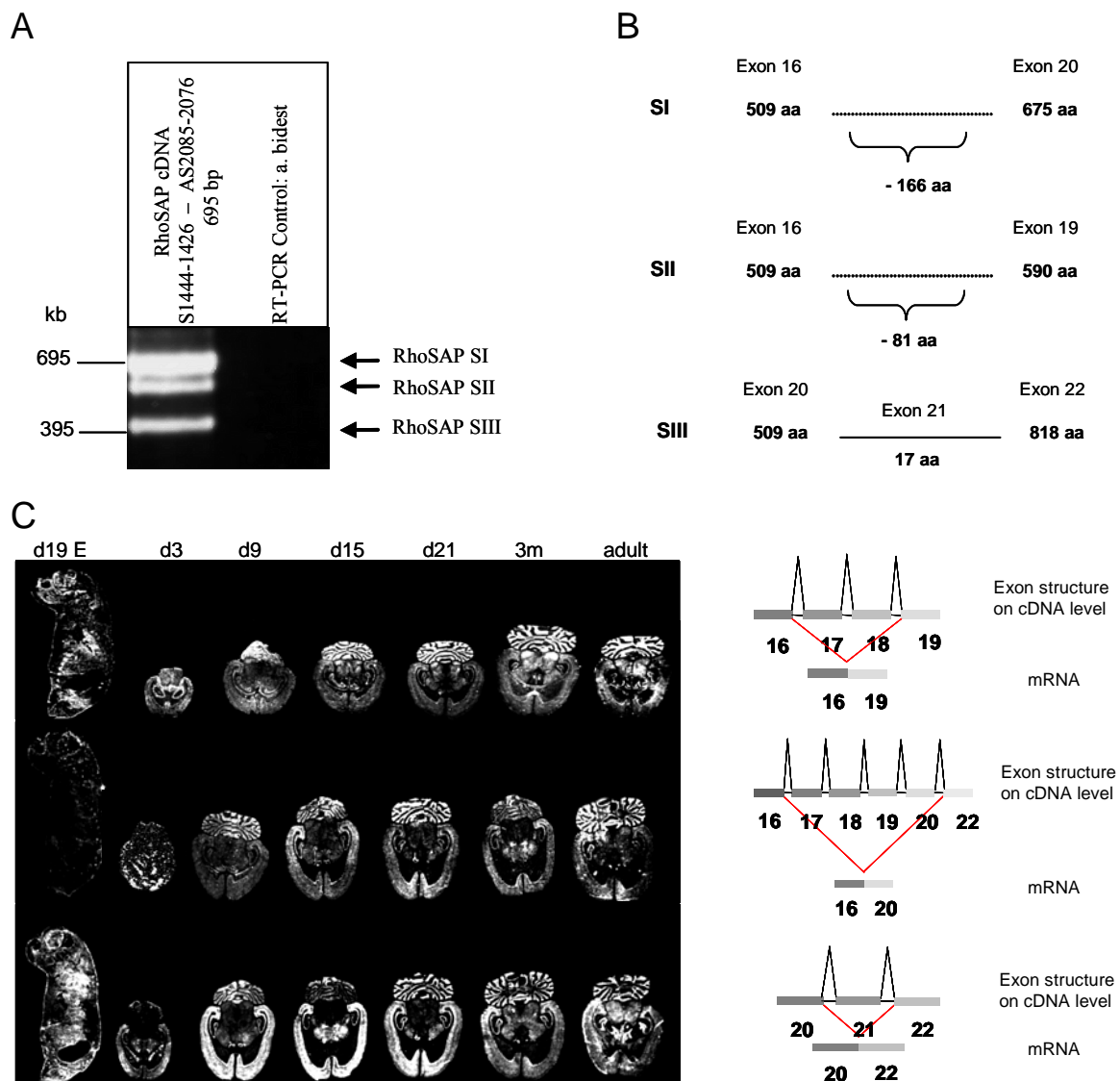


Fig. 3-6 Splice variants of RhoSAP. (A) RT-PCR using sense primer S1444-1426 and antisense primer AS2085-2076 to amplify the C-terminal part of RhoSAP cDNA resulted in two additional products (RhoSAP

SI: 400 bp, RhoSAP SII: 630bp, RhoSAP SIII: 665 bp) next to the expected 660 bp band as main PCR product. Subcloning and sequencing of these PCR products showed there were three more different splice variants of RhoSAP in rat brain. (B) Depiction of the three RhoSAP variants on aa level. (C) *In situ* hybridization illustrating the different expression patterns of RhoSAP splice variants according to the rat brain development (d19E: day 19 embryo, d3: day 3, d9: day 9, d15: day 15, d21: day 21, 3m: 3 months and 1 year old adult rat brain)

3.1.5 Generation and characterization of anti-RhoSAP antisera

To investigate RhoSAP on protein level, corresponding antisera were generated in rabbit and guinea pig. The antisera were directed against the whole protein as antigen determinant, except for the N-terminal part containing the BAR domain. Moreover, the antisera are directed against the GST-tag which was a component of the antigen produced for immunization.

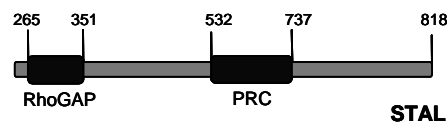


Fig. 3-7 RhoSAP epitope recognized by the antisera generated in rabbit and guinea pig. RhoSAP was cloned into pGEX-4T-2 to overexpress the GST-fusionprotein in *E. coli* cells. 300-500 µg of RhoSAP-GST were purified for immunization of rabbit and guinea pig. Antisera were generated by Pineda Antibody Service Berlin and extracted at day 120 after initial immunization.

The antisera were tested for the antibodies' specificity. Therefore, RhoSAP-GST proteins were overexpressed in *E. coli* so that the bacterial homogenate could be analyzed by Western blotting. Furthermore, the same approach was undertaken for pEGFP-RhoSAP constructs to generate fusionproteins in HeLa cells. The resulting protein bands had the correct molecular weights, including their particular tag's protein amount: 26 kDa for GST or GFP, respectively.

The calculated protein mass was analyzed in P2 brain homogenate and testis lysate. A corresponding band at 90 kDa was found representing the theoretically deduced protein weight. Another band was detected in brain homogenate at 120 kDa pointing out to the existence of another protein variant. This was supported by several antisera purifications using RhoSAP expressed as GAP domain GST-fusionprotein. Western blot investigations always yielded two protein bands underlining the idea that RhoSAP exists in two variants on protein level.

Additionally, immunoglobulin purification of the anti-RhoSAP sera resulted in the observation of several degradation bands. This might be due to the fact that antibody stabilization factors were wiped out of the sera. When comparing both sera deriving from rabbit and guinea pig, in respect to the detected bands in Western blotting, anti-RhoSAP

rabbit serum turned out to show less diffuse bands. That is why the rabbit serum was used for the subsequent immunoblotting and immunohistochemical stainings.

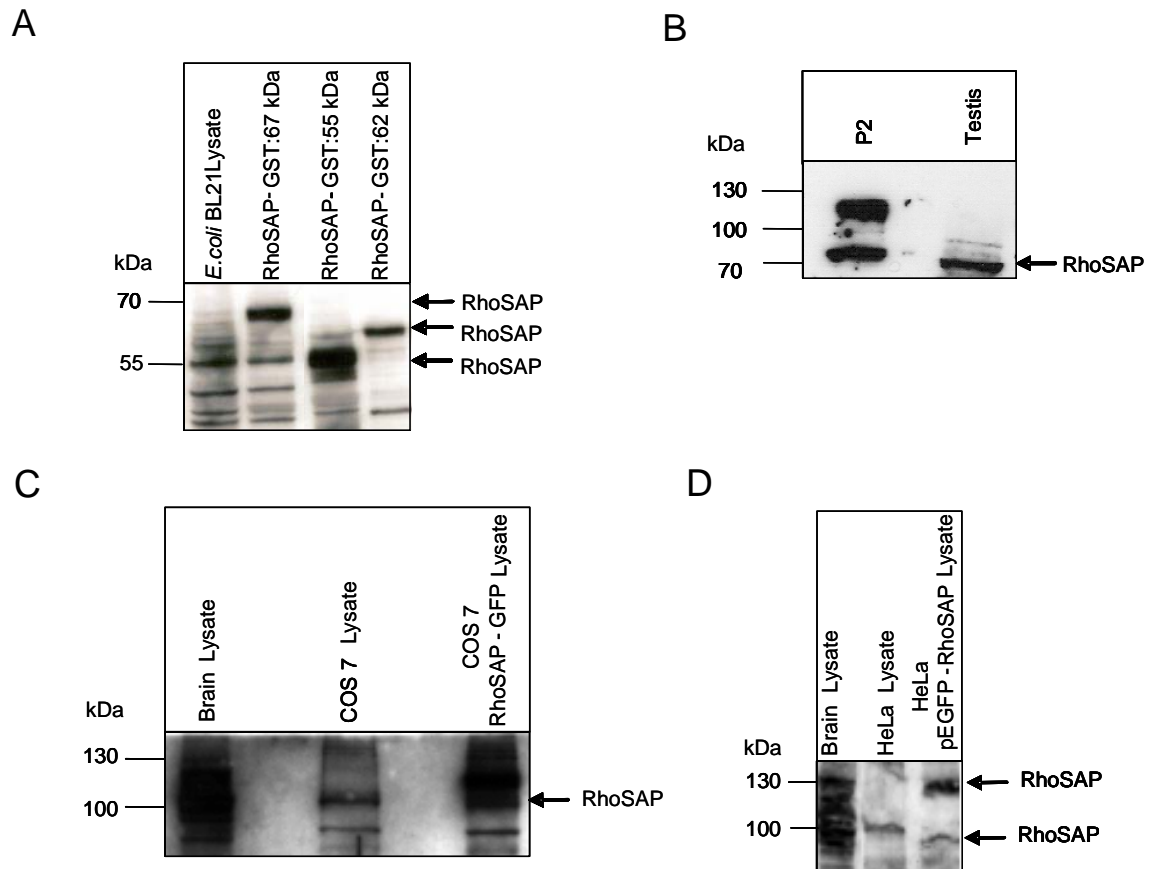


Fig. 3-8 Characterization of polyclonal rabbit anti-RhoSAP serum by immunoblotting. (A) Overexpressed pGEX-4T-2 RhoSAP variants in *E. coli* cells were lysed to load 15 μ L (20 μ g) of the bacterial lysates dissolved 1:1 in SDS-loading buffer on a 10% SDS gel. Anti-RhoSAP rabbit serum was used in a dilution of 1:5000. Bands were detected for pGEX4T-2 S1330-AS2457 at 67 kDa, for pGEX4T-2 S4-AS799 at 55 kDa, for pGEX4T-2 S781-AS1347 (B) Anti-RhoSAP (rabbit) detected two bands at 90 kDa and 120 kDa in P2 brain fraction but only one signal was received in testis homogenate at app. 70 kDa. The antiserum was diluted 1:4000. 15-20 μ g of protein were applied to each lane. (C) and (D) Pure COS7/HeLa cell lysate and recombinant RhoSAP-GFP full length containing COS7/HeLa lysates were applied in a range of 10-15 μ g protein on each lane. A clear and enriched band between 120-130 kDa was detected for the lysates containing recombinant RhoSAP. Pure lysate showed a signal at the same band size but it was weaker due to endogenous protein production. Brain lysate was used as positive control since RhoSAP is a brain protein. A reference band was detected at 100 kDa. Antibody dilution was 1:4000.

3.1.6 Profiling RhoSAP's expression in brain and other tissues

To investigate RhoSAP's abundance in different tissues, a commercial rat multiple Northern blot was hybridized with a 755 bp sized probe derived from the cDNA part corresponding to the RhoGAP domain of the molecule. A transcript of 4.4 kb was present in all tissues analyzed, indicating that RhoSAP is ubiquitously expressed. However, the expression in brain was particularly high, next to heart, liver and testis tissue. In these tissues, RhoSAP transcripts were strongly abundant, as compared to the relatively low levels found in the other tissues. Interestingly, weak subbands representing transcripts

ranging under 4.4 kb of size as well as transcripts of 1.24 kb and 0.35 kb were detected, especially in heart, muscle, and kidney or testis tissue.

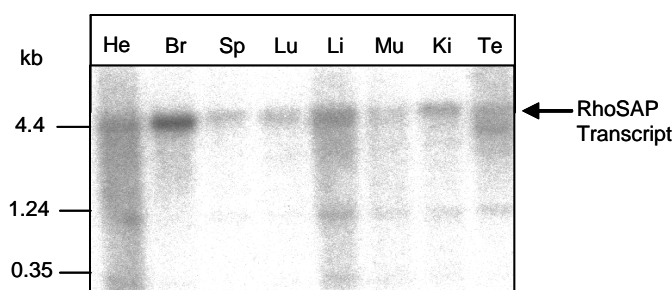


Fig. 3-9 Northern blot analysis of mRNA from different rat tissues. RNA from the tissues indicated as following: He (heart), Br (brain), Sp (spleen), Lu (lungs), Li (liver), Mu (muscle), Ki (kidney) and Te (testis) was analyzed with a 755 bp sized DNA probe. The cDNA of RhoSAP is expressed ubiquitously, but almost at a weak level. High abundance of RhoSAP transcripts were almost found in brain tissue at 4.4 kb.

Furthermore, RhoSAP was detected by Western blot analysis in different rat tissue homogenates to find out which expression pattern exists on the protein level. In this case, the protein was abundant at high levels in every tissue analyzed, except for the skeletal muscle fraction where no protein was detected at all. A band of around 90 kDa tending towards 100 kDa was present in every tissue homogenate lane in the Western blot analysis. RhoSAP expression in brain differed slightly, in the respect of finding an additional protein band at approximately 120 kDa of molecular weight.

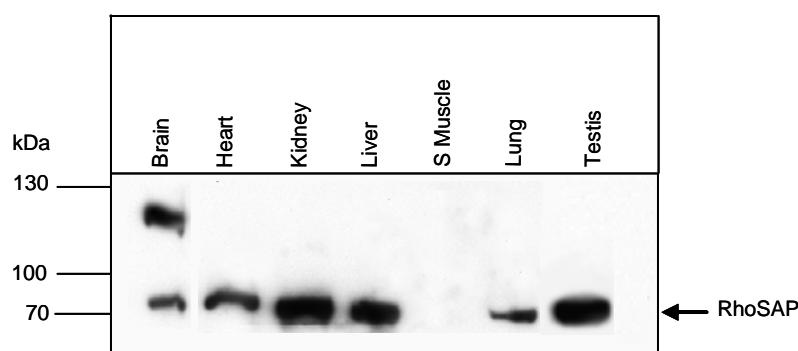


Fig. 3-10 RhoSAP expression analysis in different rat tissue homogenates. Rat tissue homogenates: brain, heart, kidney, liver, skeletal muscle, lung and testis were generated and proteins extracted in 1×RIPA buffer. A total of 20 µg of proteins were loaded on each lane of a 10% SDS gel to carry out Western blotting. RhoSAP protein bands were detected in each homogenate at around 90 kDa, except for skeletal muscle homogenate. The expression in brain revealed a second band at 120 kDa. Rabbit anti-RhoSAP was diluted 1:5000.

To further characterize the distribution of RhoSAP in brain tissue, *in situ* hybridizations were performed with rat brain cryoslices of different stages of development. The expression of the mRNA significantly increases in the cerebellum between postnatal day

d15 and d21 whereas at d3 no transcripts were detected and at d15, the protein occurred gradually. RhoSAP transcripts were at a relatively high level in hippocampus from d9 throughout the adult stage of development. Cortex contained lower levels of transcript which were already present from d3 on at a relative constant level. Remarkably, there was a slight diminution of transcripts after 3 months which then rose again in adult rats.

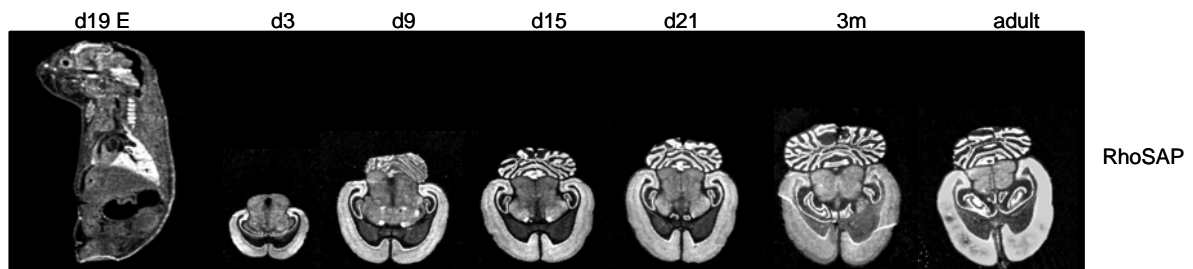
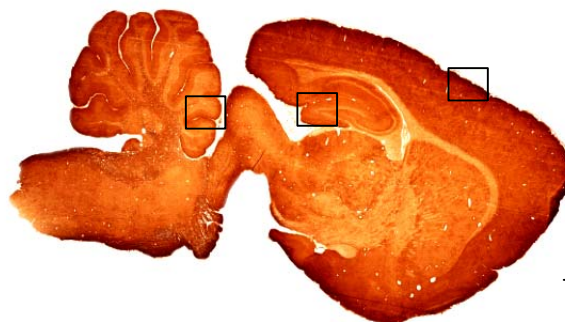


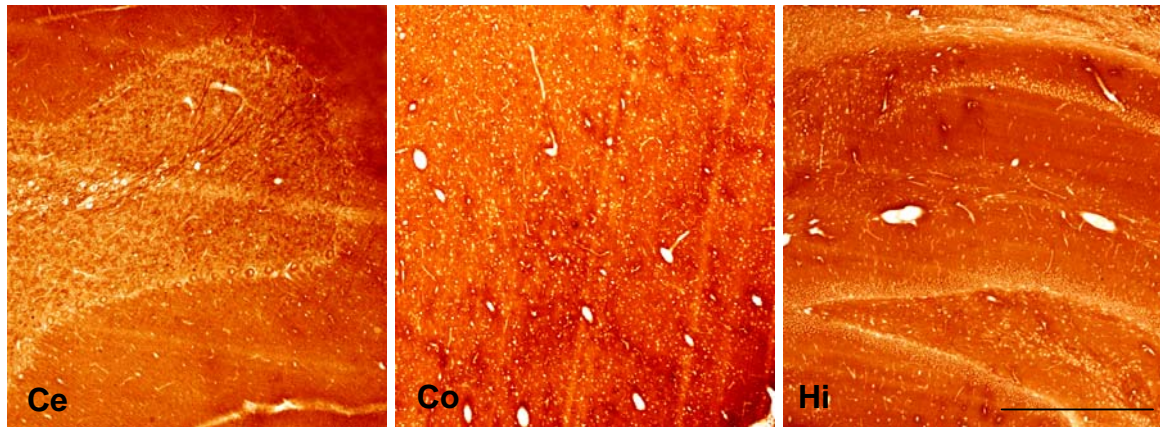
Fig. 3-11 Study on the RhoSAP expression pattern in different brain regions in a developmental time frame. RhoSAP gene expression was demonstrated by *in situ* hybridization of horizontal brain tissue cryosections with a RhoSAP-specific oligo (2.2.9). A 19 days old embryo (d19E), postnatal day 3, 9, 15 and 21 (d3-d21), 3 months and 1 year (adult) old brains were utilized for 8 μ m thick cryoslices. Distribution of RhoSAP mRNA was mainly concentrated in cerebellum, hippocampus and cortex.

In correspondence, the performed DAB staining confirmed that cortex, cerebellum and hippocampus show a regular expression pattern of RhoSAP. Differing from the former time line observation, specific patterns at different developmental stages (16 days, 3 months, 1 year) were not detectable. Purkinje cell layer in cerebellum was detected by anti-RhoSAP as well as hippocampal specific regions as CA1, CA2, CA3 and the dentate gyrus.

A



B



C

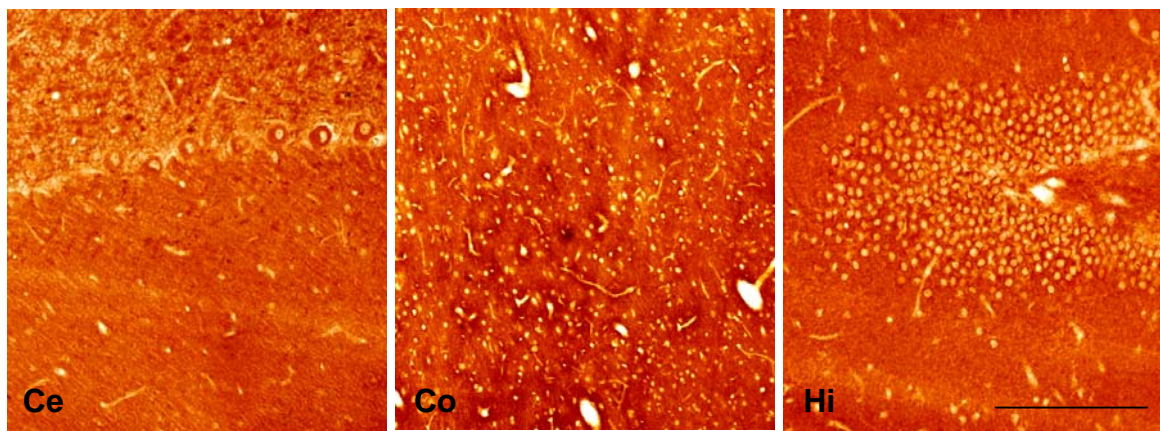


Fig. 3-12 Immunohistochemical labeling with 3,3-deaminobenzidine of frontal rat brain sections using rabbit anti-RhoSAP. The RhoGAP protein RhoSAP is widely abundant in the rat brain. Illustrations depicting parts of the cerebellum, the cortex and the hippocampus prove, the protein is highly expressed in specialized brain areas. Anti-RhoSAP 1:1000; scale bar (A) 5 mm and (B) 500 μ m and (C) 250 μ m resolution.

To analyze the developmental expression profile on protein level in cortex, cerebellum and hippocampus, rat homogenates were tested by Western blotting. Strikingly, in cortex and hippocampus, RhoSAP is not expressed at the embryonic stage of development, but was first detected at day 4. Comparing both brain regions, hippocampus amazingly expresses only the 90 kDa sized variant of RhoSAP, whereas cortex showed the brain specific band of 120 kDa, too. The protein expression pattern of cerebellum differs strongly from the other regions considered. Firstly, there is less protein expression in general due to weaker bands correlating with a smaller amount of RhoSAP being present in cerebellum. Moreover, the molecule was already detected in the embryo stage. From this stage on until day 4, two protein forms of 120 kDa and 130 kDa were found as well as the typical 100 kDa protein which was detected as the third protein variant at day 4. Continuing the time line, the 130 kDa band of RhoSAP vanished at day 8, 16 and after 1 month, to reappear after 1 year of development again. The same was valid for the 100 kDa band which

disappeared in 1 month old animals and was redetected in adult cerebellum homogenate. These results point out that RhoSAP does not only exist as one form of protein, but there are putative protein variants.

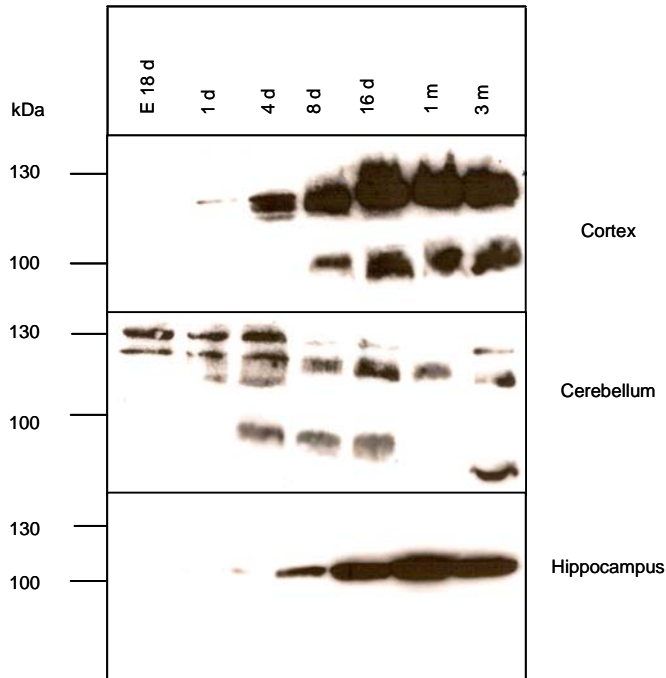


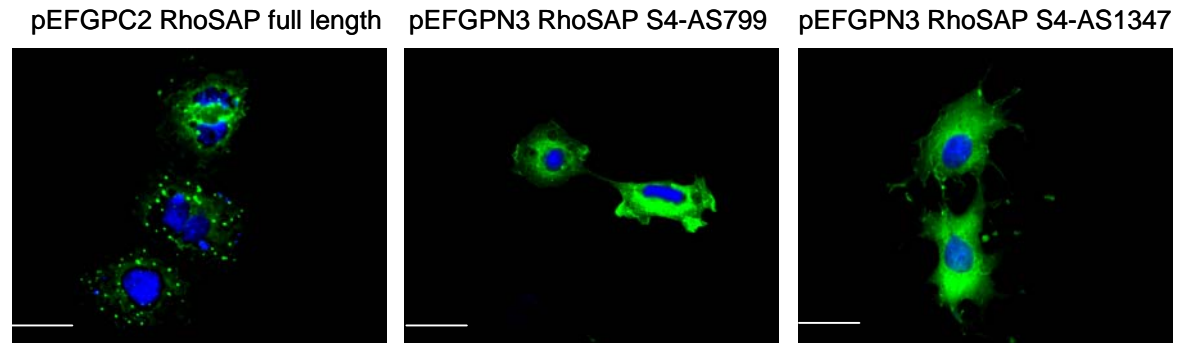
Fig. 3-13 Time line of RhoSAP protein expression in cortex, cerebellum and hippocampus. A total amount of 20 µg cortex, cerebellum and hippocampal tissue lysate was applied on a 10% SDS gel for Western blot analysis (anti-RhoSAP rabbit: 1:5000). Only one variant of RhoSAP is highly enriched in the developing hippocampus (100 kDa) but cannot be found in embryo and at postnatal day 1 and 4. This is similar to the protein's expression profile in cortex which not only contained a 100 kDa band at postnatal day 8 until 3 months (d8-3m) but an additional band at 120 kDa. In contrast cerebellum's profile significantly deviated from cortex and hippocampus.

3.1.7 Recombinant expression of RhoSAP in COS7 cells

Postulating a specific localization pattern of recombinant RhoSAP proteins, COS7 cells were firstly transfected with GFP with RhoSAP fusion proteins of different sizes. Constructs were generated by cloning RhoSAP DNA fragments *via EcoRI* and *Sall* restriction sites into the pEGFPC2 vector, tagging GFP to the N-terminus of the fusion protein. This seemed to be disturbing, regarding the low transfection efficiencies and partially lethal effects, these plasmids caused on the transfection outcome. A specific feature was the observation that transfecting the RhoSAP full length construct, cloned into pEGFPC2, resulted in the expression of RhoSAP at certain spots where it seemed to accumulate. Opposite to this observation was the finding of relatively homogenous transfections when using pEGFPN3-RhoSAP constructs. In this case, the GFP was tagged

C-terminal. In general, no significant differences were observed concerning the cell lines. HeLa or COS7 cells led to the same findings.

A



B

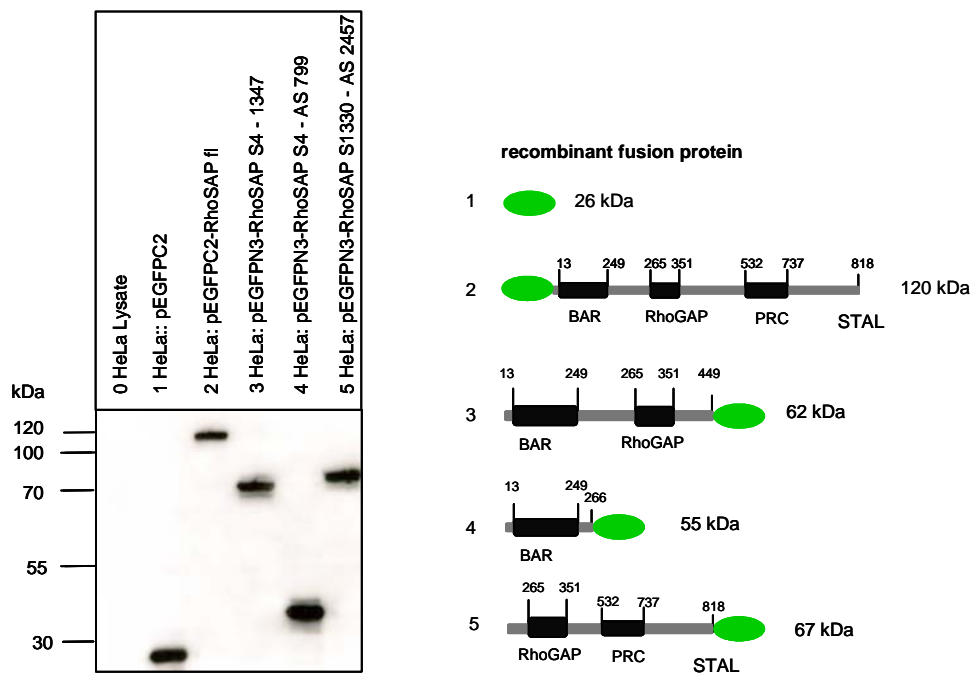


Fig. 3-14 Expression analyses of GFP-RhoSAP fusion proteins in HeLa cells. (A) HeLa cells were transfected with the expression plasmids as indicated above in the pictures. To visualize the cell nuclei, DAPI staining (1:10000) was performed. N-terminal fusion of GFP to RhoSAP full length resulted in a dot (accumulated RhoSAP) signal that was spread around the nucleus and throughout the whole cell. This was found to be true not for all transfected HeLa cells in the case of pEGFPC2-RhoSAP full length. (B) Western blot analysis: HeLa cells were transfected with different sized expression plasmids of RhoSAP, as given in the blot figure. Recombinant fusion proteins and corresponding molecular weights resulting from the expression of pEGFP-RhoSAP constructs are illustrated next to the Western blot diagram. Expressions were tested by anti-GFP (1:1000) directed against the GFP tags of each fusionprotein. 10 μ g of HeLa lysate was loaded on each lane of a 10% SDS gel. Pure HeLa lysate serves as negative control and HeLa lysate transfected with pEGFPC2 alone was used as reference. Scale bar 20 μ m.

3.1.8 Localization of RhoSAP in hippocampal neurons

RhoSAP was identified through a yeast two-hybrid screen using the PDZ domain of ProSAP2/Shank3 as bait. This protein interaction domain is characteristic for proteins of the PSD which may recruit receptors and adhesion molecules through interaction with a corresponding C-terminal PDZ-interacting motif. By using hippocampal neurons as a model system to investigate the localization of RhoSAP and to study possible interactions with proteins of the PSD, RhoSAP was overexpressed as full length GFP-fusion protein firstly. It was confirmed that RhoSAP distributes in the soma of developing neurons and localizes in dendrites, too. In some dendritic parts, the protein was found to localize relatively homogeneous. However, RhoSAP was also accumulating at specific points causing a dotted pattern in some areas of the dendrite.

Unfortunately, overexpression of pEGFP-RhoSAP constructs of different lengths turned out to be difficult due to the observation, that hippocampal neurons mostly died some hours after transfection. This might also explain low transfection rates, so that transfection procedures itself were undertaken at day 1 or 2 of neuronal development to be analyzed after 7 days at the latest.

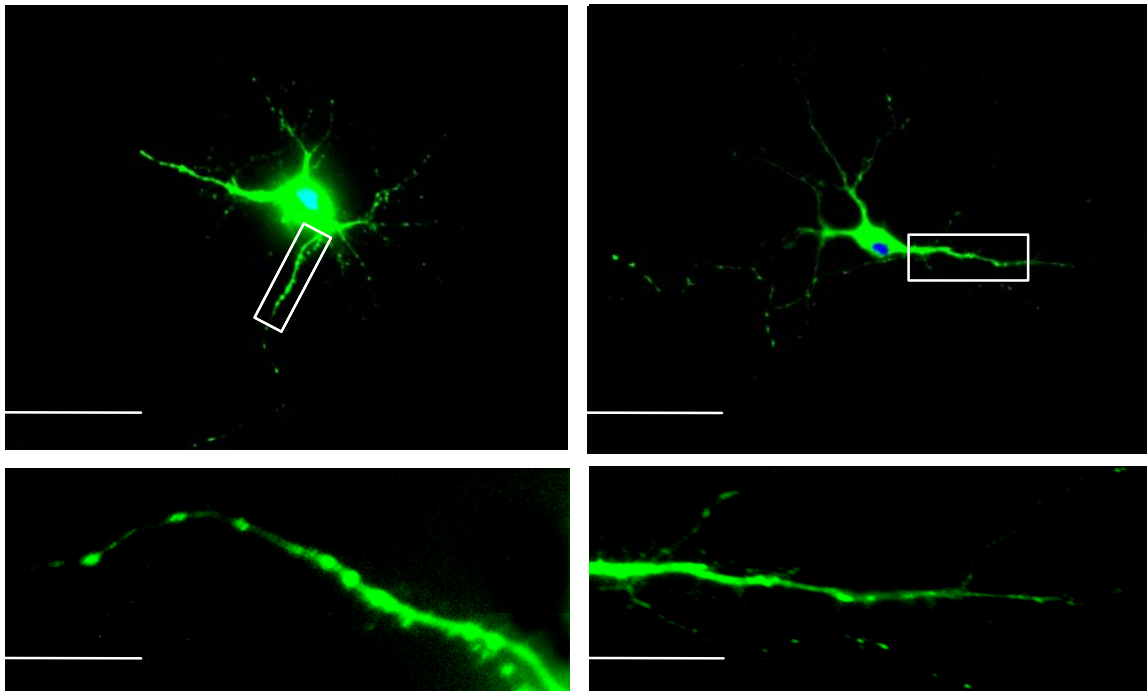


Fig. 3-15 Overexpressed RhoSAP-GFP in hippocampal neurons. 1 day old hippocampal neurons at a density of 6×10^4 cells/ well were transfected with full length RhoSAP-pEGFP constructs and continuously cultured for 1 week at 37°C (3.2 % CO₂). Cells were then fixed in 4% paraformaldehyde, sealed with MOLWOL containing DAPI and analyzed by fluorescence microscopy. Transfection rate was < 1%. Scale bar 20 µm.

Moreover, it was shown that RhoSAP is expressed endogenously in hippocampal neuron culture. The molecule was not detected before day 3 of differential development with a signal at 120 kDa.

The protein expression augmented successively from day 7 until day 14. Surprisingly, a second signal emerged at 100 kDa corresponding to an alternative spliced variant of RhoSAP. At day 14, the protein species of 120 kDa size, almost vanished.

From day 21, the amount of expressed protein began to decline. At day 21 of hippocampal neuron differentiation, only one band could be observed at 100 kDa which is weaker than the signals found at day 7 and 14. Furthermore, the second band at 120 kDa, completely disappeared.

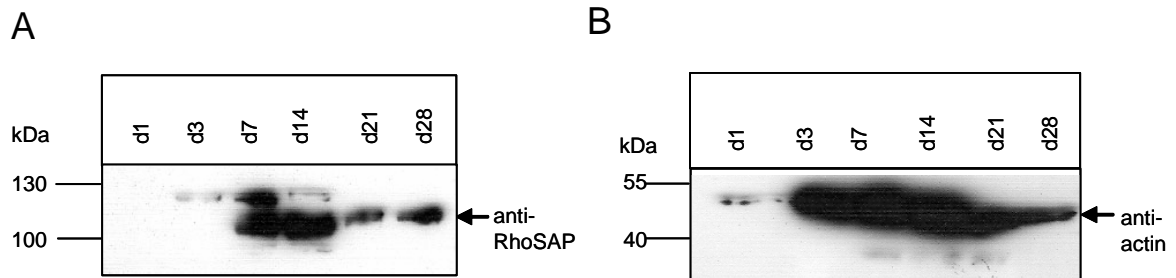
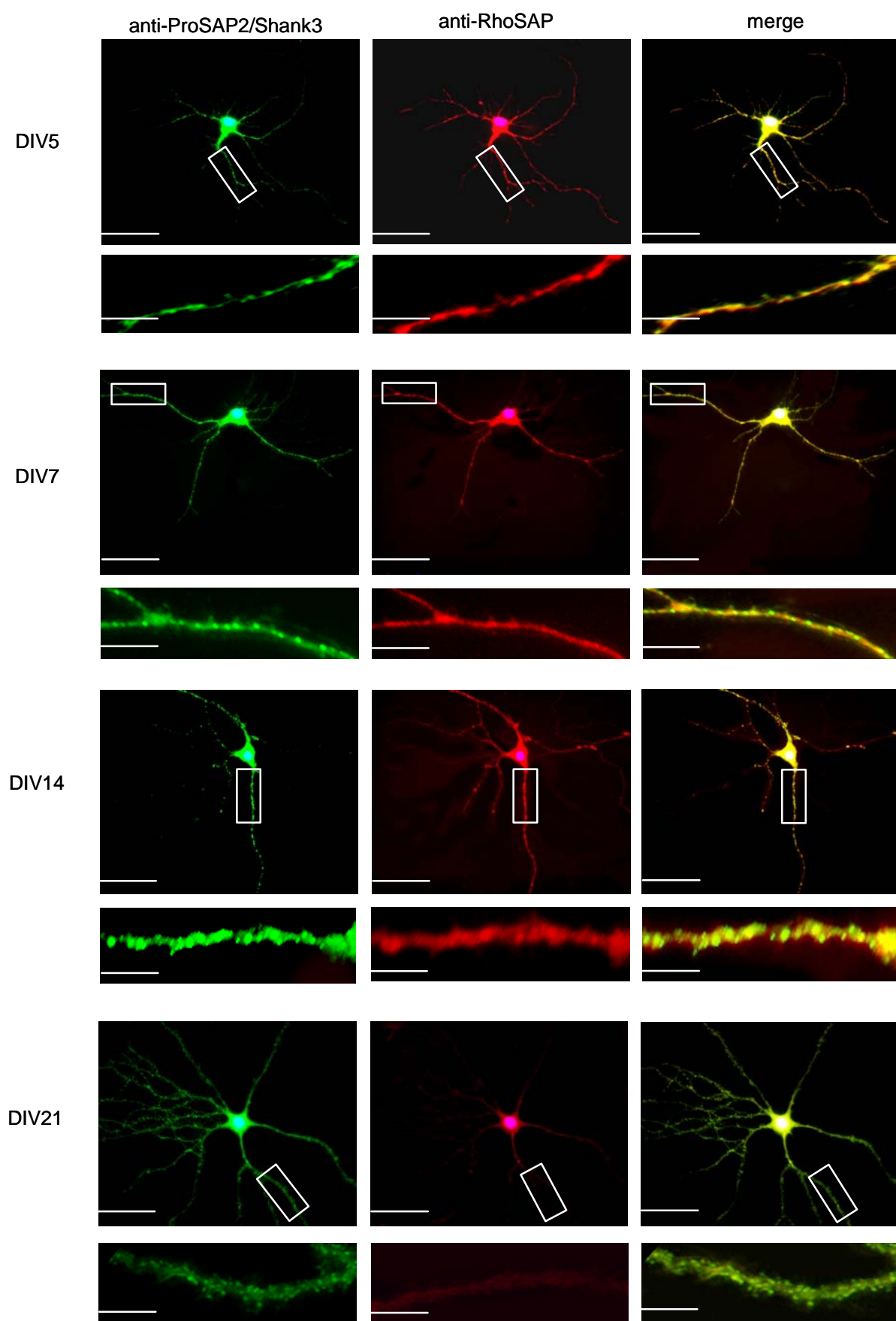


Fig. 3-16 Time line of RhoSAP in primary hippocampal neuron culture. (A) Cell lysate from cultured hippocampal neurons at d1, d3, d7, d14, d21 and d28 of differentiation were analyzed by Western blot (10 μ g total protein per lane; anti-RhoSAP was used 1:2500). The endogenous expression level of RhoSAP increases from day 3 and declines at d21 again. Note the two variants of protein are expressed at d7 and d14 whereas at d3, the 120 kDa variant is observed only and later on from d21, the 100 kDa protein is detected. (B) Referentially, the same lysates were examined by anti-actin (1:5000) to assure that probes had been prepared carefully and the same amounts of protein had been applied on the SDS gel.

To further characterize the localization of RhoSAP at the synaptic level, primary hippocampal neurons were co-immunostained with anti-RhoSAP, anti-ProSAP2/Shank3 as postsynaptic and anti-Bassoon as presynaptic markers, respectively, to find out whether RhoSAP was a genuine postsynaptic molecule. Besides the finding, it was localized postsynaptically using anti-ProSAP2/Shank3 as PSD marker, the whole coimmunostaining performed in a time line frame, clearly showed that RhoSAP started to vanish from the PSD at d21. That is why colocalizations were not detected in hippocampal neurons older than 3 weeks.

Some postsynaptic molecules could be found at the presynapse, too. To investigate, if this was the case for RhoSAP, anti-Bassoon representing a presynaptic molecule was utilized in another developmental study to verify that RhoSAP is a postsynaptic molecule. Coimmunostainings did not reveal any colocalizations with Bassoon.



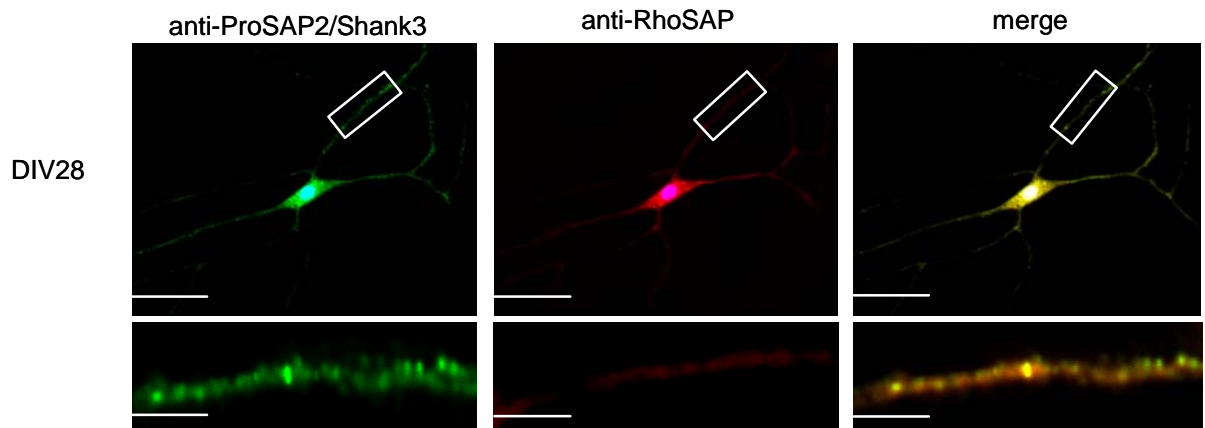
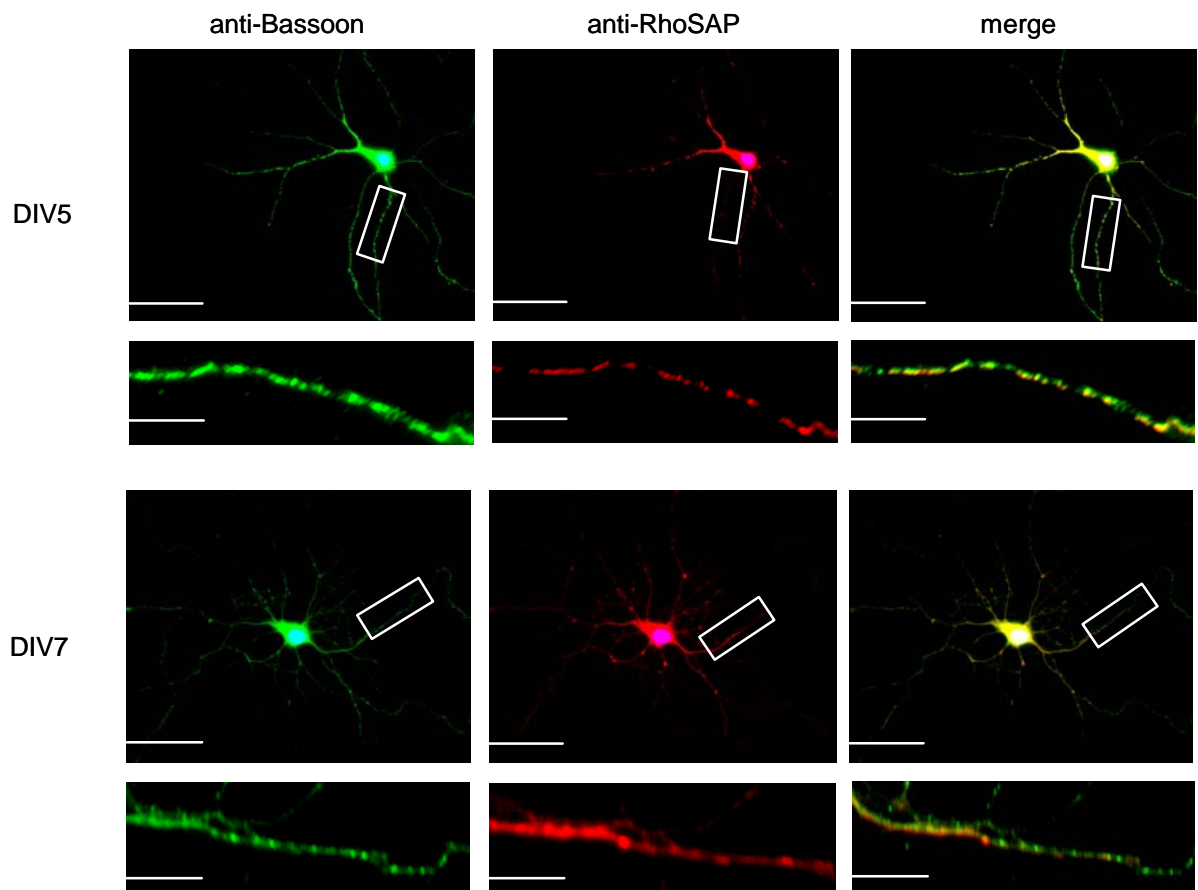


Fig. 3-17 Time line of RhoSAP and ProSAP/Shank3 colocalizations. Colocalization pattern of RhoSAP and ProSAP2/Shank3 in hippocampal neurons. The coimmunostainings were performed at day 5 (DIV5), 7 (DIV7), 14 (DIV14), 3 weeks (DIV21) and 1 month (DIV28) old cells. Anti-RhoSAP was used in a dilution of 1:4000 to be counterstained with Alexa-568-anti-rabbit 1:1000. Anti-ProSAP2/Shank3 was used 1:1000 and was coimmunoprecipitated by Alexa-488-anti-rabbit in a dilution of 1:1000. Hippocampal neurons were cultured in 24-well plates at a cell density of 4×10^4 cells/well. Fixation in 4% paraformaldehyde was followed by coimmunostainings and DAPI treatment to visualize the nucleus in vital cells.



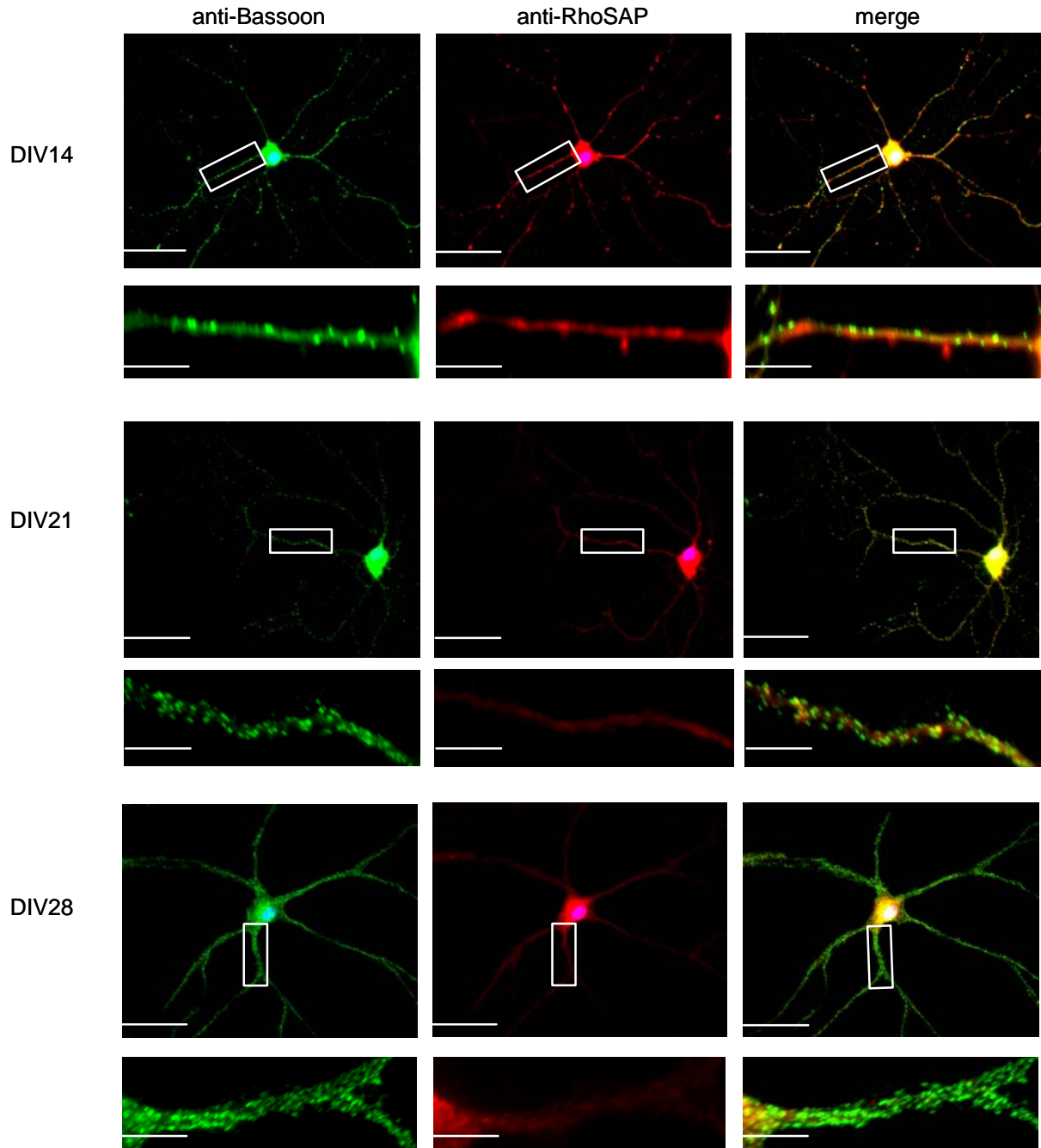


Fig. 3-18 Time line of RhoSAP and Bassoon localization. Localization pattern of RhoSAP and Bassoon in hippocampal neurons. The coimmunostainings were performed at day 5 (DIV5), 7 (DIV7), 14 (DIV14), 3 weeks (DIV21) and 1 month (DIV28) old hippocampal culture. Anti-RhoSAP was used in a dilution of 1:4000 to be counterstained with Alexa-568-anti-rabbit 1:1000. Anti-Bassoon was used 1:1000 and was coimmunoprecipitated by Alexa-488-anti-rabbit in a dilution of 1:1000. Hippocampal neurons were cultured in 24-well plates at a cell density of 4×10^4 cells/well. Fixation in 4% paraformaldehyde was followed by coimmunostainings and DAPI treatment to visualize the nucleus in vital cells.

3.1.9 Subcellular distribution of RhoSAP in neurons

To confirm the result that RhoSAP was a postsynaptic molecule, subcellular neuronal fractions were continuously purified by ultracentrifugation and extraction steps. PSD fractions were stepwise highly enriched from light membrane homogenate containing soluble postsynaptic and presynaptic proteins from the synaptic proteins.

Through Western blotting with anti-RhoSAP, the molecule was detected at a very weak level in PSD fractions as compared to the high abundance in synaptosome enriched protein fraction. This could mean, RhoSAP is associated with the insoluble part of the PSD protein network anchored to the synaptic membrane. As control, an anti-ProSAP2/Shank3 was immunoprecipitated with subcellular fractions to characterize the quality of the PSD fractionation.

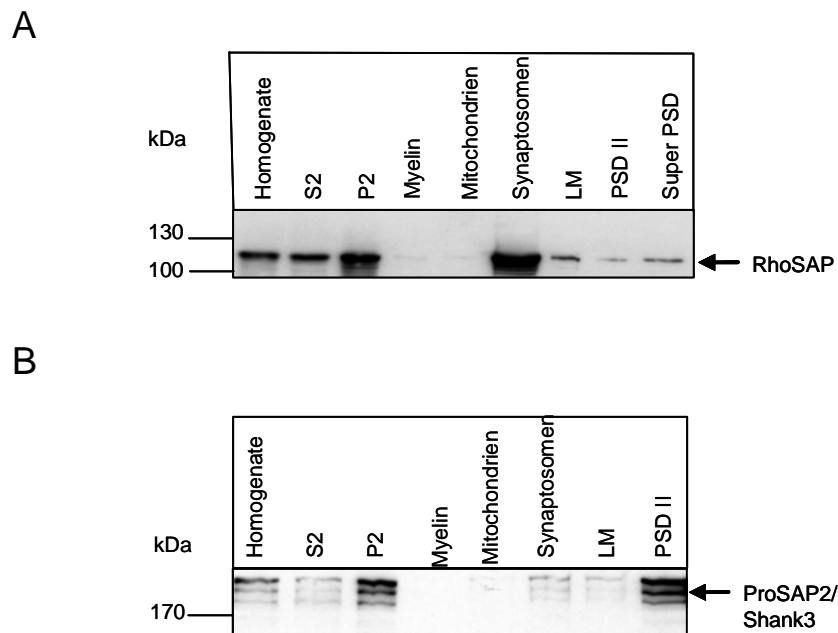


Fig. 3-19 Biochemical detection of RhoSAP in subcellular protein enriched fractions of the rat brain. Subcellular ultracentrifugally purified fractions: homogenate, S2 (soluble fraction), P2 (second pelleted fraction), myelin, mitochondria, synaptosomes, light membrane and postsynaptic densities fractions (PSD II, Super PSD) have been loaded with 20 µg protein per lane on a 10% SDS gel for Western blot analysis. Anti-RhoSAP rabbit was diluted 1:4000. A second Western blot was carried out as a control by using anti-ProSAP2/Shank3 (1:1000) as a prominent PSD marker. Enrichment in PSDs has been verified. (A) Anti-RhoSAP Western blot. (B) Anti-ProSAP2/Shank3 Western blot to testify each fractions quality and verify enrichment of postsynaptic membranes.

Furthermore, EM investigations with 3 weeks old hippocampal neurons were in accordance to the results pointing out to a postsynaptic localization of RhoSAP. In several studies, preembedding staining with anti-RhoSAP showed a punctuate signal in dendrites and the postsynaptic density. To underline the specificity of this result, cell nuclei were analyzed to demonstrate that stainings did not occur in this part of the neuron. Additionally, stainings in postsynaptic densities appeared irregularly, so that less than 10% of the analyzed neurons showed a clear localization of RhoSAP in the PSD.

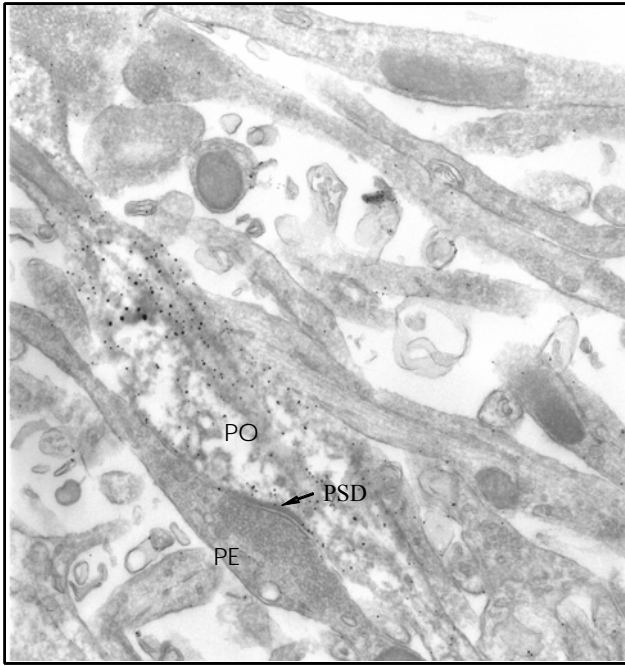
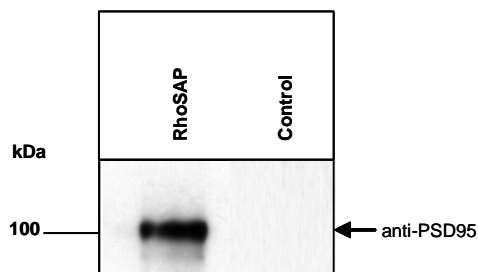


Fig. 3-20 RhoSAP signal detection in the postsynapse by electron microscopy. 70 nm ultra-thin sections of rat hippocampal neurons were electronmicroscopically investigated using the pre-embedding procedure. Anti-RhoSAP was diluted 1:1000. Magnification $\times 25,000$ and $\times 90,000$; PO: postsynapse, PE: presynapse.

To further clarify whether RhoSAP was a molecule related to other postsynaptic proteins, coimmunoprecipitations of RhoSAP with PSD95 and coimmunostainings of hippocampal neurons were performed. The precipitation study resulted in the detection of a 95 kDa sized band in Western blot analysis. The staining of postsynaptic densities by anti-PSD95 coincided with the signal from RhoSAP, which confirmed that RhoSAP is present in a PSD complex. Together with the preceding data, these observations reinforced the suggestion that RhoSAP is a molecule related to the PSD.

A



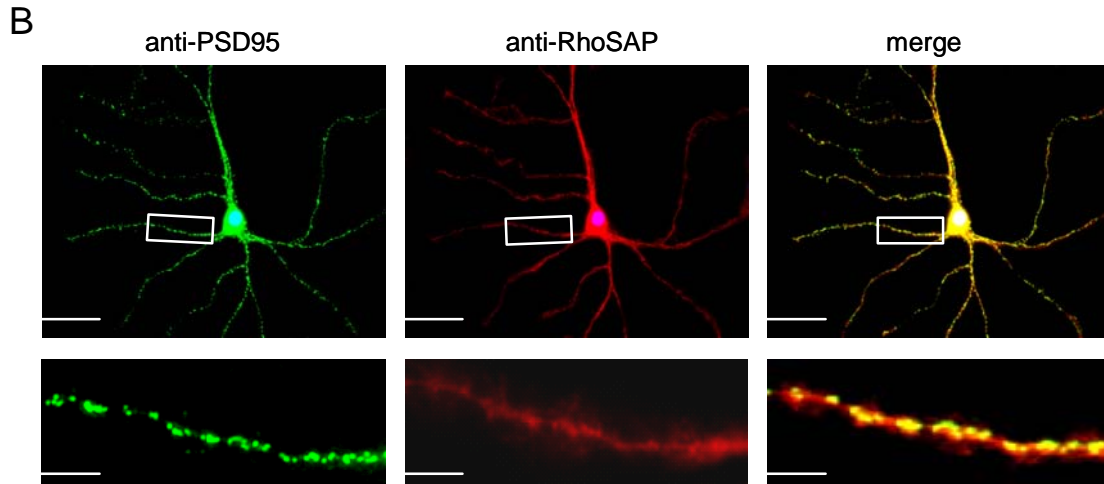


Fig. 3-21 Association of RhoSAP with PSD95 and visualization of RhoSAP's presence in synaptic spines. (A) To analyze RhoSAP's association with the PSD95 complex at postsynaptic sites, the molecule was coimmunoprecipitated with a scaffold marker of the postsynapse: PSD95. By Western blot investigation, a signal at 95 kDa was detected in the coimmunoprecipitate, demonstrating an associative link between PSD95 and RhoSAP. (B) In 14 days old hippocampal neuron culture, PSD95 and RhoSAP clearly colocalize in dendritic spines, observable all along the dendritic arbor. Anti-PSD95 was diluted 1:1000, anti-RhoSAP 1:4000. Scale bar corresponds to 25 μm in the overview, to 10 μm in the insert.

3.2 Isolation and analysis of RhoSAP's protein interaction partners

3.2.1 Verification of RhoSAP's association with ProSAP2/Shank3

To further examine whether ProSAP2/Shank3 and RhoSAP were abundant together in a complex, biochemical coimmunoprecipitation studies were performed. ProSAP2/Shank3 was found to co-immunoprecipitate with RhoSAP. The protein was mapped as the typical triple band at 170 kDa on a Western blot. That finding indicated that ProSAP2/Shank3 must be one associative molecule in a broader protein complex that comprises more than protein molecules next to RhoSAP. However, no signal could be observed using anti-ProSAP2/Shank3 to coimmunoprecipitate RhoSAP. As a result, anti-RhoSAP did not reveal a band at 100 kDa and/or 120 kDa, respectively, by Western blotting.

Another hint of relevance showing an association was noted by pull-down data. Coupling RhoSAP-GFP recombinant protein to magnetobeads and incubating with overexpressed ProSAP2/Shank3-GFP lysate resulted in the detection of three bands at 170 kDa when analyzing the coimmunoprecipitates with anti-ProSAP2/Shank3 on a nitrocellulose membrane. Interestingly, the *vice versa* assay did not lead to the detection of a band for RhoSAP. That might be due to stereochemical reasons preventing correct hydrophobic interactions so that both molecules are behaving associative.

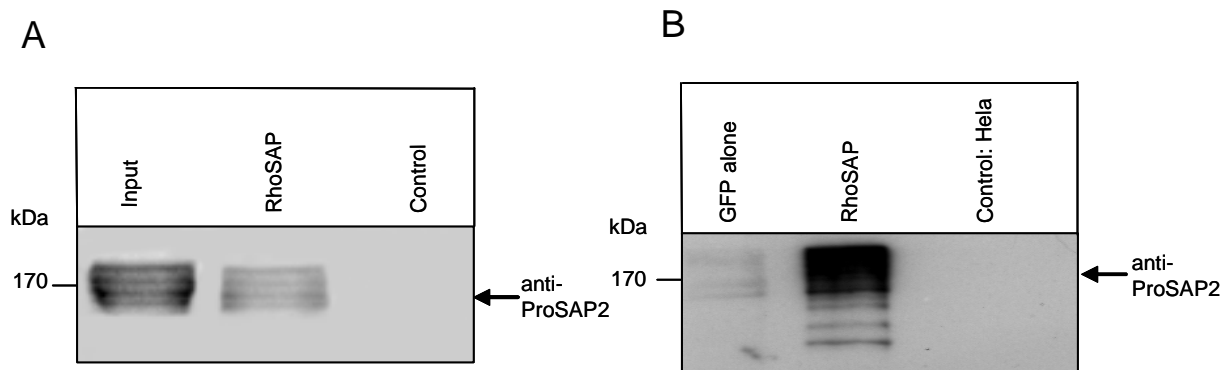


Fig. 3-22 Coimmunoprecipitations from rat brain lysate; pull-down experiment with RhoSAP-GFP and colocalization study of syndapin-GFP and pDsRed-PDZ domain. (A) Coimmunoprecipitations of ProSAP2/Shank3 from rat brain lysate with μ MAC coupled anti-RhoSAP. Pure rat brain lysate as input subjected to anti-ProSAP2/Shank3 (1:1000) revealed the typical triple band at 170 kDa. RhoSAP coimmunoprecipitated with ProSAP2/Shank3 in comparison to empty μ MAC beads, which did not precipitate as no signal was detected. (B) Pull-down analysis: RhoSAP-GFP immunoprecipitated with ProSAP2/Shank3 (antibody was used 1:1000).

3.2.2 Identification of novel binding partners by a yeast two-hybrid screen

To identify proteins that interact with RhoSAP's C-terminus, a GAL4-BD construct (pACT-2) coding for the sequence segment: 442 aa - 818 aa, including the proline rich clusters and the STAL PDZ binding motif was used as bait in a yeast two-hybrid screen of a rat brain cDNA library. The bait construct was transformed into Y187 yeast cells whereas AH109 served as host for rat brain cDNA library.

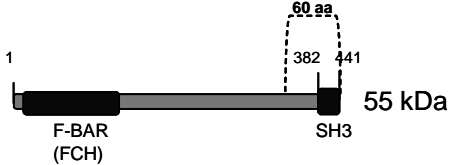
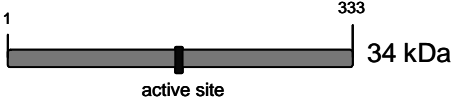
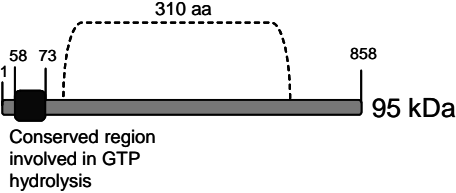
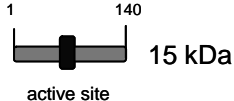
Of 6.4×10^6 transformants that were screened, 82 colonies of mated yeast grew on leucine, tryptophan and histidine negative agar plates and activated β -galactosidase. Subsequent preliminary *EcoRI/XhoI* restriction analysis, revealed 28 clones which were further investigated by DNA sequencing to discover their corresponding protein function.

One of the prey sequences coded for full length syndapin I (*S. sapiens*) and Pacsin 1 (*R. norvegicus*), respectively. It is an FCH and SH3 domain containing protein that has been described to be an important mediator for dynamin I and contributes to linking endocytosis to cytoskeletal dynamics (Kessels & Qualmann, 2006).

The 441 aa long protein and its SH3 domain mapped to the proline rich clusters located in the C-terminal part of RhoSAP.

Gliap, Cystatin C and EF-2 were among the other identified proteins which had been described as functional molecules and showed an open reading frame in the pACT2 vector (prey) when analyzing there sequences in pACT-2.

Tab. 3-1 Molecules interacting with RhoSAP's C-terminus (yeast two-hybrid screen)

Name of the prey protein/ Accession Number of EMBL-EBI Bank	Number of clones found in the Y2H	Functional profile of the interacting protein	Domain structure of the prey protein
Syndapin I (AF139492)	1 (#71-5)	<ul style="list-style-type: none"> - plays a role in vesicle formation and transport - binds dynamin I, synaptojanin, synapsin I and N-WASP - homo- and heterodimerizes with other Syndapins 	 <p>55 kDa</p>
Gliap (AJ427914)	2 (# 69-1; # 73-1)	<ul style="list-style-type: none"> - L-asparaginase that might be involved in astroglial production of L-aspartate which in turn acts as an excitatory neurotransmitter in brain 	 <p>34 kDa</p>
EF2 (AF000576)	1 (#43-1)	<ul style="list-style-type: none"> - GTP-binding elongation factor that interacts with release factors that bind to ribosomes to induce release of the peptide 	 <p>95 kDa</p>
Cystatin C (BC101872)	2 (#12-1; #47-1)	<ul style="list-style-type: none"> - inhibitor of cysteine proteinases and acts as local regulator of this enzyme activity - inhibits cathepsins B, H and L 	 <p>15 kDa</p>

3.2.3 Confirmation of RhoSAP interaction with syndapin I

To test further for an association between RhoSAP and syndapin I that were found to interact in a yeast two-hybrid system, coimmunoprecipitation and pull-down investigations were undertaken. Immobilizing anti-RhoSAP to Protein A and subsequent incubation with rat brain lysate, showed that syndapin I was a part of the formed protein complexes. As a result, anti-syndapin I had unambiguously detected a band at 55 kDa in a Western blot analyzing the immunoprecipitate. In contrast, the *vice versa* approach, using anti-syndapin I to co-immunoprecipitate RhoSAP did not show a band at 100 or 120 kDa as it was expected.

The same was stated for the pull-down experiment, using immobilized recombinant RhoSAP-GFP and syndapin I-GFP lysate for immunoprecipitation. It was shown that anti-Syndapin I detected the 55 kDa band again, supporting the yeast two-hybrid data found previously. However, immunoprecipitation was not observed *vice versa*. It is important to point out, lysates were purified before applications but despite might have contained endogenous other proteins from the destroyed HeLa cells, next to the actual overexpressed RhoSAP-GFP or syndapin-GFP. Thus, this could explain partially why binding was proved in one direction only.

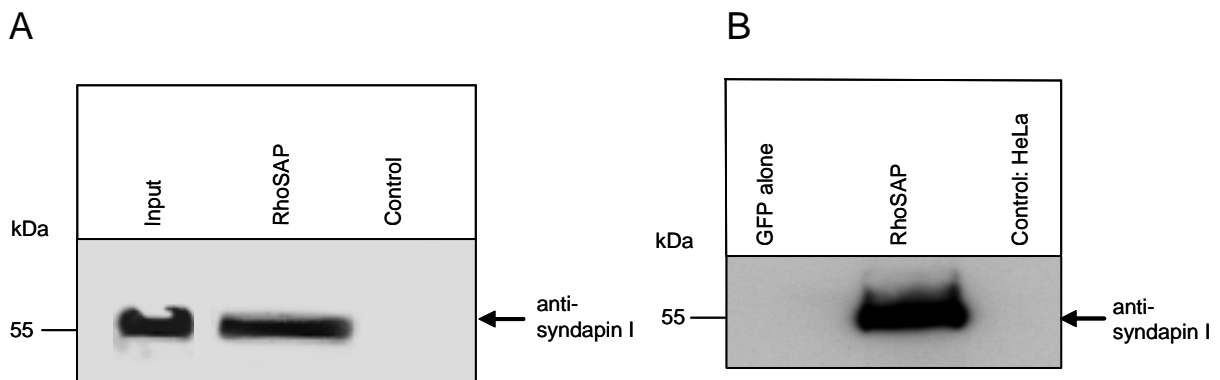


Fig. 3-23 Coimmunoprecipitations from rat brain lysates, pull-down experiment with RhoSAP-GFP and colocalization study of Syndapin-GFP and FlagRich2 which was counterstained with Alexa 647.

(A) Syndapin I was coimmunoprecipitated from rat brain lysates with anti-RhoSAP. The abundance of the 55 kDa sized protein was confirmed in rat brain lysate (input), too. To substantiate the positive signals, a negative probe which did not contain μ MAC beads coupled to anti-RhoSAP but instead beads and rat brain lysate were united alone. After applying each approach on a 12% SDS gel, subjected anti-syndapin I (1:1000) did not detect a signal in the lane of the negative control. (B) Pull-down analysis: RhoSAP-GFP isolated from HeLa cells was incubated with syndapin-GFP, extracted from HeLa cells as well. The following Western blot investigation to track syndapin I (antibody used 1:1000) as associative molecule of RhoSAP, led to the detection of a syndapin I signal at 55 kDa molecular weight. Substituting syndapin-GFP lysate with GFP lysate showed that no band at 55 kDa could be traced in the Western blot analysis.

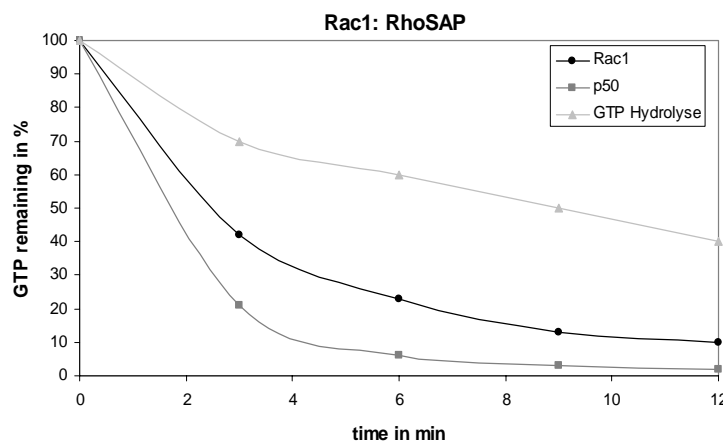
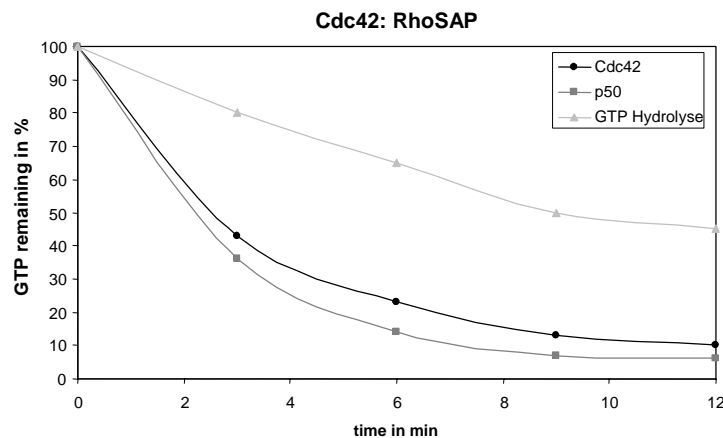
3.3 Functional analysis of RhoSAP

3.3.1 Investigation of GAP activity

To determine the function of the RhoGAP domain of RhoSAP, the *in vitro* GTPase activity using the RhoGAP domain as GST-fusionprotein was tested. When incubated with Cdc42 and Rac1, the RhoGAP domain could significantly stimulate the GTPase activity of both GTPases whereas RhoA failed to show a stimulating effect. The RhoGAP domain proved to have quite similar GAP efficiency toward Cdc42 and Rac1 compared to GTP hydrolysis alone as negative control. After 2 minutes of reaction initiation, nearly 80% of bound radioactive GTP had already been hydrolyzed in presence of RhoSAP's GAP domain. In

contrast, GTP hydrolysis of Cdc42-GTP or Rac1-GTP without RhoGAP only showed intrinsic hydrolysis indicated by 70-80% radioactive GTP remaining bound to the Cdc42 and Rac1. When testing RhoA, presence or absence of recombinant RhoGAP did not yield any differences. By both approaches, it was discovered that not more than 20% of radioactive GTP has been hydrolyzed after 12 minutes of reaction time, meaning intrinsic hydrolysis and RhoA reaction coincided. Conclusively, RhoSAP's GAP domain had no catalytic activity for RhoA.

In addition, the presence of higher concentrations of the RhoGAP domain (1-3 $\mu\text{g}/\mu\text{l}$) strongly triggered the stimulatory effect for Cdc42 and Rac1 compared to RhoA which did not show any enhancement of GTP hydrolysis. These results indicate that RhoSAP's GAP domain is active for some Rho GTPases *in vitro*.



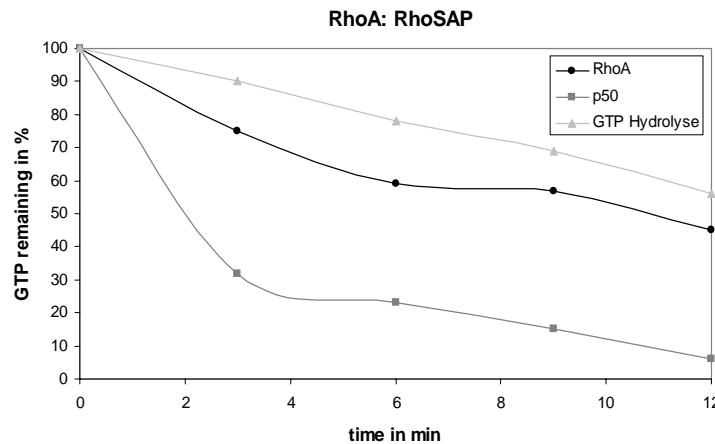


Fig. 3-24 The RhoGAP domain of RhoSAP stimulates Cdc42, Rac1 but not RhoA GTPase activities *in vitro*. The GTPase activities were measured in the presence and absence of the recombinant RhoGAP domain (188 aa: residues 255-445). RhoGAP domain stimulated activities are represented by filled circles, GTP hydrolysis corresponding to the same approach but without GAP protein is represented by closed triangles and in every diagram, p50 GAP stimulating activity is depicted by filled squares. p50 as reference was measured to positively control the experiments. 10 μ Ci of [γ - 32 GTP]-GTP was used per approach.

3.3.2 Investigation of endocytic activity

The initial aim of the endocytosis assay was to explore the potential implication of RhoSAP with respect to endocytic activities.

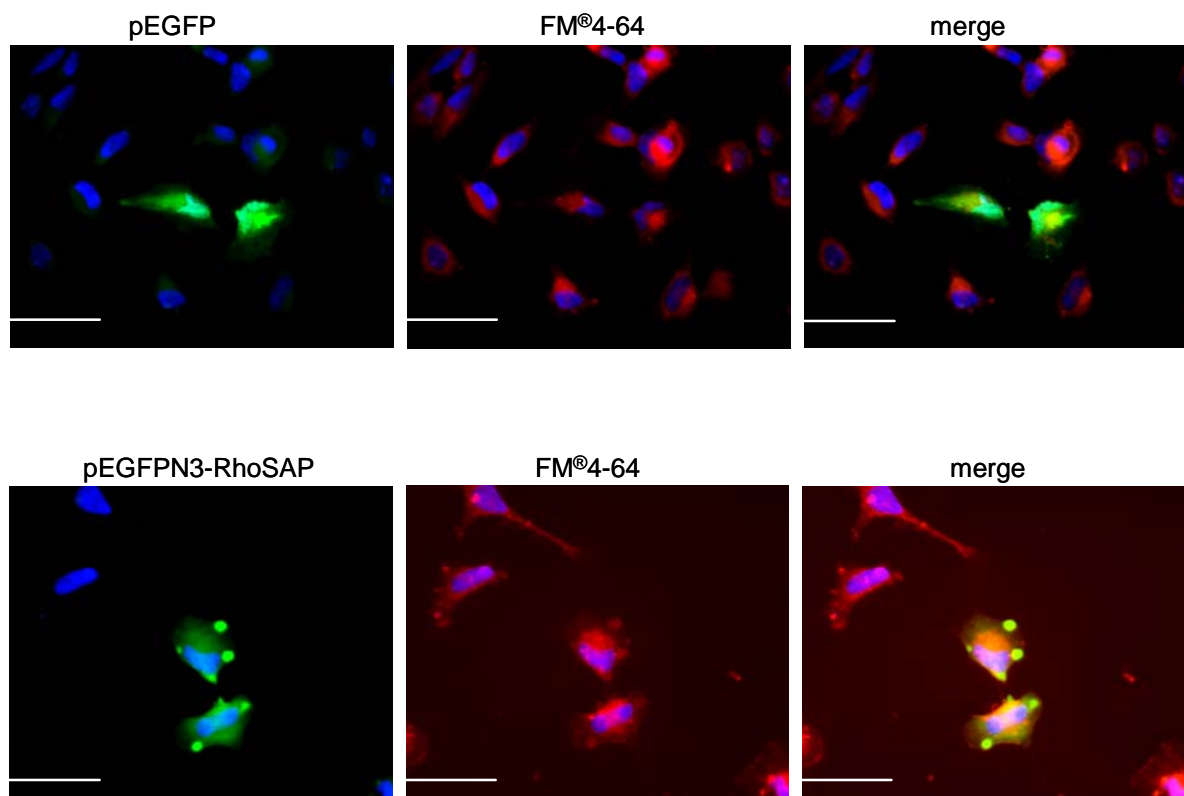
Due to the finding that RhoSAP was in association with ProSAP2/Shank 3 and syndapin I, it was hypothesized that the molecule plays a role in membrane trafficking, mainly in endocytic events, as this is the case for AMPA and NMDA receptor recycling at the synapse. Syndapin I was already described to mediate an interconnection of cytoskeletal rearrangements and endocytosis (Kessels & Qualmann, 2006). It interacts with N-WASP, an F-actin polymerization regulator and dynamin I, a GTPase facilitating vesicles' detachment from membranes. Moreover, dynamin I which is a component of the postsynapse (Gray *et al.* 2003, Peng *et al.* 2004) interacts with ProSAP2/Shank3 (Vallee *et al.*, 2001) and Homer, two important scaffold molecules of the PSD.

In this study, FM[®] 4-64 was used to indicate endocytic activity. Vesicles removed from the cell into the extracellular space after treatment with FM[®] 4-64 that triggered endocytosis. The number of vesicles generated in each approach was counted for 30 cells to conclude indirectly that endocytic activity rested on the same level, increased or decreased during recombinant expression of RhoSAP-GFP, ProSAP-GFP, syndapin-GFP, RhoSAP-GFP with ProSAP-GFP and RhoSAP-GFP with syndapin-GFP, respectively, compared to the control: pEGFP. Transfected cells were identified by their green fluorescent staining.

On the one hand it was explored that RhoSAP-GFP and ProSAP-GFP transfection enhanced vesicle production massively compared to pEGFP as reference and the double transfection approaches, respectively.

On the other hand, the lower rates of formed vesicles in the double transfection approaches did not reflect their huge size that was observed in contrast to the single transfection approaches. It remained speculative to assume that in double transfected assays, vesicles tended to fuse stronger because of a very high endocytic activity. Counting the vesicle numbers always referred to an end point of endocytosis. The course in which vesicles had united was not considered, so that the result of fewer vesicles needed not to necessarily represent a weaker endocytic activity.

Distribution of GFP-proteins being present in the same cells after cotransfection was investigated by Alexa-568 staining that had been done separately with all double transfected approaches. Obviously, cotransfection rates lay between 5-10% for RhoSAP-GFP stained anti-Alexa-568 (red), 10-15% for ProSAP-GFP marked with Alexa-568 red fluorescence and 10-20% for synadpin I-GFP parallel red fluorescently stained, respectively.



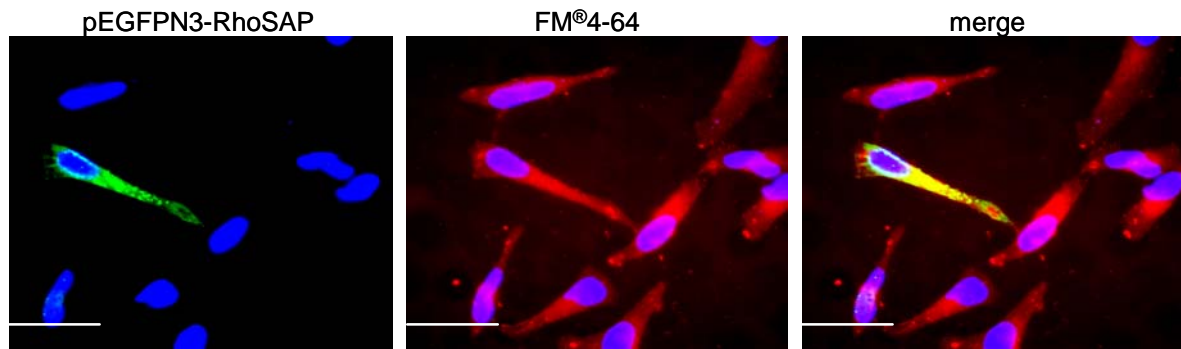
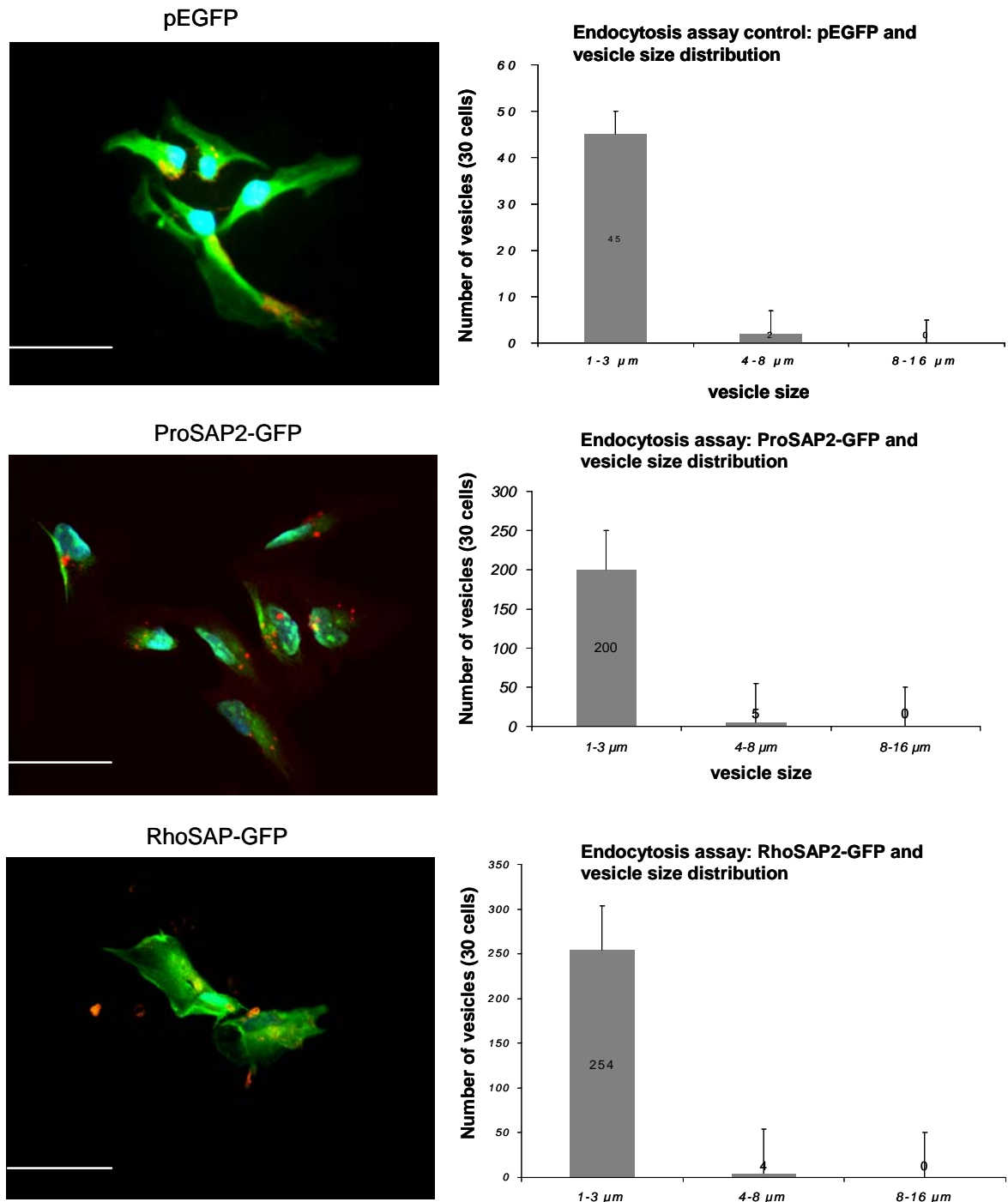


Fig. 3-25 FM4-64 staining of HeLa cells transfected with the RhoSAP full length constructs. HeLa cells were transfected with C-terminally fused GFP RhoSAP constructs. In order to preliminarily elicit if RhoSAP were found to colocalize with endocytic vesicles, cells were treated with FM[®] 4-64 (5 μ g/mL in HBSS) on ice. Reaction ran for 10 minutes. After fixation and analysis, the red fluorescent dye overlapped with the green fluorescent protein signal, both in the cell itself and vesicles taking off during endocytosis. Bar indicates 20 μ m.



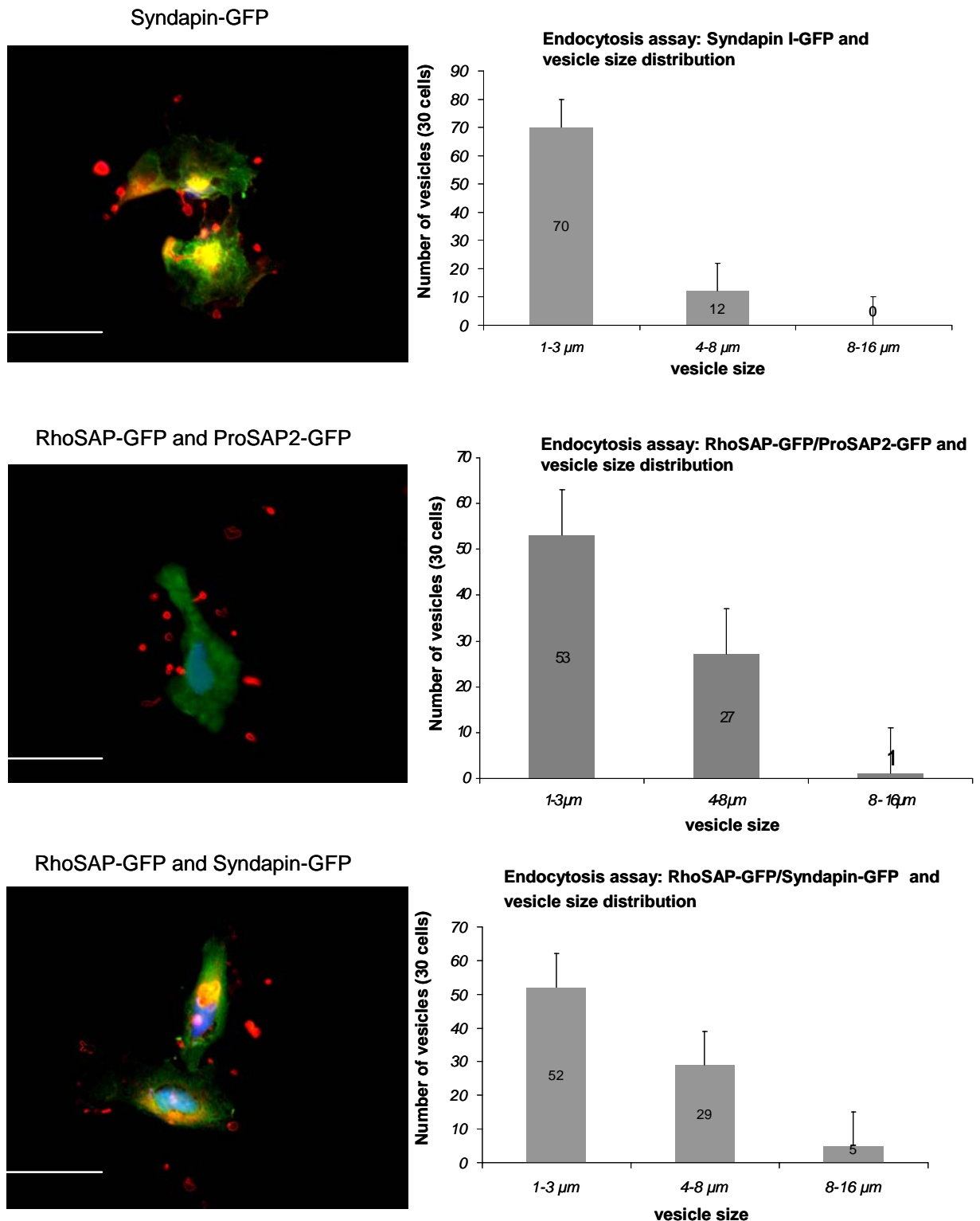


Fig. 3-26 FM[®] 4-64 endocytosis assay to investigate RhoSAP with regard to an endocytic stimulating influence. HeLa cells were single transfected with pEGFP, pEGFP-ProSAP2/Shank3, pEGFP-RhoSAP, pEGFP-syndapin I and double transfected with pEGFP-RhoSAP and pEGFP-ProSAP or pEGFP-syndapin I, respectively. FM[®] 4-64 stainings were performed for 10 minutes. After fixation in 4% paraformaldehyde, endocytic activity was analyzed by fluorescence microscopy through counting all vesicles that had emerged from one cell. For each approach, 30 cells were investigated to determine the statistical significance. Vesicles were divided into three size classes: 1-3 μm, 4-8 μm and 8-16 μm. Vesicle number of RhoSAP-GFP and ProSAP/Shank3-GFP ranges between 200 and 250 compared to 45 vesicles for pEGFP transfected HeLa cells. The majority was sized 1-3 μm. In contrast, double transfections of RhoSAP-GFP and ProSAP2/Shank3-GFP or syndapin I-GFP, respectively resulted in approx 50 vesicles for 30 cells. Double

transfections were undertaken to discover possible mediator effects for RhoSAP association partners. Surprisingly, both double transfection approaches generated a total of about 30 vesicles (30 cells) between 4-8 μm of diameter. This might have been caused by vesicles fusion which could be a sign for high endocytic activity. DNA was stained with DAPI (blue) in all panels. Bar indicates 20 μm . To verify distribution of GFP recombinant expressed proteins, Alexa 568 (red fluorescence) stainings had been performed for one construct each in every co-transfection assay. Transfection rates reached 5-10% for RhoSAP-GFP, 10-15% for ProSAP-GFP and 10-20% for syndapin I-GFP.

To validate the statistical significance of the endocytosis assay, the counted vesicle numbers for each approach were examined by a Mann-Whitney Rank Sum test. Data showed statistical relevance.

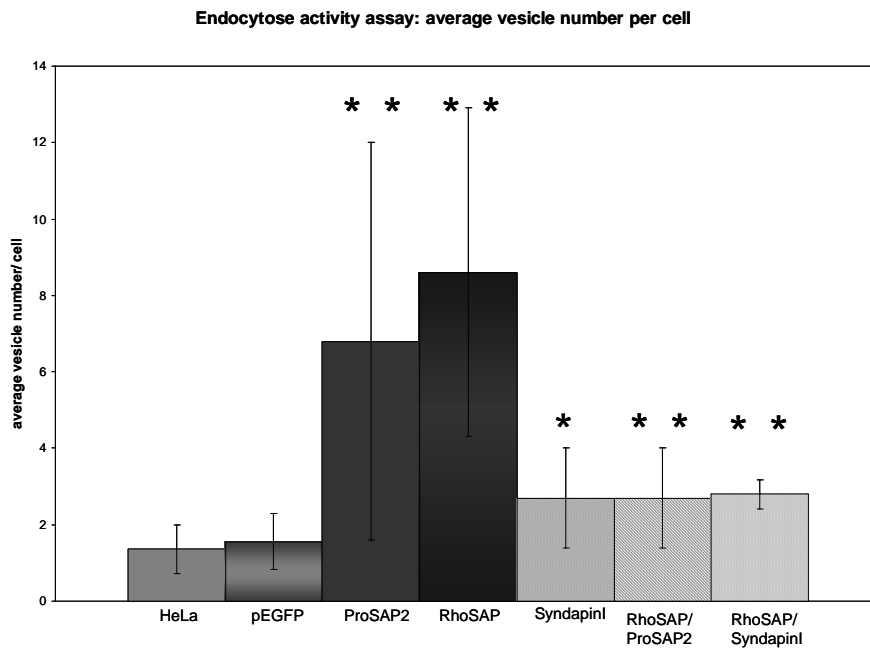


Fig. 3-27 Role of RhoSAP in endocytosis under the additional influence of ProSAP2 and syndapin I.

(C) To prove statistical relevance to decide if endocytosis activity changed for the approaches with the single or double transfection approaches, a Mann-Whitney Rank Sum test underlined statistical significant differences among pEGFP (control) and all other approaches. Asterisks indicate: *p = 0,002 and *p<0,001 relative to control.

3.3.3 Investigation of intracellular membrane trafficking

To explore whether RhoSAP played a role in endocytosis only or was also abundant in endosomal turn-over representing intracellular membrane trafficking, Rab5-GFP and Rab11-GFP had been used to study colocalization. Members of the large Rab family of GTPases regulate trafficking specificity by assembling specific molecular complexes and membrane microdomains (Mohrmann & van der Sluijs, 1999). In the case of Rab5, which mediates endocytic turn-over from the plasma membrane to early endosomes, LTD-inducing stimuli promote GDP-GTP exchange. This in turn activates Rab5 and subsequent signaling cascades are triggered to internalize AMPA receptors (Brown *et al.*, 2005).

To distinguish endogenous RhoSAP from recombinant green fluorescent tagged Rab5 and Rab11 proteins, respectively, it was counterstained by red fluorescent Alexa 568.

Colocalizations were especially observed for co-transfections with Rab5-GFP, evaluating the merged pictures from GFP transfection and Alexa counter staining. As a result, RhoSAP was observed to be in an associative complex with Rab5-GFP. This directs suggestions to further analyze RhoSAP function in endosomal membrane traffic events in the neuron.

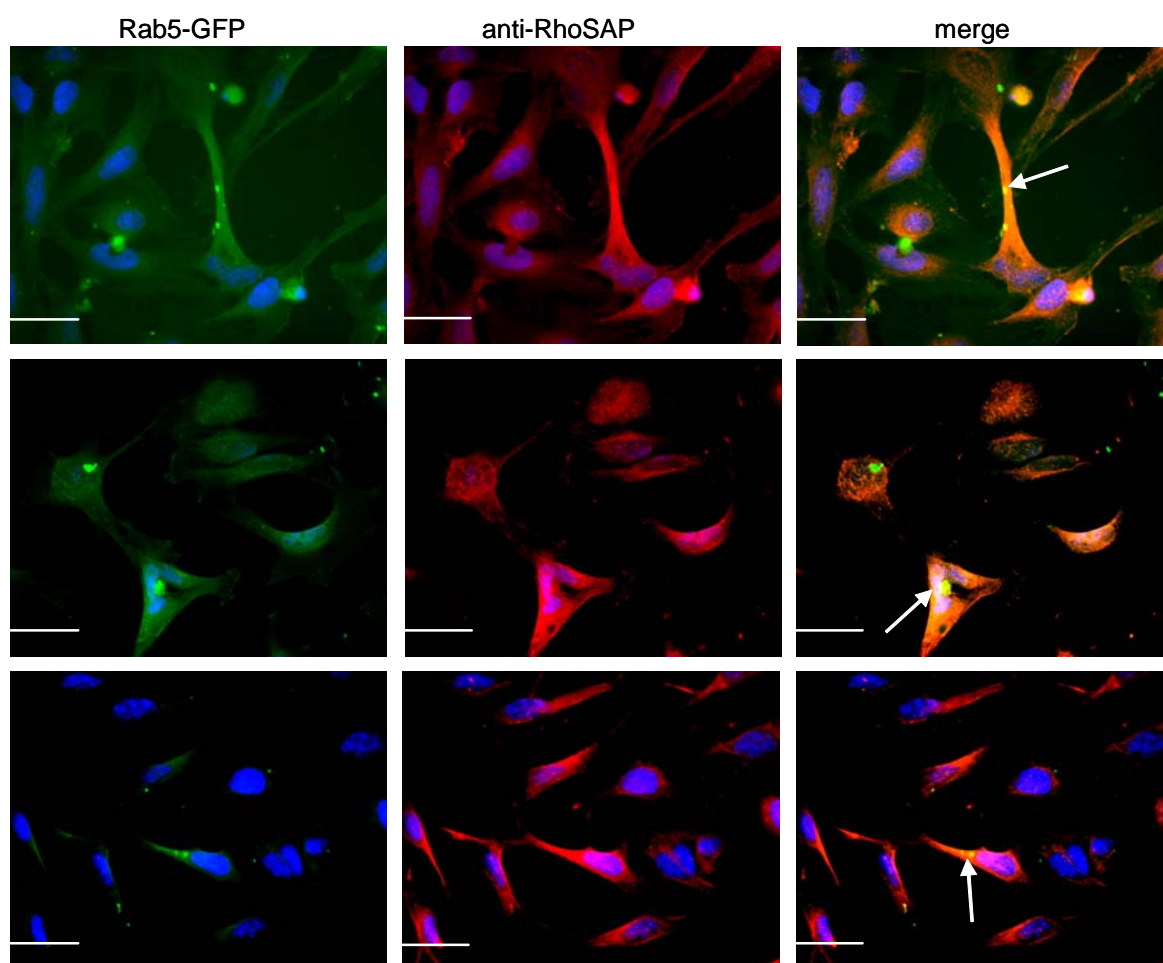


Fig. 3-28 Colocalization of Rab5-GFP and endogenous RhoSAP. Rab5-GFP transfection caused the generation of vesicles, pinching off from HeLa cells. Signaling RhoSAP by counter staining with Alexa 568 (1:1000) clearly determined vesicles with yellow color, indicating Rab5 and RhoSAP were distributed in an associative pattern. Bar determines scale of 20 μm .

3.3.4 Investigation of RhoSAP's effect on the cytoskeleton in cell culture

The actin cytoskeleton mediates a variety of essential biological functions, providing a structural framework for cell shape and polarity, which is the driving force for cells to move and divide. Rho GTPases are key regulators of the actin cytoskeleton, and furthermore, through their interaction with multiple target proteins, they ensure

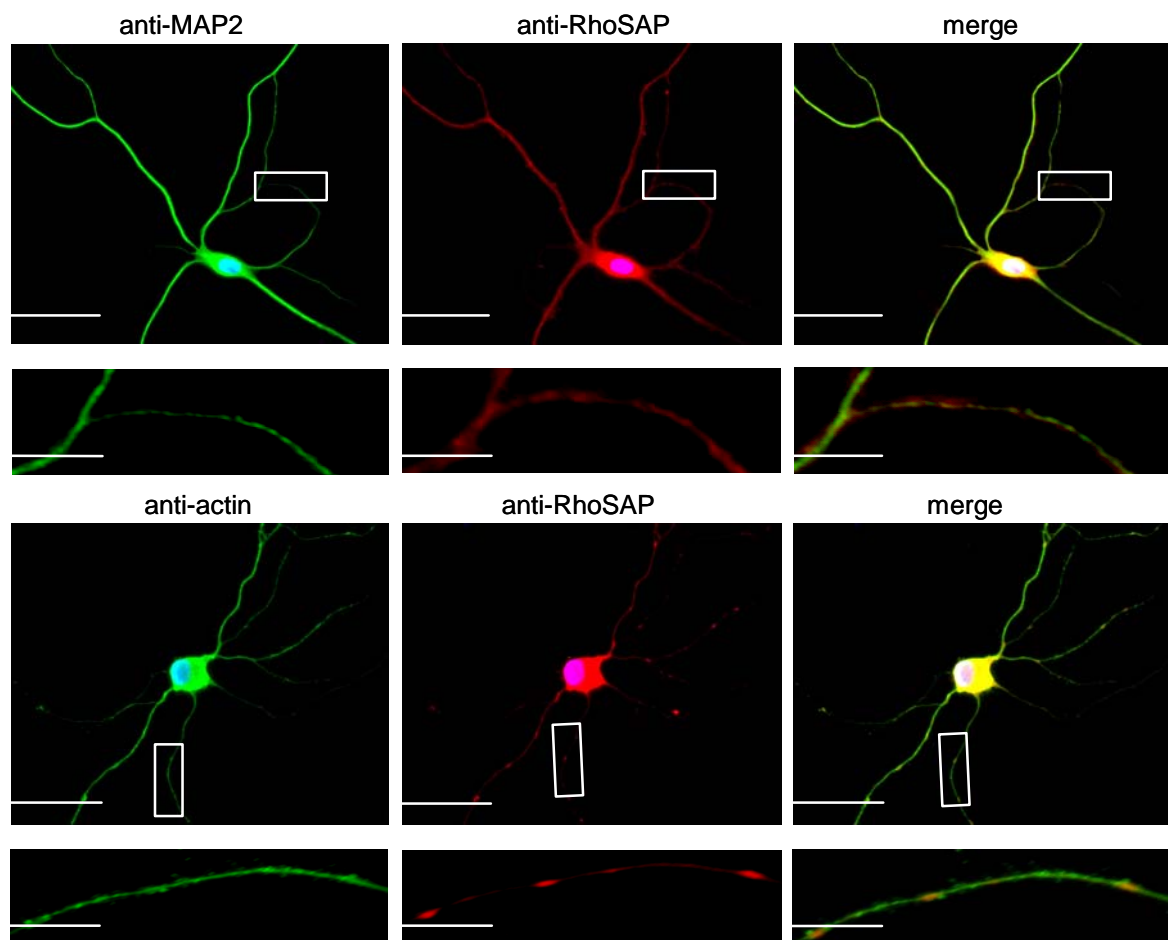
coordinated control of other cellular activities such as gene transcription and adhesion (Hall 1998). Moreover, the development and structural plasticity of dendritic arbors are governed by several factors that include small GTPases like Rac1 and Cdc42. In fact, activated Rac1 was substantiated to selectively increase branch additions and retractions, as did Cdc42 but to a lesser extent (Li *et al.*, 2000).

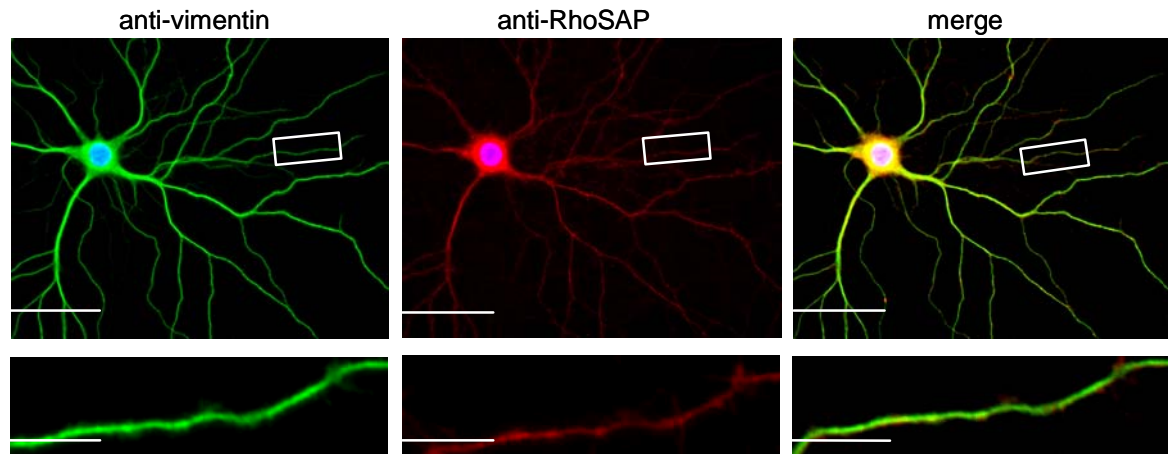
To this end, studies on colocalization of RhoSAP and cytoskeletal elements were undertaken. MAP2, representing a microtubuli interacting protein; actin being the basic component of actin cytoskeleton and vimentin as neurofilament were chosen to assess if RhoSAP, as Rac1 and Cdc42 active RhoGAP molecule was related to the internal scaffold of the neuron.

All three cytoskeletal markers colocalized with RhoSAP in the soma of hippocampal neurons. In hippocampal dendrites, only vimentin appeared to colocalize with RhoSAP.

To further test whether RhoSAP was present in association with the actin cytoskeleton, RhoSAP-GFP (aa: 1-449) was transfected in HeLa cell line and probed with Phalloidin to mark the F-actin of the cells. By all accounts, no overlapping of fluorescence intensities was observable; hence RhoSAP had no direct effect on the actin cytoskeleton.

A





B

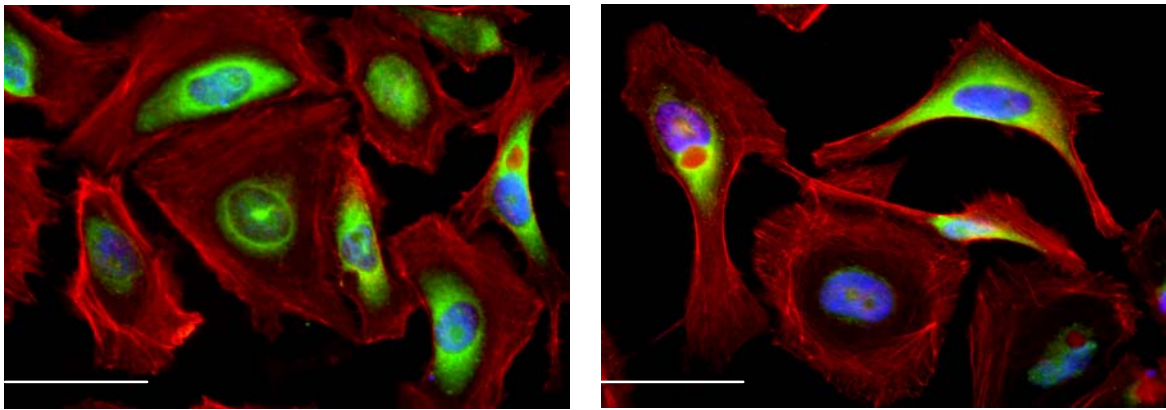


Fig. 3-29 RhoSAP effect on cytoskeletal elements: MAP2, actin and vimentin. (A) To substantiate possible co-localizations of RhoSAP and MAP2, actin and/or vimentin, respectively, 14 day old hippocampal cell culture were targeted by specific antibodies (working solution 1:1000) for the cytoskeletal markers. RhoSAP does coincide with MAP2, actin and vimentin in the neuronal soma whereas colocalization in the dendritic arbor was traced for vimentin (neurofilament) only. Scale bar 30 μm . (B) Expressing recombinant pEGFPN3-RhoSAP (aa: 1-449) transiently in cell line (HeLa) to be counterstained by Phalloidin (Texas-Red 1:1000) revealed no significant association of actin and RhoSAP. Thus, this finding is consistent with what was determined for the dendritic arbor in hippocampal neurons, previously. Scale bar 40 μm .

4 Discussion

Long-term and working memory storage in the brain is explained by changes in the strength of synapses in neural networks. These changes are regulated by many biochemical signaling pathways in the postsynaptic spines of excitatory synapses. The regulation of the small Rho GTPases Cdc42 and Rac1 in spines provide insights into how actin cytoskeletal rearrangements and postsynaptic membrane trafficking are coordinated to play a role in synaptic plasticity.

The main objective of this thesis work was to investigate the role of RhoSAP, a Rho GTPases-activating protein starting from its pivotal interaction with ProSAP2/Shank3, one of the major scaffold molecules in the postsynapse.

4.1 Neuronal localization of RhoSAP and Rho GTPase signaling

Over the past years, it has become clear that the Rho family of GTPases plays an important role in various aspects of neuronal development (Govek *et al.*, 2005). Among the various processes are neurite outgrowth (Yoshizawa *et al.*, 2002), axonal pathfinding (Ng *et al.*, 2002), vesicle trafficking (Sudhof 1995) and exo-/endocytosis (Wucherpfenning *et al.*, 2003). Given that RhoSAP, a RhoGAP molecule, was identified from a rat brain cDNA library to interact with ProSAP2/Shank3 by an Y2H, subsequent investigations addressed the question in how far this molecule was brain specific. Several experimental approaches were performed to solve this problem. On the one hand, RhoSAP was identified in different tissues as heart, spleen, lung, liver, skeletal muscle, kidney, testis and brain on the transcript and protein level so that no brain-specificity could be confirmed. The latter exhibited a first sign that there must be putative variants of the RhoSAP protein. Only in brain tissue, two bands were detected at 100 kDa and 120 kDa, respectively, by Western blotting. On the transcript level, the strongest expression signal was attained in brain mRNA at 4.4 kb of size. Again, two smaller signals were detected which enforced the assumption of putative splice variants. Due to RhoSAP's phylogenetic relation to nadrin of about 50%, and the finding that the nadrin molecule comprises two more splice variants, the discovery of three more putative splice variants of RhoSAP concurred with the previous observations (Furuta *et al.*, 2002; 3.1.4). Unfortunately, it could not be convincingly determined which splice variant corresponded with the protein bands in SDS gels. The calculated molecular weight for RhoSAP was to 90 kDa. The determined splice variants in contrast account for approx 72 kDa, 81 kDa and 88 kDa which in turn means that there's no direct proof for the shorter protein forms of RhoSAP on the

protein level taking the detected 100 and 120 kDa bands into account. Possibly, the protein shows a different migration behavior in gel electrophoresis. All splice variants are characterized by the deletion of exons located in the PRD of RhoSAP. However, indications infer a protein form which lacks the BAR domain which could account for the 100 kDa protein (3.1.6).

Distinction of splice variants on the transcript level in rat brain determined by *in situ* hybridization, revealed that the 71 kDa variant I is expressed in hippocampus at postnatal day 3, whereas this signal seems to become weaker and slowly vanishes in the adult stages of development. However, in cerebellum a strong signal can be obtained along the time line. Splice variant II behaves similarly. But differences can be found in the embryonic stage of development where signals are absent. In contrast to the latter variants, splice variant III displays clear signals in cerebellum, hippocampus and cortex. Remarkably, RhoSAP's expression profile augments from postnatal day 9 on in cortex and suddenly declines from postnatal d21 on (3.1.4). In summary, all these three different expression patterns might be explained by distinct roles fulfilled in different brain regions in association with a particular stage of neuronal development. Since splice variants occurred in the C-terminus, this could be an important regulatory domain of the protein.

On the other hand, it was substantiated that RhoSAP is a genuine PSD molecule. This could be proved by PSD95 and ProSAP2/Shank3 coimmunoprecipitations and electron microscope imaging. By this means, it could be demonstrated that RhoSAP seems to be in a complex with ProSAP2/Shank3 and PSD95. Electron microscopically findings coincided with the results obtained from the biochemical approach, however, it illustrated that RhoSAP might be a protein with regulatory function since it could not be found in every postsynapse.

More information of RhoSAP localization to the PSD came from costainings with ProSAP2/Shank3 in hippocampal neuron culture. Amazingly, colocalizations with ProSAP2/Shank3 are disrupted from postnatal d21. It can be speculated that RhoSAP is downregulated due to some Rho signaling response which effects RhoSAP crucially in the later stage of development.

Overexpressing RhoSAP as full length recombinant GFP protein resulted a diffuse intracellular punctuate pattern which could suggest a coaccumulation with intracellular membranes. This in turn, could point to an involvement in intracellular membrane trafficking. In this context, it is particularly interesting that distinct RhoSAP-GFP fusion proteins did not yield positive transfection results. Cells from primary hippocampal culture appeared to die shortly after receiving RhoSAP as fusion protein. An exception is made by constructs with C-

terminal fused GFP tags. Those constructs, especially the shortened form of RhoSAP, comprising the BAR domain only, led to much better results. In these cases transfection efficiency in cell lines was not more than 5%. The difference found could be explicable by a possible dominant negative effect that does not occur when RhoSAP's BAR domain is overexpressed only.

However, pictures showing hippocampal neurons transfected with RhoSAP-GFP full length clearly demonstrated that RhoSAP accumulated in spots within the dendrite. Next to this, it was distributed throughout the neuronal soma. Cloning of RhoSAP into other target vectors with smaller molecular tags will be done in the near future to check if these findings are caused by the vector construct itself or by RhoSAP.

This work identified RhoSAP, a RhoGAP that is active for Rac1 and Cdc41, two small GTPases of the Rho family. Hence, some hypothesis to which extend RhoSAP is involved in certain Rho signaling pathways can be drawn from that.

Rho proteins control the organization of the actin cytoskeleton in eukaryotic cells. Activation of Rac promotes *de novo* actin polymerization at the cell periphery to form lamellipodial extensions and membrane ruffles. For instance, the phosphatidylinositol 4-phosphate 5-kinase is a Rac target and is responsible for the generation of PIP₂ molecules that are essential together with Rac1 for the release of capping proteins from the ends of actin filaments (Machesky 1998).

In contrast, Cdc42 influences N-WASP activation, as well as other F-actin interacting proteins triggering actin polymerization and dendritic spine formation by Arp2/3 activation to form filopodia or microspikes (Nobes & Hall, 1995; Govands *et al.*, 2005).

Cross-talk between Rho proteins has been observed, in particular, Cdc42 is a strong activator of Rac1. That means filopodial extensions are usually associated with lamellipodial extensions. Additionally, Cdc42 and Rac1 can activate the Lin-11, Isl-1 and Mec-2 kinase (LIMK) by concerted activation of p21-activated kinase (PAK). The LIMK phosphorylate Cofilin which activates actin nucleation (Newey *et al.*, 2005).

Finally, Rac and Cdc42 have been implicated in cell movement, axonal guidance, cytokinesis and morphological changing processes involving changes in cell shape and polarity (an Aelst & d'Souza-Schorey, 1997).

4.2 RhoSAP, membrane trafficking and actin dynamics

During neuronal development and synaptogenesis, coordination of membrane trafficking, cell substrate adhesion and actin reorganization is required for protrusive activity of neuronal dendrites and spines. Actin organization is regulated by Rho family GTPases and with a contribution to the endocytic cycle, confers to extend the dendritic spines in response to stimulation of chemical synapses (de Curtis 2001). Consequently, these interconnected processes must be fine-regulated by Rho GTPases stimulating or inhibiting factors, such as GAP proteins. Indeed, it was demonstrated that a class of ArfGAP molecules: the GIT proteins which affect endocytosis colocalize with p95APP1, a marker of large endocytic vesicles. Deficits in GAP activity led to the accumulation in abnormal recycling compartments which underline the significance of GAP proteins in endocytic events (Claing *et al.*, 2000).

Discovering putative interaction partners of RhoSAP revealed an interesting endocytosis-related protein: synaptic dynamin-associated protein I (syndapin I). By the means of a two-hybrid screen, 375 aa of RhoSAP's C-terminus including its proline rich clusters directly interacted with 60 aa of the C-terminal part of syndapin I comprising its SH3 domain (3.2.1). This two-hybrid approach was independently confirmed by other assays. First, the validity of the result received by the genetic approach was examined through retransformation assays tested with X-Gal to confirm the bait and prey vector constructs interacted *in vitro*.

Other than that, it is known that the transcriptional and translational apparatus in yeast can frequently deviate from the usual mode. Although syndapin I was found with a medium frequency, the fact that it was discovered in two independent screens (transformation efficiency: 6.4×10^6) gave reason for continuing to investigate this interaction. Hence, upon coimmunoprecipitation of RhoSAP with brain lysate, the eluate contained syndapin I. The same proved to be true for the pull-down approach using overexpressed RhoSAP- and syndapin-GFP (3.2.3).

Syndapin I, a dynamin I-binding protein of 52 kDa was first described in rat brain (Qualmann *et al.*, 1999). It can be involved in multiple protein-protein interaction via a SH3 domain at the C-terminus and its F-BAR domain in the N-terminus. Whereas the SH3 domain binds to the site 2 PxxP motif of dynamin's proline rich domain (PRD), the F-BAR domain typically binds to phospholipids. In particular, these are phosphatidylserine membranes that are caused to form tubules *in vitro* via F-BAR domains (Anggono & Robinson, 2007; Itoh *et al.*, 2005). To be functional active, BAR domains have to dimerize. In the case of the human homologue of syndapin I: PACSIN, F-BAR domains form tetramers of about 240 kDa, which build-up a

huge beta barrel structures. By this oligomerization effect, multiple SH3 binding partners as well as other BAR proteins can simultaneously participate in endocytosis (Halbach *et al.*, 2007). Among other clathrin-mediated endocytosis promoting factors, syndapin I is the essential phospho-sensor of dynamin I. Thereby, the membrane-associated GTPase is able to trigger the pinching off of endocytic vesicles (Anggono *et al.*, 2006). When perturbing syndapin I, membranous cisternae massively accumulate at the sites of release; though this is not associated with the formation of coated pits. Conversely, this indicates that syndapin I is required to facilitate clathrin-mediated endocytosis (CME) (Andersson *et al.*, 2008).

To elucidate RhoSAP's function with regard to a stimulating effect on clathrin-mediated endocytosis, HeLa cells were transfected with RhoSAP-GFP and its releasing endocytic vesicles were marked with FM[®] 4-64, a red fluorescent dye. As a result, the green fluorescent signal merged with the red fluorescent vesicle signal which implied co-localization of RhoSAP with endocytic vesicles. Thereby, a preliminary hint on cellular level was obtained supporting the idea that RhoSAP is involved in endocytosis (3.3.2).

Further studies, coexpressing RhoSAP with syndapin I-GFP and ProSAP2/Shank3-GFP showed that the endocytic stimulating effect, measured by the number of emerging vesicles, was raised compared to controls (pure and pEGFP vector transfected HeLa cells). Notably, HeLa cells overexpressing RhoSAP-GFP and ProSAP-GFP alone had a higher stimulating effect than the co-expressions. Intriguingly, ProSAP-GFP's impact on endocytosis was increased in contrast to cells expressing RhoSAP-GFP. One possible explanation for this result might be the fact that dynamin-2 is specifically associated with ProSAP/Shank (Okamoto *et al.*, 2001). Consequently, the direct interaction might stronger accelerate endocytosis. It is not yet clear, if RhoSAP interacts with dynamin in any kind. Taking up, the two-hybrid data of RhoSAP's C-terminus, other dynamin or endocytic proteins; except for syndapin I could not be identified.

The cotransfection results, however, might point out to a decelerated or inhibited effect on endocytosis. An explanation can be taken from the fact that the endocytic protein intersectin1 which can function as GEF for Cdc42 is a critical activator for N-WASP and specifically accelerates actin assembly (Hussain *et al.*, 2001). Consistently, it can be speculated that RhoSAP's GAP activity together with syndapin I or ProSAP2/Shank3 could have a negative feed-back effect on the actin cytoskeleton. In accordance, N-WASP's association with syndapin and dynamin would be decreased as well (Rohatgi *et al.*, 2000; Qualmann *et al.*, 1999). Moreover, syndapin interacts with Son of sevenless (Sos), a Ras/Rac GEF which was implicated to regulate actin dynamics and extensively contributes to endocytic proceedings

(Wasiak *et al.*, 2001). Thus, it can be hypothesized that RhoSAP is an antagonist which downregulates ProSAP2/Shank3 and dynamin's interaction that leads in turn to a reduction of the endocytic promoting effect.

Thereby, endocytosis might be further fine regulated concerning dynamin's interaction partners. Moreover, associations among proteins are dynamic and transient resulting in their fast formation, breakage or degradation. Imaginable, that basal protein turn-over might have some impact on the outcome of the endocytosis experiments.

To verify the received results, it is advisable to investigate the transferrin receptor uptake by FACS measurements for comparison.

In addition, it was tested if endosomal trafficking proteins, such as the two small GTPases: Rab5 or Rab11 were colocalizing with RhoSAP in HeLa cells. Surprisingly, RhoSAP especially accumulated with Rab5 in intracellular vesicles indicating a potential function in the secretory pathway (3.1.7).

Since synaptic vesicle recycling has been proposed to depend on proteins which coordinate membrane and cytoskeletal dynamics, it is not surprising that the F-BAR domain containing syndapin I interact with N-WASP, along with dynamin, amphiphysin and endophilin. Accordingly, N-WASP, which associates with the Arp2/3 complex, triggers local actin polymerization specifically at sites of endocytosis. The mechanism of vesicle fission appears to take place only if N-WASP interacts with accessory proteins, such as syndapin I, but also with other BAR proteins such as endophilin and amphiphysin. These proteins were suggested to be molecular links between membrane trafficking and cortical cytoskeletal dynamics. Syndapin I mutants incapable of self-associating failed to act as multivalent organizers coordinating vesicle fission and actin polymerization (Kessels & Qualmann, 2006).

In this context, it has to be mentioned that N-WASP's WH2 domain, mediates dynamic attachment between membranes and the growing ends of actin filaments to sustain membrane vesicle movement (Cuo *et al.*, 2007). At the same time, the VCA region in N-WASP's C-terminus was determined to be crucial for activation of Arp2/3 and critical to induce dendritic spine and synapse formation via actin nucleation (Wegner *et al.*, 2008).

A characteristic colocalization pattern for RhoSAP and syndapin I in hippocampal neurons could not be detected when staining with the particular antibodies. Since RhoSAP does not only localize to PSDs but is found throughout the soma and dendrites in a diffuse manner, it can be postulated that none of both molecules supports a clear co-accumulation of the other (data not shown). Thus, indicating that both proteins are mostly cytoplasmic and they are not colocalizing at specific neuronal areas, for instance endocytic zones in the dendritic spine

head. But instead, they could require stimulation and other protein factors to be specifically targeted at sites of synaptic activity. In this context, future experiments with glutamate stimulation to excite excitatory synapses and the subsequent signaling cascades in the PSD can help to enlighten this aspect of RhoSAP-syndapin association.

Further colocalization studies with actin and other cytoskeletal elements like tubulin or MAP2, respectively did not demonstrate a connection of RhoSAP and the cytoskeleton (3.3.4). This can be seen as confirmation that RhoSAP interacts with ProSAP2/Shank3 which connects it indirectly to the cytoskeleton due to its association with cortactin and α -fodrin. An exception represents vimentin, which clearly merged with RhoSAP during fluorescence analysis, depicting colocalization characteristics.

In summary, there is a growing body of evidence for a yet unknown role of RhoSAP in CME and intracellular membrane trafficking to the PSD. However, by now it cannot be determined exactly in how far the RhoSAP-syndapin I interaction is interconnected with the cytoskeleton and effects endosomal trafficking in general. Since AMPA or NMDA receptor recycling is underlied by these processes and thought to play a fundamental role in synaptic plasticity, the regulatory significance of RhoGAP proteins cannot be underestimated. One option to further address the role of RhoSAP in membrane trafficking would be to perform RNAi experiments to understand what impact its loss will have on endocytosis.

To this end, also more sensitive assays like *in vivo*-imaging need to be applied to study the endocytic and cytoskeletal dynamics in neurons effected by the RhoSAP-syndapin and RhoSAP-ProSAP2/Shank3 interaction, respectively.

4.3 Hypothesis for the function of RhoSAP in neurons

Internalization of postsynaptic receptors (*e.g.* AMPARs and NMDARs), lipids, and other cargos at the postsynaptic membrane involves several different pathways. There is growing evidence that F-actin plays a direct role in endocytic events so that the actin cytoskeleton seems to be an integral part of membrane turn-over in cells (Engquist-Goldstein & Drubin, 2003). However, it has to be mentioned that the role of actin in endocytosis has been somewhat discussed controversial in the literature. Actin polymerization has been reported to be necessary (Lamaze *et al.*, 1997; Yazar *et al.*, 2005) or dispensable (Boucrot *et al.*, 2006; Fujimoto *et al.*, 2000).

Several proteins, for instance dynamin, syndapin, cortactin and N-WASP have been identified that may function at the interface between the membrane cytoskeleton and the endocytic vesicle-budding machinery (Qualmann & Kessels, 2002).

The first indication of an involvement of RhoGTPases in CME came from studies by Lamaze *et al.* (1996), who showed that constitutively active mutants of either Rho or Rac could block transferrin-receptor mediated endocytosis, while Cdc42 regulates endocytosis in immature dendrites. This provides a first hint to a regulatory function of RhoGAP proteins in CME. Concretely, RhoGTPases might participate by modulating phosphoinositide metabolism, through regulation of the enzymes affecting phosphoinositide turnover (Symons & Rusk, 2003; Malecz *et al.*, 2000). Furthermore, Rac and Cdc42 are also important determinants of dendritic structure, particularly with respect to dendritic branching and remodeling, though Cdc42 appears to have a milder effect on dendritic outgrowth compared to Rac (Ng *et al.*, 2002).

For this purpose, the molecular mechanisms involved in the regulation of synaptic receptors are essential to understanding how synaptic plasticity is regulated. Significantly, less is known about the regulation of synaptic NMDARs compared with AMPARs which have been both implicated to have a major influence in the establishment and maintenance of synaptic plasticity. NMDARs are crucial for the induction of specific forms of synaptic plasticity, such as LTP and LTD. However, AMPARs have to be present and forwardly activated otherwise the synapse, only containing NMDRs would remain silent (Prybylowski & Wendhold, 2004). Generally, NMDARs are stabilized and retained at the postsynapse by an attachment to PSD95 through a PDZ domain interacting with the NR2 subunit. Intriguingly, the distal C-terminus of the subunit NR2B was found to enable the association of adaptor protein 2 (AP-2) through a YEKL motif (Prybylowski *et al.*, 2005). AP-2 is a CME accessory protein which resides closer to the PSD than clathrin and dynamin (Racz *et al.*, 2004). It also interacts with GluR2, an AMPAR subunit and acts LTD-dependently in AMPA receptor trafficking (Lee *et al.*, 2002). In addition, Pérez-Otano *et al.* (2006) have shown that syndapin I regulates the endocytic removal of NMDARs. The developmentally regulated NR3A subunit is selectively bound by its NPF motif which assembles together with synadpin C-terminal domain, dynamin and clathrin in a complex upon NMDARs association with AP-2. Recruitment of the clathrin endocytic machinery might be therefore regulated by more CME related proteins, such as small GTPases and GAPs. Endocytic trafficking events are considered to be positioned at endocytic zones (EZ), adjacent to the PSD. Dynamin-3, abundant in the EZ but also in the PSD, displays a physical link to Homer and mGluR5. Enlargement of dendritic spine heads depends on the synaptic recruitment of Homer into the postsynapse, which in conjunction with the scaffold family of ProSAP/Shanks promotes maturation of dendritic spines and causes accumulation of IP₃-receptors at the SERs of PSDs (Gray *et al.*, 2003; Lu *et al.*, 2007).

Alternatively, it has been proposed that plasticity induced growth of dendritic spines are a consequence from exocytic trafficking from intracellular recycling endosomes providing membranes for outgrowth. Endosomal turn-over is induced after LTP-inducing stimuli, e.g. glutamate activation (Park *et al.*, 2006).

Another component of the CME which was detected in clathrin-coated pits, is cortactin, a ProSAP/Shank and dynamin 2 interacting molecule. Dynamin 2 itself interacts with Shank1 through its PRD (Cao *et al.*, 2003; Okamoto *et al.*, 2001).

Itoh *et al.* (2005) demonstrated the cooperative antagonizing effect of dynamin and actin in membrane tubulation. Analysis of cells expressing high levels of BAR-proteins, such as endophilin and F-actin binding protein1, usually inducing massive tubulation, had a much smaller impact on tubulation or no effect, if dynamin-2 was co-overexpressed in COS-7 cells. BAR domain proteins bind small GTPases via their regulatory modules for these enzymes, strongly suggesting their cooperation with small GTPases in the control of cellular processes at the membrane-cytosol interface (Habermann 2004). One of these processes is the regulation of actin, and this is particularly linked to Cdc42 and N-WASP, two proteins shown to participate in endocytosis (Kakimoto *et al.*, 2004; Benesch *et al.*, 2005; Innocenti *et al.*, 2005). In this thesis RhoSAP was identified as a novel putative ProSAP/Shank and syndapin I interacting molecule. In neurons, ProSAP/Shank is one of the major scaffolding molecules targeting and clustering distinct signaling molecules with NMDAR receptors. In contrast, syndapin I is an interconnecting regulator between actin polymerization and NMDA receptor recycling.

Taken together, these data led to the proposal of the following working-model of RhoSAP function (Fig. 4-1). Additionally, this thesis should provide a framework to assess RhoSAP's function in the PSD at a molecular level.

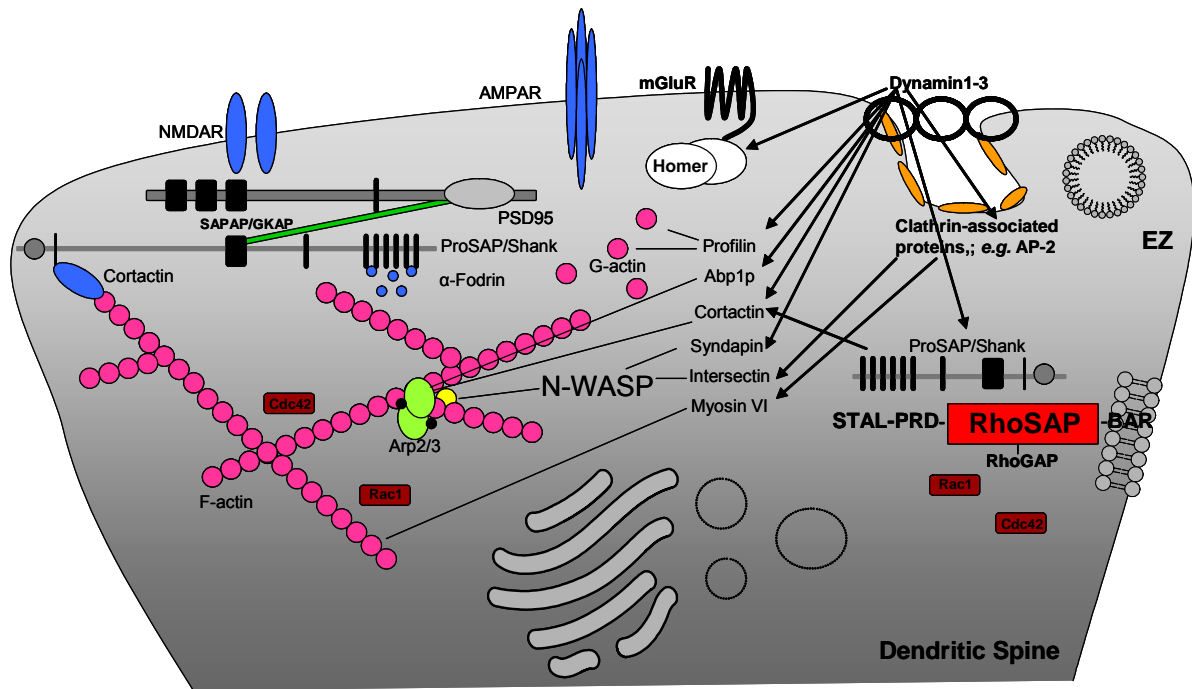


Fig. 4-1 Working-model for the protein-protein interactions identified as potential links between components of the endocytic and the actin cytoskeletal machine. Two types of functional links are crucial for the interaction of endocytic components with the actin cytoskeleton. First, actin polymerization can occur via direct binding of activators (Abp1, cortactin) or via the activation of N-WASP which is recruited to clathrin-forming vesicles by modular scaffolding proteins of the CME (syndapin, intersectin). Second, endocytic proteins interact with F-actin (Myosin IV) and G-actin (profilin) and are implicated to significantly tether and modulate both machineries. RhoSAP is a RhoGAP, active for Rac1 and Cdc42. Due to the finding that it binds to major scaffolds of the PSD (ProSAP2/Shank3) and endocytic zones (syndapin), RhoSAP could act as regulatory mediator between small GTPases influenced signaling cascades common to ProSAP/Shank and CME. RhoSAP is anchored to the postsynaptic membrane via its BAR domain. Simultaneously, it regulates Rac1 which has been implicated in phosphoinositol metabolism but at the same time regulates the actin cytoskeleton. Additionally, dynamin-2, is a component of the ProSAP/Shank-cortactin complex that affects actin dynamics. Since RhoSAP interacts with the PDZ domain of ProSAP/Shank, it is indirectly connected to PSD95 that physically links to ProSAP/Shank through IRSp53. PSD95 in turn clusters NMDARs through one of its PDZ domains. The NR2 subunit associates with AP-2, a CME accessory protein. Because dynamin-3 is found in complex with Homer, metabotropic GluR signaling is indirectly linked to ProSAP/Shank. Homer has been further implicated in IP₃-receptor signaling. Attributably, RhoSAP influences the cytoskeleton indirectly due to its interaction with ProSAP2/Shank3 and at the mean time it can regulate through the small GTPases Cdc42 and Rac1.

Syndapin I, another interacting partner of RhoSAP also interacts with dynamin and regulates NMDAR recycling. It associates with N-WASP's PRD domain through its SH3 domain and causes actin polymerization within an activation complex consisting of Abi1 and WAVE.

During synaptogenesis, when dendritic spines start to differentiate upon LTP stimuli, the cytoskeletal and endocytic machinery is of importance to realize morphological changes of the postsynaptic densities. Neither cytoskeletal rearrangements nor receptor (e.g. AMPA) trafficking can be considered alone to sufficiently explain synaptic plasticity of PSDs. Modified and extended from Smythe & Ayscough, 2006.

4.4 Conclusion

This thesis project demonstrated that RhoSAP, a GAP down-regulating Cdc42 and Rac1 of the Rho GTPases, is a novel binding partner for the PDZ domain of the ProSAP/Shank family. This means, it is indirectly linked to the actin cytoskeleton, since ProSAP2/Shank3 provides a link over the pp1 domain which interacts with Cortactin. PSD localization for RhoSAP was proved biochemically in PSD fractions, detected by immunofluorescent staining

with ProSAP2/Shank3 in a developmental time line and monitored by electron microscope. Remarkably, RhoSAP's expression profile begins to decrease at the adult stage after continually augmenting during neuronal development.

Along with ProSAP2/Shank3, RhoSAP interacts with syndapin I, a CME accessory protein which itself is associated with N-WASP, one of the actin polymerization stimulating factors. Again, the RhoGAP molecule might be connected to the actin cytoskeleton indirectly. Due to its activity for Cdc42 and Rac1, it can be speculated that it coregulates dendritic development, especially spine morphogenesis because both RhoGTPases belong to the major GTPases which effect cytoskeletal dynamics. This in turn is the prerequisite for morphological changes of spine structure after chemical stimuli deriving from the presynaptic CAZs targeting the postsynaptic densities.

The fact that syndapin I also binds components of the endocytic machinery, as does N-WASP leads to the hypothesis that RhoSAP might be a regulator of actin and endocytic activity at PSDs. This hypothesis is substantiated by the finding that RhoSAP alone incites endocytosis in cell line but in conjunction with ProSAP2/Shank3 or syndapin I; this effect is decreased. Accordingly that implies: RhoSAP participates as fine tune feed-back regulator for the interconnection of actin cytoskeleton and endocytic zones, which are predominantly found at highly active synapses.

In conclusion, RhoSAP might be an important player for spine development and thus, for synaptic plasticity.

5 Summary

The postsynaptic side harbors a highly dynamic protein network machinery – the postsynaptic density (PSD), which receives and integrates neurotransmitter signals.

Synapse assembly, maturation, maintenance and plasticity depend on multifaceted protein-protein and protein-lipid interactions within the PSD. To understand the synaptic physiology at a molecular level, genetic approaches as the yeast two-hybrid screen, studies in cultivated hippocampal neurons with the overexpressed protein of interest but also *in vitro* proteinbiochemical arrays have been used to determine signaling in the PSD.

The objective of this work was to functionally characterize postsynaptic related signaling molecules that directly interact with ProSAP2/Shank3, one of the major scaffold proteins in the PSD. It is one of the main components to build up the architectural framework of postsynaptic densities in dendritic spines.

Thereafter, the physiological relevance of the obtained data was to be further tested by *in vitro* cell cultural studies in cell lines and rat hippocampal neurons, a well established synaptic model system.

To this end, the thesis focuses on RhoSAP, a Rho GTPase-activating protein. The data to characterize RhoSAP as a postsynaptic molecule can be divided into two sections:

1. RhoSAP, a RhoGAP protein is a novel interaction partner of ProSAP2/Shank3 in brain.

A yeast two-hybrid screen of a rat brain cDNA library was initially performed with the objective to find new interaction partners for ProSAP2/Shank3's PDZ domain. RhoSAP, a RhoGAP protein was identified coding for 818 aa (~90 kDa). This molecule harbors a RhoGAP domain, proline rich motifs and a BAR domain that is responsible for lipid tubulation and curvature. The direct interaction of ProSAP2/Shank3 occurred via RhoSAP's STAL sequence in its C-terminus. The interaction was confirmed by coimmunoprecipitation, pull-down assay and colocalization studies in cultured hippocampal neurons. Accordingly, RhoSAP is enriched in the PSD along with ProSAP and other scaffold proteins of the postsynapse, *e.g.* PSD95.

RhoSAP is highly expressed in hippocampus, cerebellum and in cortex. The level of RhoSAP increases during development, what coincides with the maturation of synaptic contacts. Surprisingly, it starts to decrease again at a more adult stage of brain development. Further investigation revealed that different isoforms of RhoSAP exist in

the nervous system. Three splice variants of 2000 bp, 2237 bp and 2462 bp in size were found on the transcript level. On protein level, two putative RhoSAP molecules appeared at 70 kDa in a Western blot experiment and at 120 kDa, the last form was shown to be brain-specific.

Due to the fact that proline rich clusters preferably interact with SH3 motifs, another yeast two-hybrid screen with RhoSAP's C-terminus including proline rich stretches as bait was performed to find new interactions. Among the identified interaction partners was syndapin I, a dimer protein associating with dynamin I, endophilin and amphiphysin. Since syndapin I enhances endocytosis, the protein pointed out to a potential function of RhoSAP in endocytic events in dendritic spines. This hypothesis was also favored by the fact that BAR domain proteins are involved in clathrin-mediated endocytosis.

2. RhoSAP is active for small Rho GTPases and boosts endocytic activity in cell line.

A GAP activity assay confirmed that RhoSAP's GAP domain is active for Rac1 and Cdc42 *in vitro*. Both Rho GTPases are important to promote membrane ruffling, lamellipodium, filopodium and actin fiber formation. The implications of RhoSAP's down regulatory effect on Rho signaling have to be further elucidated.

Studies in HeLa cells revealed that RhoSAP promotes endocytosis which could be demonstrated by FM[®] 4-64 dye analysis. After transfection of RhoSAP, the number of stained pinched off membranous vesicles augmented, in contrast to basal endocytosis taking place in untransfected cells.

In fact, exo-/endocytosis is very important for AMPA receptor cycling at PSDs, as this contributes to the distribution pattern of receptors in the postsynaptic membrane to enhance or weaken synaptic input. That means in turn, synaptic vesicle recycling and subsequent intracellular membrane traffic imply an important aspect in determining dendritic spine structure besides cytoskeletal rearrangements.

Conclusively, this work contributes to a better understanding of RhoSAP, a RhoGAP protein of the PSD that might contribute to a functional connection of the cytoskeleton, the scaffold backbone of PSDs, and the fine tuning of endocytic events in dendritic spines.

This could provide a better understanding of how the concerted cross-talk of Rho signaling, cytoskeletal dynamics and membrane trafficking facilitates spine morphological changes in response to stimulated chemical synapses.

6 References

- Abo, A., Pick, E., Hall, A., Trotty, N., Teahan, C.G., and Segal, A.W. (1991) Activation of the NADPH oxidase involves the small GTP-binding protein p21rac1. *Nature* **353**, pp. 668-670
- Adams, A.E., Johnson, D.I., Longnecker, R.M., Sloat, B.F., and Pringle, J.R. (1990) CDC42 and CDC43, two additional genes involved in budding and the establishment of cell polarity in the yeast *Saccharomyces cerevisiae*. *J Cell Biol* **111**, pp. 131-142
- Ahnert-Hilger, G., Hölting, M., Große, G., Pickert, G., Mucke, C., Nixdorf-Bergweiler, B., Bouquet, P., Hofmann, F., and Just, I. (2004) Differential effects of Rho GTPases on axonal and dendritic development in hippocampal neurons. *J Neurochem* **90**, pp. 9-18
- Allen, W.E., Zicha, D., Ridley, A.J., and Jones, G.E. (1998) A role for Cdc42 in macrophage chemotaxis. *J Cell Biol* **141**, pp. 1147-1157
- Andersson, F., Jakobsson, Löw, P., Shupliakov, O., and Brodin, L. (2008) Perturbation of syndapin/PACSIN impairs synaptic vesicle recycling evoked by intense stimulation. *J Neurosci* **28**, pp. 3925-3933
- Anggono, V., Smillie, K.J., Graham, M.E., Valova, V.A., Cousin, M.A., and Robinson, P.J. (2006) Syndapin I is the phosphorylation-regulated dynamin I partner in synaptic vesicle endocytosis. *Nat Neurosci* **9**, pp. 752-760
- Anggono, V., and Robinson, P.J. (2007) Syndapin I and endophilin I bind overlapping proline-rich regions of dynamin I: role in synaptic vesicle endocytosis. *J Neurochem* **102**, pp. 931-943
- Bader, M.F., Doussau, F., Chasserot-Golaz, S., Vitale, N., and Gasman, S. (2004) Coupling actin and membrane dynamics during calcium-regulated exocytosis: a role for Rho and ARF GTPases. *Biochem Biophys Acta* **1742**, pp. 37-49
- Bar-Sagi, D., and Hall, A. (2000) Ras and Rho GTPases: A family reunion. *Cell* **103**, pp. 227-238
- Barfod, E.T., Zheng, Y., Kuang, W.J., Hart, M.J., and Evand, T. (1993) Cloning and expression of a human CDC42 GTPase-activating protein reveals functional SH3-binding domain. *J Biol Chem* **268**, pp. 26059-26062
- Baron, M.K., Boeckers, T.M., Vaida, B., Faham, S., Gingery, M., Sawaya, M.R., Salyer, D., Gundelfinger, E.D., and Bowie, J.U. (2006) An architectural framework that may lie at the core of the postsynaptic density. *Science* **27**, pp. 531-535
- Barrett, T., Xiao, B., Dodson, E.J., Dodson, G., and Ludbrook, S.B. (1997) The structure of the GTPase-activating domain from p50. *Nature* **385**, pp. 458-461
- Behnia, R., and Munro, S. (2005) Organelle identity and the signposts for membrane traffic. *Nature* **438**, pp. 597-604

Benesch, S., Polo, S., Lai, F.P., Anderson, K.I., Stradal, T.E., Wehrland, J., and Rottner, K. (2005) N-WASP deficiency impairs EGF internalization and actin assembly at clathrin-coated pits. *J Cell Sci* **118**, pp. 3103-3115

Bernards, A. (2003) GAPs galore! A survey of putative Ras superfamily GTPase-activating proteins in man and *Drosophila*. *Biochim Biophys Acta* **1603**, pp. 47-82

Bernards, A., and Settleman, J. (2004) GAP control: regulating the regulators of small GTPases. *Trends Cell Biol* **14**, pp. 377-385

Billuart, P., Bienvenu, T., Ronce, N., des Portes, V., Vinet, M.C., Zemni, R., Crollius, H.R., Carrié, A., Fauchereau, F., Cherry, M., Briault, S., Hamel, B., Fryns, J.P., Beldjord, C., Khan, A., Moraine, C., and Chelly, J. (1998) Oligophrenin-1 encodes a RhoGAP protein in X-linked mental retardation. *Nature* **392**, pp. 923-926

Boeckers, T.M., Kreutz, M.R., Winter, C., Zuschratter, W., Smalla, K.H., Sanmarti-Vila, L., Wex, H., Langnaese, K., Bockmann, J., Garner, C.C. and Gundelfinger, E.D. (1999a) Proline-rich synapse-associated protein-1/cortactin binding protein 1(ProSAP/CortBP1) is a PDZ-domain protein highly enriched in the postsynaptic density. *J Neurosci* **19**, pp. 6506-6518

Boeckers, T.M., Winter, C., Smalla, K.H., Kreutz, M.R., Bockmann, J., Seidenbrecher, C., Garner, C.C., and Gundelfinger, E.D. (1999b) Proline-rich synapse associated proteins ProSAP1 and ProSAP2 interact with synaptic proteins of the SAPAP/GKAP family. *Biochem Biophys Res Commun* **264**, pp. 247-258

Boeckers, T.M., Mameza, M.G., Kreutz, M.R., Bockmann, J., Weise, C., Buck, F., Richter, D., and Gundelfinger, E.D. (2001) Synaptic scaffolding proteins in rat brain. Ankyrin repeats of the multidomain Shank protein family interact with the cytoskeletal protein alpha-fodrin. *J Biol Chem* **276**, pp. 40104-40112

Boeckers, T.M., Bockmann, J., Kreutz, M.R., and Gundelfinger, E.D. (2002) ProSAP/Shank proteins – a family of higher order organizing molecules of the postsynaptic density with an emerging role in human neurological disease. *J Neurochem* **81**, pp. 903-910

Boeckers, T.M. (2006) The postsynaptic density. *Cell Tis Res* **326**, pp.409-422

Bokoch, G.M., Vlahos, C.J., Wang, Y., Knaus, U.G., and Traynor-Kaplan, A.E. (1996) Rac GTPase interacts specifically with phosphatidylinositol 3-kinase. *Biochem J* **315**, pp. 775-779

Borhardt, A., Bojesen, S., Haas, O.A., Fuchs, U., and Bartelheimer, D. (2000) The human GRAF gene is fused to MLL in a unique t (5;11)(q31;q23) and both alleles are disrupted in three cases of myelodysplastic syndrome/ acute myeloid leukaemia with a deletion 5q. *PNAS* **97**, pp. 9168-9173

Boucrot, E., Saffarian, S., Massol, R., Kirchhausen, T., and Ehrlich, M. (2006) Role of lipids and actin in the formation of clathrin-coated pits. *Exp Cell Res* **312**, pp.4036-4048

- Bourgeron, T., Ehrenreich, H., and Brose, N. (2008)** Reduced social interaction and ultrasonic communication in a mouse model of monogenic heritable autism. *PNAS* **5**, pp. 1710-1715
- Bourgeron, T. (2007)** The possible interplay of synaptic and clock genes in autism spectrum disorders. *Cold Spring Harb Symp Quant Biol* **72**, pp. 645-654
- Bouton, A.H., Kanner, S.B., Vines, R.R., Wang, H.C., Gibbs, J.B., and Parsons, T.J. (1991)** Transformation by pp60src or stimulation of cells with epidermal growth factor induces the stable association of tyrosine phosphorylated cellular proteins with GTPase-activating protein. *Mol Cell Biol* **11**, pp. 945-953
- Bos, J.L., Rehmann, H., and Wittinghofer, A. (2007)** GEFs and GAPs: Critical elements in the control of small G proteins. *Cell* **129**, pp. 865-877
- Bradtke, F., and Dotti, C.G. (1999)** The role of local actin instability in axon formation. *Science* **283**, pp. 1931-1934
- Bredt, D.S., and Nicoll, R.A. (2003)** AMPA receptor trafficking at excitatory synapses. *Neuron* **40**, pp. 361-379
- Brouns, M.R., Matheson, S.F., and Settleman, J. (2001)** p190 RhoGAP is the principal Src substrate in brain and regulates axon outgrowth, guidance and fasciculation. *Nat Cell Biol* **3**, pp. 361-367
- Brown, T.C., Tran, I.C., Backos, D.S., and Esteban, J.A. (2005)** NMDA receptor-dependent activation of the small GTPase Rab5 drives the removal of synaptic AMPA receptors during hippocampal LTD. *Neuron* **45**, pp. 81-94
- Cao, H., Orth, J.D., Chen, J., Weller, S.G., Heuser, J.E., and McNiven, M.A. (2003)** Cortactin is a component of clathrin-coated pits and participates in receptor-mediated endocytosis. *Mol Cell Biol* **23**, pp. 2162-2170
- Carlin, R.K., Grab, D.J., Cohen, R.S., and Siekevitz, P. (1980)** Isolation and characterization of postsynaptic densities from various brain regions: enrichment of different types of postsynaptic densities. *J Cell Biol* **86**, pp. 831-843
- Carlisle, H.J., and Kennedy, M.B. (2005)** Spine architecture and synaptic plasticity. *Trends Neurosci* **28**, pp. 182-187
- Chang, J.H., Gill, S., Settleman, J., and Parsons, S.J. (1995)** c-Src regulates the simultaneous rearrangement of actin cytoskeleton, p190RhoGAP, and p120RasGAP following epidermal growth factor stimulation. *J Cell Biol* **130**, pp. 355-368
- Chapdelaine, P., Vignola, K., and Fortier, M.A. (2001)** Protein estimation directly from SDS-PAGE loading buffer for standardization of samples from cell lysates or tissue homogenates before Western blot analysis. *Biotechniques* **31**, pp. 478-482
- Chien, C.-T., Bartel, P.L., Sternglanz, R., and Fields, S. (1991)** The two-hybrid system: A method to identify and clone genes for proteins that interact with a protein of interest. *PNAS* **88**, pp. 9578-9582

- Cicchetti, P., Mayer, B.J., Thiel, G., and Baltimore, D. (1992)** Identification of a protein that binds to the SH3 region of Abl and is similar to Bcr and GAP-rho. *Science* **257**, pp. 803-806
- Cichowski, K., Santiago, S., Jardim, M., Johnson, B.W., and Jacks, T. (2003)** Dynamic regulation of the Ras pathway via proteolysis of the NF1 tumor suppressor. *Genes Dev* **17**, pp. 449-454
- Claing, A., Perry, S.J., Achiriloaie, M., Walker, J.K., Albanesi, J.P., Lefkowitz, R.J., and Premont, R.T. (2000)** Multiple endocytic pathways of G protein-coupled receptors delineated by GIT sensitivity. *PNAS* **97**, pp. 1119-1124
- Cote, J.F., and Vuori, K. (2002)** Identification of an evolutionary conserved superfamily of DOCK180-related proteins with guanine nucleotide exchange activity. *J Cell Sci* **115**, pp. 4901-4913
- Cotman, C.W., Banker, G., Churchill, L., and Taylor, D. (1974)** Isolation of postsynaptic densities from rat brain. *J Cell Biol* **63**, pp. 441-445
- Cuo, C., Wong, D.T., Gierke, S., Chang, V., and Taunton, J. (2007)** Mechanism of actin network attachment to moving membranes: barbed end capture by N-WASP WH2 domain. *Cell* **9**, pp. 901-913
- de Curtis, I. (2001)** Cell migration: GAPs between membrane traffic and the cytoskeleton. *EMBO reports* **2**, pp. 277-281
- David, C., McPherson, P.S., Mundigl, O., and de Camilli, P. (1996)** A role of amphiphysin in synaptic vesicle endocytosis suggested by its binding to dynamin in nerve terminals. *PNAS* **93**, pp. 331-335
- Diekmann, D., Brill, S., Garrett, M.D., Trotty, N., and Hsuan, J. (1991)** Bcr encodes a GTPase-activating protein for p21rac. *Nature* **351**, pp. 400-402
- Dong, H., O'Brien, R.J., Fung, E.T., Lanahan, A.A., Worley, P.F., and Huganir, R.L. (1997)** GRIP: a synaptic PDZ domain-containing protein that interacts with AMPA receptors. *Nature* **386**, pp. 279-284
- Downward, J. (1990)** The Ras superfamily of small GTP-binding proteins. *Trends Biochem Sci* **15**, pp. 469-72
- Du, Y., Weed, S.A., Xiong, W.C., Marshall, T.D., and Parsons, J.T. (1998)** Identification of a novel cortactin SH3 domain-binding protein and its localization to growth cones of cultured neurons. *Mol Cell Biol* **18**, pp. 5838-5851
- Durand, C.M., Betancur, C., Boeckers, T.M., Bockmann, J., Chaste, P., Fauchereau, F., Nygren, G., Rastam, M., Gillberg, I.C., Anckarsäter, H., Sponheim, E., Oubran-Botor, H., Delorme, R., Chabane, N., Mouren-Simeoni, M.C., de Mas, P., Bieth, E., Rogé, B., Héron, D., Burgien, L., Gillberg, C., Leboyer, M. and Bourgeron, T. (2007)** Mutations in the gene encoding the synaptic scaffolding protein Shank3 are associated with autism spectrum disorders. *Nat Genet* **39**, pp. 25-27

- Dresbach, T., Qualmann, B., Kessels, M.M., Garner, C.C. and Gundelfinger, E.D. (2001)** The presynaptic cytomatrix of brain synapses. *Cell Mol Life Sci* **58**, pp. 94-116
- Engert, F., and Bonhoeffer, T. (1999)** Dendritic spine changes associated with hippocampal long-term synaptic plasticity. *Nature* **399**, pp.66-70
- Engquits-Goldstein, A.E., and Drubin, D.G. (2003)** Actin assembly and endocytosis: from yeast to mammals. *Annu Rev Cell Dev Biol* **19**, pp. 287-332
- Esteban, J.A. (2003)** AMPA receptor trafficking. *Mol Inter* **3**, pp. 375-385
- Faix, J., and Grosse, R. (2006)** Staying in shape with formins. *Dev Cell* **10**, pp. 693-706
- Farsad, K., and de Camilli P. (2003)** Mechanisms of membrane deformation. *Opin Cell Biol* **15**, pp. 372-381
- Farsad, K., Ringstad, N., Takei, K., Floyd, S.R., Rose, K., and de Camilli, P. (2001)** Generation of high curvature membranes mediated by direct endophilin bilayer interactions. *J Cell Biol* **155**, pp.193-200
- Feinberg, A.G. and Vogelstein, B. (1983)** A technique for radiolabeling DNA restriction endonuclease fragments to high specific activity. *Anal Biochem* **132**, pp.6-13
- Fernandez-Borja, M., Janssen, L., Verwoerd, D., Hordijk, P., and Neefjes, J. (2005)** RhoB regulates endosomal transport by promoting actin assembly on endosomal membranes through Dial1. *J Cell Sci* **118**, pp. 2661-2270
- Fields, S., and Song, O. (1989)** A novel genetic system to detect protein-protein interactions. *Nature* **340**, pp. 245-246
- Fojimoto, L.M., Roth, R., Heuser, J.E., and Schmid, S.L. (2000)** Actin assembly plays a variable, but not obligatory role in receptor mediated endocytosis in mammalian cells. *Traffic* **1**, pp. 161-171
- Fransson, A., Ruusala, A., and Aspenström, P. (2003)** Atypical Rho GTPases have roles in mitochondrial homeostasis and apoptosis. *J Biol Chem* **278**, pp. 6495-6502
- Frost, A., Rushika, P., Roux, A., Spasov, K., Destaing, O., Egelman, E.H., de Camilli, P., and Unger, V.M. (2008)** Structural basis of membrane invagination by F-BAR domains. *Cell* **132**, pp. 807-817
- Furuta, B., Harada. A., Kobayashi, Y., Takeuchi, K., Kobayashi, T., and Umeda, M. (2002)** Identification and functional characterization of nadrin variants, a novel family of GTPase activating protein for Rho GTPases. *J Neurochem* **82**, pp. 1018-1028
- Fütterer, K., and Machesky, L.M. (2007)** „Wunder“ F-BAR domains: going from pits to vesicles. *Cell* **129**, pp. 655-657
- Garner, C.C., Nash, J. and Haganir, R.L. (2000)** PDZ domains in synapse assembly and signaling. *Trends Cell Biol* **10**, pp. 274-280

- Gasman, S., ChasseroT-Golaz, S., Malacombe, M., Way, M., and Bader, M.F. (2004)** Regulated exocytosis in neuroendocrine cells: a role for subplasmalemmal Cdc42/N-WASP-induced actin filaments. *Mol Biol Cell* **15**, pp. 520-531
- Goley, E.D., Rodenbusch, S.E., Martin, A.C., and Welch, M.D. (2004)** Critical conformational changes in the Arp2/3 complex are induced by nucleotide and nucleation promoting factor. *Mol Cell* **16**, pp. 269-279
- Goslin, K., and Banker, G. (1991)** Rat hippocampal neurons in low-density culture: culturing nerve cells. *MIT Press*, Cambridge MA, pp. 251-281
- Govek, E.E., Newey, S.E., and van Aelst, L. (2005)** The role of the Rho GTPases in neuronal development. *Genes Dev* **19**, pp.1-49
- Govind, S., Kozma, R., Monfries, C., Lim, L., and Ahmed, S. (2001)** Cdc42Hs facilitates cytoskeletal reorganization and neurite outgrowth by localizing the 58-kD insulin receptor substrate to filamentous actin. *J Cell Biol* **152**, pp. 579-594
- Gray, N.W., Fourgeaud, L., Huang, B., Chen, J., Cao, H., Oswald, B.J., Hémar, A., and McNiven, M. (2003)** Dynamin 3 is a component of the postsynapse, where it interacts with mGluR5 and Homer. *Cur Biol* **13**, pp. 510-515
- Gundelfinger, E.D., Boeckers, T.M., Baron, M.K., and Bowie, J.U. (2006)** A role for zinc in synapse assembly. *Trends Biochem Sci* **31**, pp. 366-373
- Gundelfinger, E.D., and tom Dieck, S. (2000)** Molecular organization of excitatory chemical synapses in the mammalian brain. *Naturwissenschaften* **87**, pp. 513-523
- Habermann B. (2004)** The BAR-domain family of proteins: a case of bending and binding? *EMBO reports* **5**, pp. 250-255
- Halbach, A., Mörgelin, M., Baumgarten, M., Milbrandt, M., Paulsson, M., and Plomann, M. (2007)** PACSIN 1 forms tetramers via its N-terminal F-BAR domain. *FEBS J* **274**, pp. 773-782
- Hall A. (1998)** Rho GTPases and the actin cytoskeleton. *Science* **279**, pp. 509-511
- Harada, A., Furuta, B., Takeuchi, K., Itakura, M., Takahashi, M., and Umeda, M. (2000)** Nadrin, a novel neuron-specific GTPase-activating protein involved in regulated exocytosis. *J Biol Chem* **275**, pp. 36885-36891
- Heukeshoven J., and Dernick, R (1988)** Improved silver staining procedure for fast staining in PhastSystem Development Unit. I. Staining of sodium dodecyl sulfate gels. *Electrophoresis* **9**, pp. 28-32
- Hering, H., and Sheng, M. (2001)** Dendritic spines: structure, dynamics and regulation. *Nat Rev Neurosci* **2**, pp. 880-888
- Hildebrand. J.D., Taylor, J.M., and Parsons, J.T. (1996)** An SH3 domain-containing GTPase-activating protein for Rho and Cdc42 associates with focal adhesion kinase. *Mol Cell Biol* **16**, pp. 3169-3178

- Hoffman, G.R., Nassar, N., and Cerione, R.A. (2000)** Structure of the Rho family GTP-binding protein Cdc42 in complex with multifunctional regulator RhoGDI. *Cell* **100**, pp. 345-356
- Howard, L., Nelson, K.K., Maciewicz, R.A., and Blobel, C.P. (1999)** Interaction of the metalloprotease disintegrins MDC9 and MDC15 with two SH3 domain containing proteins, endophilin I and SH3PX1. *J Biol Chem* **274**, pp. 31693-31699
- Huang, M., Duhadaway, J.B., Prendergast, G.C., and Laury-Kleintop, G.C. (2007)** RhoB regulates PDGFR-beta trafficking and signaling in vascular smooth muscle cells. *Atheroscler Thromb Vasc Biol* **27**, pp. 2597-2605
- Hussain, N.K., Jenna, S., Glogauer, M., Quinn, Q.C., Wasiak, S., Kay, B.K., Stossel, T.P., Lamarche-Vane, N., McPherson, P.S. (2001)** The endocytic scaffolding protein intersectin1 regulates actin dynamics via Cdc 42 and N-WASP. *Nat Cell Biol* **3**, pp. 927-932
- Innocenti, M., Zucconi, A., Disanza, A., Frittoli, E., Areces, L.B., Steffen, A., Stradal, T.E., Fiore, P.P.D., Carlier, M.-F., and Scita, G. (2004)** Abi1 is essential for the formation and activation of a WAVE2 signaling complex. *Nat Cell Biol* **6**, pp. 319-327
- Innocenti, M., Gerboth, S., Rottner, K., Lai, F.P., Hertzog, M., Stradal, T.E., Frittoli, E., Didry, D., Polo, S., Disanza, A. et al. (2005)** Abi1 regulates the activity of N-WASP and WAVE in distinct actin-based processes. *Nat Cell Biol* **7**, pp. 969-976
- Itoh, T., Erdmann, K.S., Roux, B., Habermann, B., Werner, H., and de Camilli, P. (2005)** Dynamin and the actin cytoskeleton cooperatively regulate plasma membrane invagination by BAR and F-BAR proteins. *Dev Cell* **9**, pp. 791-804
- Itoh, T., and de Camilli, P. (2006)** BAR, F-BAR (EFC) and ENTH/ ANTH domains in the regulation of membrane-cytosol interfaces and membrane curvature. *Biochim Biophys Acta* **1761**, pp. 897-912
- Jaffe, A.B., and Hall, A. (2005)** Rho GTPases: Biochemistry and Biology. *Annu Rev Cell Dev Biol* **21**, pp. 247-269
- Jaffer, Z.M., and Chernoff, J. (2004)** The Cross-Rho's of cell-cell adhesion. *J Biol Chem* **279**, pp. 35123-35126
- Jamain, S., Radyushkin, K., Hammerschmidt, K., Granon, s., Boretius, S., Varoqueaux, F., Ramanantsoa, N., Gallego, J., Ronnenberg, A., Winter, D., Frahm, J., Fischer, J., Bourgeron, T., Ehrenreich, H., and Brose, N. (2008)** Reduced social interaction and ultrasonic communication in a mouse model of monogenic heritable autism. *PNAS* **5**, pp. 1710-1715
- Kakimoto, T., Katoh, H., and Negishi, M. (2004)** Identification of splicing variants of Rapostilin, a novel RND2 effector that interacts with N-WASP and induces neurite branching. *J Biol Chem* **279**, pp. 14104-14110
- Karnoub, A.E., Symons, M., Campbell, S.L., and Der, J.C. (2004)** Molecular basis for Rho GTPase signaling specificity. *Breast Canc Res Treat* **84**, pp. 61-71

- Keep, N.H., Barnes, M., Barsukov, I., Badii, R., Lian, L.Y. Segal, A.W., Moody, P.C., and Roberts, G.C. (1997)** A modulator of Rho family G proteins, RhoGDI, binds these G proteins via an immunoglobulin-like domain and a flexible N-terminal arm. *Structure* **5**, pp. 623-633
- Kim, E., and Sheng, M. (2004)** PDZ domain proteins of synapses. *Nat Rev Neurosci* **5**, pp. 771-781
- Kjøller, L., and Hall, A. (1999)** Signaling to Rho GTPases. *Exp Cell Res* **253**, pp. 166-179
- Kovar, D.R. (2006)** Molecular details of formin-mediated actin assembly. *Curr Opin Cell Biol* **18**, pp. 11-17
- Kozma, R.S., Ahmed, S., Best, A., and Lim, L. (1995)** The Ras-related protein Cdc42Hs and bradykinin promote formation of peripheral actin microspikes and filopodia in Swiss 3T3 fibroblasts. *Mol Cell Biol* **15**, pp. 1942-1952
- Kreienkamp, J.H., and Dityatev, A. (2004)** The magic of synaptogenesis. Meeting on spinogenesis and synaptic plasticity. *EMBO Rep* **5**, pp.1125-1129
- Lamarche, N., and Hall, A. (1994)** GAPs for Rho-related GTPases. *Trends Genet* **10**, pp. 436-440
- Lamarche, N., Tapon, N., Stowers, L., Burbelo, P.D., Aspenstrom, P., Bridges, T., Chant, J., and Hall, A. (1996)** Rac and Cdc42 induce actin polymerization and G1 cell cycle progression independently of p65PAK and the JNK/SAPK MAP kinase cascade. *Cell* **87**, pp. 519-529
- Lamaze, C., Fujimoto, L.M., Jin, H.L., and Schmid, S.L. (1997)** The actin cytoskeleton is required for receptor-mediated endocytosis in mammalian cells. *J Biol Chem* **272**, pp. 20332-20325.
- Lamaze, C., Chuang, T.H., Terlecky, L.J., Bokoch, G.M., and Schmid, S.L. (1996)** Regulation of receptor-mediated endocytosis by Rho and Rac. *Nature* **382**, pp. 177-179
- Lang, C., Barco, A., Zablow, L., Kandel, E.R., Siegelbaum, S.A., and Zakharenko, S.S. (2004)** Transient expansion of synaptically connected dendritic spines upon induction of hippocampal long-term potentiation. *PNAS* **101**, pp. 16665-16670
- Lanzetti, L. (2007)** Actin in membrane trafficking. *Curr Opin Cell Biol* **19**, pp. 453-458
- Lau, C.G., and Zukin, R.S. (2007)** NMDA receptor trafficking in synaptic plasticity and neuropsychiatric disorders. *Nat Rev Neurosci* **8**, pp. 413-426
- Lee, S.H., Liu, L., Wang, Y.T., and Sheng, M. (2002)** Clathrin adaptor AP2 and NSF interact with overlapping site of GluR2 and play distinct roles in AMPA receptor trafficking and hippocampal LTD. *Neuron* **36**, pp. 661-674
- Leung, T., How, B.E., Manser, E., and Lim, L. (1993)** β -chimaerin, a new GTPase-activating protein for p21rac, is specifically expressed during the acrosomal assembly stage in rat testis. *J Biol Chem* **268**, pp. 3813-3816

- Li, Z., van Aelst, L., and Cline, H.T. (2000)** Rho GTPases regulate distinct aspects of dendritic arbor growth in *Xenopus* central neurons in vivo. *Nat Neurosci* **3**, pp. 217-224
- Li, W.L., Hornshaw, M.P., van der Schore, R.C., Watson, R., Tate, S., Casetta, B., Jimenez, C.R., Gouwenberg, Y., Gundelfinger, E.D., Smalla, K.H., and Smit, A.B. (2004)** Proteomics analysis of rat brain postsynaptic density. *J Biol Chem* **279**, pp. 987-1002
- Li, R. (2007)** Cytokinesis in development and disease: variations on a common theme. *Cell Mol Life Sci* **64**, pp. 3044-3058
- Lichte, B., Veh, R.W., Meyer, H.E., and Kilimann, M.W. (1992)** Amphiphysin, a novel protein associated with synaptic vesicles. *EMBO J* **11**, pp. 2521-2530
- Ligeti, E., Dagher, M.C., Hernandez, S.E., Koleske, A.J., and Settleman, J. (2004)** Phospholipids can switch the GTPase substrate preference of a GTPase-activating protein. *J Biol Chem* **279**, pp. 5055-5058
- Lim, S., Sala, C., Yoon, J., Park, S., Kuroda, S., Sheng, M., and Kim, E. (2001)** Sharpin, a novel postsynaptic density protein that directly interacts with the Shank family of proteins. *Mol Cell Neurosci* **17**, pp. 385-397
- Lu, J., Helton, T.D., Blanpied, T.A., Racz, B., Newpher, T.M., Weinberg, R.J., and Ehlers, M.D. (2007)** Postsynaptic positioning of endocytic zones and AMPA receptor cycling by physical coupling of dynamin-3 to homer. *Neuron* **55**, pp. 874-889
- Luna, A., Matas, O.B., Martinez-Menaguerz, J.A., Mato, E., Duran, J.M., Ballesta, J., Way, M., and Egea, G. (2002)** Regulation of protein transport from the Golgi complex to the endoplasmic reticulum by Cdc42 and N-WASP. *Mol Biol Cell* **13**, pp. 866-879
- Luscher, C., Xia, H., Beattie, E.C., Carrol, R.C., von Zastrow, M., Malenka, R.C., and Nicoll, R.A. (1999)** Role of AMPA receptor cycling in synaptic transmission and plasticity. *Neuron* **24**, pp. 649-658
- Macara, I.G., and Spang, A. (2006)** Closing the GAP between polarity and vesicle transport. *Cell* **125**, pp. 419-421
- Machensky, L.M. (1998)** Cytokinesis: IQGAPs find a function. *Curr Biol* **8**, pp. R202-R205
- Malenka, R.C., and Nicoll, R.A. (1999)** Long-term potentiation – a decade of progress? *Science* **285**, pp. 1870-1874
- Matsuzaki, M., Honkura, N., Ellis-Davies, G.C. and Kasai, H. (2004)** Structural basis of long-term potentiation in single dendritic spines. *Nature* **429**, pp. 761-766
- Mohrmann K., and van der Sluijs, P. (1999)** Regulation of membrane transport through the endocytic pathway by RabGTPases. *Mol Membr Biol* **16**, pp. 81-87
- Montgomery, J.M., Zamorano, P.L., and Garner, C.C. (2004)** MAGUKs in synapse assembly and function: an emerging view. *Cell Mol Life Sci* **61**, pp. 911-929
- Moon, S.Y., and Zheng, Y. (2003)** Rho GTPase-activating proteins in cell regulation. *Trends Cell Biol* **13**, pp. 13-22

- Mullins, R.D., Stafford, W.F., and Pollard, T.D. (1997)** Structure, subunit topology, and actin binding activity of the Arp2/3 complex from *Acanthamoeba*. *J Cell Biol* **136**, pp. 331-343
- Musacchio, A., Cantley, L.C. and Harrison, S.C (1996)** Crystal structure of the breakpoint cluster region-homology domain from phosphoinositide 3-kinase p85 alpha subunit. *PNAS* **93**, pp. 14373-14378
- Naisbitt, S., Kim, E., Tu, J.C., Xiao, B., Sala, C., Valtschanoff, J., Weinberg, R.J., Worley, P.F., and Sheng, M. (1999)** Shank, a novel family of postsynaptic density proteins that binds to the NMDA receptor/PSD-95/GKAP complex and cortactin. *Neuron* **23**, pp. 569-582
- Nassar, N., Hoffman, G.R., Manor, D., Clardy, J.C., and Cerione, R.A. (1998)** Structures of Cdc42 bound to the active and catalytically comprised forms of Cdc42GAP. *Nat Struc Biol* **5**, pp. 1047-1052
- Newey, S.E., Velamoor, V., Govek, E.-E., and van Aelst, L. (2005)** Rho GTPases, dendritic structure, and mental retardation. *J Neurobiol* **64**, pp. 58-74
- Ng, J., Nardine, T., Harms, M., Tzu, J., Goldstein, A., Sun, Y., Dietzl., G. Dickson, .J., and Luo, L. (2002)** Rac GTPases control axonal outgrowth, guidance and branching. *Nature* **416**, pp. 442-447
- Nobes, C.D., and Hall, A. (1995)** Role of actin polymerization and adhesion to extracellular matrix in Rac-and Rho-induced cytoskeletal reorganization. *J Cell Biol* **138**, pp. 53-62
- Nourry, C., Grant, S.G., and Borg, J.P. (2003)** PDZ domain proteins: plug and play! *Sci STKE* **22**, RE7
- Okamoto, P.M., Gamby, C., Wells, D., Fallon, J., and Vallee, R.B. (2001)** Dynamin isoform-specific interaction with the Shank/ProSAP scaffolding proteins of the postsynaptic density and actin cytoskeleton. *J Biol Chem* **276**, pp. 48458-48465
- Otsu, M., Hiles, I., Gout, I., Fry, M.J., and Ruiz-Larrera, F. (1991)** Characterization of two 85 kd proteins that associate with receptor tyrosine kinases, middle -T/pp60c-src complexes, and PI3-kinase. *Cell* **65**, pp. 91-104
- Park, M., Salgado, J.M., Ostroff, L., Helton, T.D., Robinson, C.G., Harris, K.M., and Ehlers, M. (2006)** Plasticity-induced growth of dendritic spines by exocytic trafficking from recycling endosomes.
- Peng, J., Kim, M.J., Cheng, D., Duong, D.M., Gygi, S.P., and Morgan, S. (2004)** Semiquantitative proteomic analysis of rat forebrain postsynaptic density fractions by mass spectrometry. *J Biol Chem* **279**, pp. 21003-21011
- Perez-Otano, I., Lujan, R., Tavalin, S.J., Plomann, M., Modregger, J., Liu, X.-B., Jones, E.G., Heinemann, S.F., Lo, D.C., and Ehlers, M.D. (2006)** Endocytosis and synaptic removal of NR3A-containing NMDA receptors by PACSIN1/syndapin1. *Nat Neurosci* **9**, pp. 611-621

- Peter, B.J., Kent, H.M., Mills, I.G., Vallis, Y., Butler, P.J.G., Evans, P.R., and McMahon, H.T. (2004)** BAR domains as sensors of membrane curvature: the amphiphysin BAR structure. *Science* **303**, pp. 495-499
- Proepper, C., Johannsen, S., Liebau, S., Dahl, J., Vaida, B., Bockmann, J., Kreutz, M.R., Gundelfinger, E.D., and Boeckers, T.M. (2007)** Abelson interacting protein 1 (Abi-1) is essential for dendrite morphogenesis and synapse formation. *EMBO J* **26**, pp. 1397-409
- Prybylowski, K., and Wendhold, R.J. (2004)** N-methyl-D-aspartate receptors: subunit assembly and trafficking to the synapse. *J Biol Chem* **279**, pp. 9673-9676
- Prybylowski, K., Chang, K., Kan, L., Vicini, S., and Wendhold, R.J. (2005)** The synaptic localization of NR2B-containing NMDA receptors is controlled by interactions with PDZ proteins and AP-2. *Neuron* **15**, pp. 845-857
- Qualmann, B., Roos, J., di Gregorio, P.J., and Kelly, R.B. (1999)** Syndapin I, a synaptic dynamin-binding protein that associates with the neural Wiskott-Aldrich syndrome protein. *Mol Cell Biol* **10**, pp. 501-513
- Qualmann, B., and Kessels, M.M. (2002)** Endocytosis and the cytoskeleton. *Int Rev Cytol* **220**, pp. 93-144
- Kessels, M.M., and Qualmann, B. (2006)** Syndapin oligomers interconnect the machineries for endocytic vesicle formation and actin polymerization. *J Biol Chem* **281**, pp. 13285-13299
- Racz, B., Blanpied, T.A., Ehlers, M.D., and Weinberg, R.J. (2004)** Lateral organization of endocytic machinery in dendritic spines. *Nat Neurosci* **7**, pp. 917-918
- Ranganathan, R., and Ross, E.M. (1997)** PDZ domain proteins: scaffolds for signaling complexes. *Curr Biol* **7**, pp. 770-773
- Ren, G., Vajjhala, P., Lee, J.S., Winsor, B., and Munn, A.L. (2006)** The BAR domain proteins: molding membranes in fission, fusion, and phagy. *Micro Mol Biol Rev* **70**, pp. 37-120
- Richnau, N., and Aspenström, P. (2001)** Rich, Rho GTPase-activating protein domain – containing protein involved in signaling by Cdc42 and Rac1. *J Biol Chem* **276**, pp. 35060-35070
- Rittinger, K., Walker, P.A., Eccleston, J.F., Smerdon, S.J., and Gamblin, S.J. (1997)** Structure at 1.65 Å of RhoA and its GTPase-activating protein in complex with a transition-state analogue. *Nature* **389**, pp. 758-762
- Rittinger, N., Taylor, W.R., Smerdon, S.J., and Gamblin, S.J. (1998)** Support for shared ancestry of GAPs. *Nature* **392**, pp. 448-449
- Rodal, A.A., Sokolova, O., Robins, D.B., Daugherty, K.M., Hippenmeyer, S., Riezman, H., Grigorieff, N., and Godde, B.L. (2005)** Conformational changes in the Arp2/3 complex leading to actin nucleation. *Nat Struc Mol Biol* **12**, pp. 26-31

- Rohatgi, R., Ma, L., Miki, H., Lopez, M., Kirchhausen, T., Takenawa, T., and Kirschner, M.W. (1999)** The interaction between WASP and the Arp2/3 complex links Cdc42-dependent signals to actin assembly. *Cell* **16**, pp. 221-231
- Rohatgi, R., Ho, H., and Kirschner, M.W. (2000)** Mechanism of N-WASP activation by Cdc42 and phosphatidylinositol 4,5-bisphosphate. *J Cell Biol* **150**, pp. 1299-1320
- Sala, C., Piech, V., Wilson, N.R., Passafaro, M., Liu, G., and Sheng, M. (2001)** Regulation of dendritic spine morphology and synaptic function by shank and homer. *Neuron* **31**, pp. 115-130
- Saras, J. and Heldin, C.H. (1996)** PDZ domain bind carboxy-terminal sequences of target proteins. *Trend Biochem Sci* **21**, pp. 455-458
- Scheffzek, K., Ahmadian, M.R., and Wittinghofer, A. (1998)** GTPase-activating proteins: helping hands to complement an active site. *Trends Biochem Sci* **23**, pp. 257-262
- Scheffzek, K., Lautwein, A., Kabsch, W., Ahmadian, M.R., and Wittinghofer, A. (1996)** Crystal structure of the GTPase-activating domain of human p120GAP and implications for the interaction with Ras. *Nature* **384**, pp. 591-596
- Schmidt, A., and Hall, M.N. (1998)** Signaling to the actin cytoskeleton. *Annu Rev Cell Dev Biol* **14**, pp. 305-338
- Schmidt, A., and Hall, A. (2002)** Guanine nucleotide exchange factors for Rho GTPases: turning on the switch. *Genes Dev* **16**, pp. 1587-1609
- Seabra, M.C. (1998)** Membrane association and targeting of prenylated Ras-like GTPases. *Cell Signal* **10**, pp. 167-172
- Self, A.J., and Hall, A. (1995)** Measurement of intrinsic nucleotide exchange and GTP hydrolysis rates. *Meth Enzymol* **256**, pp. 67-76
- Settleman, J.V., Narasimhan, V., Foster, L.C., and Weinberg, R.A. (1992)** Molecular cloning of cDNAs encoding the GAP-associated proteins p190: Implications for a signaling pathway from ras to the nucleus. *Cell* **69**, pp. 539-549
- Sheng, M., and Hoogenraad, C.C. (2007)** The postsynaptic architecture of excitatory synapses: a more quantitative view. *Annu Rev Biochem* **76**, pp. 1.1-1.25
- Sheng, M., and Kim, E. (2000)** The Shank family of scaffold proteins. *J Cell Sci* **113**, pp. 1851-1856
- Shields, J.M., Pruitt, K., McFall, A., Shaub, A., and Der, C.J. (2000)** Understanding Ras: 'it ain't over 'til it's over'. *Trends Cell Biol* **10**, pp. 147-154
- Skolnik, E.Y., Margolis, B., Mohammadi, M., Lowenstein, E., and Fischer, R. (1991)** Cloning of PI3-kinase-associated p85 utilizing a novel method for expression/cloning of target proteins for receptor tyrosine kinases. *Cell* **65**, pp. 83-90

- Smythe, E., and Ayscough, K.R. (2006)** Actin regulation in endocytosis. *J Cell Sci* **119**, pp. 4589-4598
- Snapper, S.B., Takeshima, F., Anton, I., Liu, C.H., Thomas, S.M., Nguyen, D., Dudley, D., Fraser, H., Purich, D., Lopez-Illasaca, M., Klein, C., Davidson, L., Bronson, R., Mulligan, R.C., Southwick, R., Geha, R., Goldberg, M.B., Rosen, F.S., Hartwig, J.H., and Alt, F.W. (2001)** N-WASP deficiency reveals distinct pathways for cell surface projections and micro-bial actin based motility. *Nat Cell Biol* **3**, pp. 897-904
- Soltau, M., Berhörster, K., Kindler, S., Buck, F., Richter, D., and Kreienkamp, H.-J. (2004)** Insulin receptor substrate of 53 kDa links postsynaptic shank to PSD-95. *J Neurochem* **90**, pp. 659-665
- Sonderling, S.H., Guire, E.S., Kaech, S., White, J., Zhang, F., Schutz, K., Langeberg, L.K., Banker, G., Raber, J., and Scott, J.D. (2007)** A WAVE-1 and WRP signaling complex regulates spine density, synaptic plasticity, and memory. *J Neurosci* **27**, pp. 355-365
- Stradal, T.E.B., Rottner, K., Disanza, A., Confalonieri, S., Innocenti, M., and Scita, G. (2004)** Regulation of actin dynamics by WASP and WAVE family of proteins. *Trends Cell Biol* **14**, pp. 303-310
- Sudhof, T. (1995)** The synaptic vesicle cycle. *Annu Rev Neurosci* **27**, pp. 509-547
- Takai, Y., Sasaki, T., and Matozaki, T. (2001)** Small GTP-binding proteins. *Physiol Rev* **81**, pp. 153-208
- Takanobu, N., Watabe, A.M., Tezuka, T., Yoshida, Y., Yokoyama, K., Umemori, H., Inoue, A., Okabe, S., Manabe, T., and Yamamoto, T. (2003)** p250GAP, a novel brain-enriched GTPase-activating protein for Rho family GTPases, is involved in the N-methyl-D-aspartate receptor signaling. *Mol Biol Cell* **14**, pp. 2921-2934
- Tarricone, C., Xiao, B., Justin, N., Walker, P.A., Rittinger, K., Gamblin, S.J., and Smerdon, S.J. (2001)** The structural basis of Arfapitin-mediated cross-talk between Rac and Arf signaling pathways. *Nature* **411**, pp. 215-219
- Thomas, U. (2004)** Modulation of synaptic signaling complexes by homer proteins. *J Neurochem* **81**, pp. 407-413
- Toshiki, I., and de Camilli, P. (2006)** BAR, F-BAR (EFC) and ENTH/ANTH domains in the regulation of membrane-cytosol interfaces and membrane curvature. *Biochim Biophys Acta* **1761**, pp. 897-912
- Toshiki, I., Erdmann, K.S., Roux, A., Habermann, B., Werner, H., and de Camilli, P. (2005)** Dynamin and the actin cytoskeleton cooperatively regulate plasma membrane invagination by BAR and F-BAR proteins. *Dev Cell* **9**, pp. 791-804
- Tu, J.C., Xiao, B., Yuan, J.P., Lanahan, A.A., Leoffert, K., Li, M., Linden, D.J., and Worley, P.F. (1998)** Homer binds a novel proline-rich motif and links group 1 metabotropic glutamate receptors with IP3 receptors. *Neuron* **21**, pp. 711-726

- Wasiak, S., Quinn, C.C., Ritter, B., de Heuvel, E., Barannes, D., Plomann, M., McPherson, P.S. (2001) The Ras/Rac guanine nucleotide exchange factor mammalian Son-of-sevenless interacts with PACSIN1/ syndapin I, a regulator of endocytosis and the actin cytoskeleton. *J Biol Chem* **276**, pp.266622-26628
- Wegner, A.M., Nebhan, C.A., Hu, L., Majumdar, D., Meier, K.M., Weaver, A.M., and Webb, D.J. (2008) N-WASP and the Arp 2/3 complex are critical regulators of actin in the development of dendritic spines and synapses. *J Biol Chem* **6**, pp. 15912-15920
- Wells, D.C., Fawcett, J.P., Traweger, A., Yamanaka, Y., Goudreault, M., Elder, K., Kulkarni, S., Gish, G., Irag, C., Lim, C., Colwill, K., Starostine, A., Metalnikov, P., and Pawson, T (2006) A Rich1/ Amot complex regulates the Cdc42 GTPase and apical-polarity proteins in epithelial cells. *Cell* **125**, pp. 535-548
- Welsh, C.F. (2004) Rho GTPases as key transducers of proliferative signals in glial cell cycle regulation. *Breast Cancer Res Treat* **84**, pp. 33-42
- Wennerberg, K., Rossman, K.L., and Der, C.J. (2005) The Ras superfamily at a glance. *J Cell Sci* **118**, pp.843-846
- van Aelst, L., and d'Souza-Schorey, C. (1997) Rho GTPases and signaling networks. *Gen & Dev* **11**, pp. 2295-2322
- Wherlock, M., and Mellor, H. (2002) The Rho GTPase family: a Racs to Wrchs story. *J Cell Sci* **115**, pp. 239-240
- Wittinghofer, A., and Nassar, N. (1996) How Ras-related proteins talk to their effectors. *Trends in Biochem Sci* **21**, pp. 488-491
- Wong, K., Ren, X., Huang, Y., Xie, Y., Liu, G., Saito, H., Tang, H., Wen, L., Brady-Kalnay, S., and Mei, L. (2001) Signal transduction in neuronal migration: roles of GTPase activating proteins and the small GTPase Cdc42 in the Slit-Robo pathway. *Cell* **107**, pp. 209-221
- Wucherpfenning, T., Wilsch-Brauninger, M., and Gonzalez-Gaitan, M. (2003) Role of drosophila Rab5 during endosomal trafficking at the synapse and evoked neurotransmitter release. *J Cell Biol* **161**, pp. 609-624
- Vinatier, J., Herzog, E., Plamont, M.A., Wojcik, S.M, Schmidt, A., Brose, N., Daviet, L., El Mestikawy, S., and Giros, B. (2006) Interaction between the vesicular glutamate transporter type 1 and endophilin A1, a protein essential for endocytosis. *J Neurochem* **97**, pp. 1111-1125
- Vojtek, A.B., and Der, C.J. (1998) Increasing complexity of the Ras signaling pathway. *J Biol Chem* **273**, pp. 19925-19928
- Yang, J.Y., and Widmann, C. (2001) Antiapoptotic signaling generated by caspase-induced cleavage of RasGAP. *Mol Cell Biol* **21**, pp. 5346-5358

- Yang, Y., Marcello, M., Endris, V., Saffrich, R., Fischer, R., Trendelenburg, M.F., Sprengel, R., and Rappold, G. (2006)** MEGAP impedes cell migration via regulating actin and microtubule dynamics and focal complex formation. *Exp. Cell Res* **312**, pp. 2379-2393
- Yarar, D., Waterman-Storer, C.M., and Schmid, S.L. (2005)** A dynamic actin cytoskeleton functions at multiple stages of clathrin mediated endocytosis. *Mol Biol Cell* **16**, pp. 964-975
- Yoshizawa, M., Hoshino, M., Sone, M., and Nabeshima, Y. (2002)** Expression of stef, an activator of Rac1, correlates with the stages of neuronal morphological development in the mouse brain. *Mech Dev* **113**, pp. 65-68
- Zhang, B., and Zehhof, A.C. (2002)** Amphiphysins: raising the BAR for synaptic vesicle recycling and membrane dynamics. *Traffic* **3**, pp. 452-460
- Zhu, S., Korzh, V., Gong, Z., and Low, B.C. (2008)** RhoA prevents apoptosis during zebrafish embryogenesis through activation of MEK/Erk pathway. *Oncogene* **6**, pp.1580-1589
- Ziff, E.B. (1997)** Enlightening the postsynaptic density. *Neuron* **19**, pp. 1163-1174
- Ziv, N.E., and Garner, C.C. (2004)** Cellular and molecular mechanisms of presynaptic assembly. *Nat Rev Neurosci* **5**, pp. 385-399

I would like to thank my advisor, Professor Tobias M. Böckers, for giving me the opportunity to work in his laboratory and providing me with this interesting project. I especially thank him for approving much scientific freedom to explore and discover. His promotion of my work through conference attendances, technique and soft skills workshops, weekly PhD meetings as well as his supportive behavior in terms of problem solving discussions, proved to be one of my best experiences at the institute.

Jürgen Bockmann, my second mentor always brought a useful advice to my practical work when it came to changing any assay techniques. This always improved the outcome. I am grateful for his criticism, help and encouragement.

Generally, I would like to say ‘thank you’ to all my colleagues from the laboratory with whom I had the pleasure of working with over the years. These include: Anna Dolnik, Svenja Johannsen, Andreas Grabrucker, Christian Pröpper, Bianca Vaida, Angelika Schmidt, Natalie Damm, Michael Schmeißer, Nicola Martin, Stefan Liebau and Ursula Pika-Hartlaub. I am very grateful for their good collaboration, willingness to discuss and exchange ideas. Their kind support in every aspect of ‘our’ daily endeavors in the laboratory was helpful to master a lot of unforeseen challenges.

In particular, I would like to praise Anna Dolnik for her constructive cooperation, setting up and performing cell fractionation successfully together. Moreover, she proved to be a thorough teacher for lots of other practical approaches in the lab. Special thanks are also dedicated to Renate Zienecker for her excellent technical assistance with *in situ* hybridization and Bianca Vaida for performing EM studies together.

Many special thanks also to Sybille Etter and Wolfgang Podschuweit for their kind support to master these ‘little’ tricky computer failures.

Many personal thanks to my “old” friends who were there to share my joy and problems. Thank you. I cannot enough underline my appreciation for it.

Finally, I would like to express my gratitude to my family for their financial support and their endless love for letting me pursue my dream for so long. You’ve always kept believing in the girl with the one way ticket. Thank you for standing by me through all the times. You are great.

Curriculum Vitae

Surname: Dahl
 Forename: Janine
 Date of Birth: 02/13/1980
 Place of Birth: Ludwigslust
 Nationality: German
 Address: Trollingerweg 24
 89075 Ulm, Germany

Academic Education

08/2004 - 02/2009	Graduate Research in Neurobiology Doctoral Thesis "Characterization of RhoSAP, a GAP protein related to synapses"/ Dr. biol. hum. SFB 497 B7 Project Grant Medicinal Faculty, Institute of Anatomy and Cell Biology <i>Ulm University</i>
10/2000 - 03/2004	Graduate Studies in Biochemistry Master's in Biochemistry/ Dipl.-Biochem. <i>University of Leipzig</i>
10/98 - 09/2000	Undergraduate Studies in Biochemistry <i>Ernst-Moritz-Arndt University, Greifswald</i>
09/1992 - 06/1998	University Entrance Qualification / Abitur <i>Ostseegymnasium Rostock</i>

Attended Conferences with Poster Presentations

Neuroscience 2007 San Diego, USA	"Characterization of RhoSAP: A GTPase activating protein localized in postsynaptic densities (PSDs)"
7 th Goettingen Meeting of the German Neuroscience Society 2007, Goettingen	"RhoSAP, a novel protein of vesicle cycling at the PSD"
23 rd working conference of the German Anatomical Society 2006, Wuerzburg	"RhoSAP, a novel protein of the PSD"

Publication

Proepper C., Johannsen S., Liebau S., Dahl J., Vaida B., Bockmann J., Kreutz M.R., Gundelfinger E.D., Boeckers T.M (2007) Abelson interacting protein 1 (Abi-1) is essential for dendrite morphogenesis and synapse formation. *EMBO J* **26**, pp. 1397-409